Elucidating the Novel Role for Core Binding Factor beta in Osteosarcoma Protein Translation

By

NICHOLAS ALEXANDER OLDBERG

DISSERTATION

Submitted in partial satisfaction of the requirements for the degree of

DOCTOR OF PHILOSOPHY

in

Pharmacology and Toxicology

in the

OFFICE OF GRADUATE STUDIES

of the

UNIVERSITY OF CALIFORNIA

DAVIS

Approved:

Luke A. Wittenburg, Chair

Colleen Sweeney

James Angelastro

Committee in Charge

2024

ABSTRACT OF DISSERTATION

Osteosarcoma (OS) is the most common primary bone malignancy in humans and canines, and in humans primarily affects younger patients 10-14 years of age. While considerable efforts have been put forth in new therapeutic approaches to this disease, the treatment and prognosis for OS has changed very little since the 1980s. Targeted therapeutics have made considerable progress in other cancer types, leveraging characteristics of cancer cells which differentiate them from that of normal healthy cells. In comparison to other cancers, OS is highly heterogeneic, and no single unifying driver mutation has yet been found. Development of a therapy which could overcome the high degree of heterogeneity amongst OS tumors could go a long way in improving the lives of OS patients. Targeting protein translation has been proposed as one mechanism by which to overcome tumor heterogeneity, and this dissertation focuses on studying a noncanonical role of core binding factor beta (CBFβ) as a regulator of protein translation, and elucidating whether this could represent a potential therapeutic target for OS.

Utilizing a wide array of *in vitro* assays, we have been able to demonstrate that loss of CBFβ reduces protein expression of RUNX2 in a post-transcriptional manner, and this decrease in RUNX2 protein level is not fully explained by alterations in RUNX2 stability brought about by loss of its binding partner CBFβ. Additionally, we demonstrate that loss of CBFβ also causes a decrease in global protein translation, and confirmed an interaction between CBFβ and hnRNPK which has thus far only been observed in breast cancer cells. Importantly, this interaction with hnRNPK is said to be the mechanism by which CBFβ influences protein translation, and our results corroborate those observed in breast cancer cells and suggest CBFβ may also perform this role in OS.

Reports of the interactions between CBFβ and hnRNPK or RUNX2 allude to mutual exclusivity in interaction, and with the transcriptional role of CBFβ accomplished via binding to RUNX proteins, and the translational role of CBFβ accomplished via binding to hnRNPK, it is entirely possible these two roles are antagonistic in some fashion. To investigate the relevance of certain CBFβ residues in terms of this translational role of CBFβ, and avoid confounding variables from the transcriptional role of CBFβ, we utilized point mutations to interrupt CBFβ-RUNX2 interaction. Using various in vitro assays, we validated key residues of CBFβ which are involved in its interaction with RUNX2, re-introduced this mutant form into CBFβ knockout cells, and measured alterations to RUNX2 interaction and nuclear shuttling. We confirmed that our mutant displays reduced binding to RUNX2, and drastically reduced nuclear shuttling.

Lastly, we expanded our studies from RUNX2 to the entire genome and proteome. Encouraging data thus far had suggested CBFβ may play a role in protein translation, and necessary next steps were to assess which proteins CBFβ may be interacting with in performance of this role, and elucidate which proteins may be under the translational purview of CBFβ. Using immunoprecipitation mass spectrometry we identified numerous specific interactors of CBFβ, with high enrichment in pathway analysis terms associated with protein translation. Additionally, using two different methods we generated a list of proteins which may be under the translational purview of CBFβ, and found strong enrichment of numerous cancer-associated terms among this list.

These studies establish that CBFβ participates in protein translation in OS, with many genes under its purview associated strongly with cancer in general, and OS specifically. This provides justification for future studies delving deeper into this novel role of CBFβ, and opens up another mechanism by which protein translation could be targeted therapeutically in OS.

ACKNOWLEDGEMENTS

Many people deserve my sincere appreciation for their support during my journey through graduate school. It truly does take a village. First, I would like to express my utmost gratitude to my advisor, Dr. Luke Wittenburg, for his mentorship, positive attitude, and faith in me as a researcher. He took a chance on me and gave me the opportunity to work in his lab in April 2020, at a time when my future as a graduate student, as well as that of the world at large, was uncertain. Without his support, I wouldn't be the scientist I am today, and I am forever in his debt for the wonderful opportunity he gave me.

I'd also like to thank Dr. Colleen Sweeney and Dr. James Angelastro for serving on my dissertation committee and providing guidance as I advanced through the stages of graduate school. I am so appreciative of them for making time in their busy schedules to meet with me on project updates and to read through the entirety of this work.

I'd like to thank Dr. Dayn Godinez for being the best labmate I could have ever hoped for. It was a godsend to have such a capable coworker who is also a close friend, and I am so grateful for his support, camaraderie, and the many times he helped me design my own experiments.

I'd like to thank Dr. Daniel York for being such a great colleague and a wealth of information on experiment plans and troubleshooting. Additionally, I'd like to recognize his vigilance in ensuring that everything in our shared lab space ran smoothly.

I'd like to thank my fiancée, Brittany Morris, for her unyielding support throughout my time in graduate school. She has been my rock through so many ups and downs—experiments not working, transferring labs, health challenges, and more—and I have been so fortunate to have her as my partner throughout my journey at UC Davis. Words cannot express how grateful I am to have her in my life; she is truly one of a kind. I'd also like to recognize her parents, Brian and Kim,

for their unwavering support throughout my graduate school career and for opening their home to me post-graduation. They have always asked how my research was going and provided me with encouragement in this journey, and sent me home with delicious leftovers from the many events they've hosted at their house.

I would like to thank my mom for being so supportive and involved at every step of my educational career. She worked tirelessly to find scholarships I could qualify for, which facilitated my travel to COSMOS summer camp at UC Irvine, attendance at SAT prep programs, and helped pay for my college tuition. Her commitment to me getting the best education possible played a tremendous role in my development as a scientist and as a person overall. I would also like to mention how much of a boost the frozen meals she always sent home with me were. There were many times during my graduate studies when her homemade cooking was what gave me that extra push to keep going.

I would like to thank my dad for his encouragement throughout my time in graduate school. He has made a strong effort to understand the specifics of my research to fully grasp the weight of the triumphs and pitfalls in my journey. This has meant the absolute world to me, and it has been a joy sharing updates with him as I have progressed through graduate school.

While growing up, I faced several health challenges and was diagnosed with juvenile rheumatoid arthritis at a very young age. My dad found a program called Healthy Families, which allowed us to afford my prescription for a new drug that had just come on the market, Enbrel. This health program and Enbrel changed my life in two significant ways: health-wise, they gave me the ability to move my joints freely and return to the physical activities I loved so dearly; and career-wise, witnessing the miraculous transformation in my body brought about by Enbrel inspired me to pursue pharmacology as a field of study.

I would also like to thank my grandma, Sara Oldberg, for supporting my passion for science and providing me with such interesting reading material when I was growing up. She was an avid reader and would always give me her *Discover* magazines after she was done reading them. Discussing these articles with her are memories I will forever cherish, and they deepened my resolve that becoming a scientist was the career path for me.

I would like to thank my high school AP Biology teacher, Ms. Said, for leading such an incredible class that it inspired me to pursue a B.S. in Biochemistry, ultimately guiding me down the path I am on now. In her class, I learned numerous advanced techniques that are uncommon at the high school level, and the passion she displayed for her subject was formative in my journey to become the scientist I am today.

I would like to thank Dr. Randy Hampton for granting me the opportunity to work in his lab at UC San Diego as an undergraduate and for giving me my first exposure to scientific research. I learned so much during my time in his lab, and I will always be grateful for his tutelage and support when I was just starting out my research career.

I would like to thank Dr. Mehran F. Moghaddam and Dr. Julius Apuy for their mentorship and for being such fantastic role models during my time at Celgene. Working with them was the first time I witnessed how a PhD can broaden your mind and allow you to truly think outside the box. Prior to working at Celgene I had been unsure about pursuing a PhD, but being around them convinced me that this was the path for me.

I would also like to thank Yang Tang for her incredible mentorship and encouragement during my time at Celgene. It was such a privilege to work under someone who was such a kind and nurturing leader. Working on developing new therapies under her guidance has been one of the best experiences of my career.

I would like to thank my friends, both those I made in the PTX program and those from college and beyond, for being such a great support system throughout this journey. Whether I needed to vent about the ups and downs of my work or simply enjoy some time away from the rigors of school, they were always there for me.

Finally, I'd like to thank Skeler, one of my favorite electronic music producers. Grad school often entails very long hours in the lab, and his music gave me the energy and focus to keep pushing forward no matter what. His songs have been the soundtrack of my time in graduate school, and I am forever grateful to him for sharing his art with the world.

DEDICATION

I would like to dedicate this work to all scientific researchers—past, present, and future—and celebrate their tenacity in pushing the envelope and bringing new discoveries that benefit humanity. As scientists, we truly stand on the shoulders of giants, and the work of today is only possible because of the strong commitment of those who came before us.

TABLE OF CONTENTS

LIST OF TABLES AND FIGURES

Chapter 2

Chapter 3

Chapter 4

Chapter 1

Literature Review and Project Rationale

Osteosarcoma

Incidence and Prognoses

Osteosarcoma (OS) is the most common form of primary bone cancer in humans and canines (1), with ~1,000 new cases diagnosed per year in the United States (2,3). The age of diagnosis with OS has a bimodal age distribution, with the first, and largest, peak in the 10-14-year-old age group, with the second for patients aged 65+ (4). The early age of presentation in patients makes OS somewhat of an outlier in the field of oncology, as the average age at diagnosis for all cancer patients is 66 years (3). OS can present in a variety of bones in the body, however the lower long bones are the most common, comprising ¾ of all early-onset diagnoses (2). Within the bone, OS most often occurs at the metaphysis (4), the portion of bone between the diaphysis (middle shaft) and epiphysis (rounded end) which contains the growth plate.

The lung is far and away the most common site of metastasis in OS patients, and 20-30% of patients already harbor clinically detectable metastatic lesions at time of diagnosis (5,6). Importantly, for metastases to be clinically detectable they must be large enough to be seen by imaging techniques, resulting in small lesions often remaining undiscovered. This presents a clear limitation, and the fraction of OS patients harboring metastatic lesions at time of diagnosis is likely far higher, closer to ~50% by some estimations (7). When presenting with localized disease at time of diagnosis, patients with OS have an estimated five-year survival rate of 60-80% (8), but for those with clinically detectable metastases this plummets to ~20% (6,9).

Treatment Options

Advancements in mechanisms to treat OS have lagged behind that of cancer in general, and the current treatment regimen has remained essentially unchanged over the past 30 years (10). The standard treatment of OS is so-called MAP therapy, standing for Methotrexate, Adriamycin, and cisPlatin, with or without ifosamide (11). When introduced in the 1980's, MAP therapy represented a considerable improvement in treatment of OS. Prior to this, the standard approach to OS was amputation, which was not only gruesome, but sadly yielded a paltry 5-year survival rate of ~17% for patients with OS (12). Although nearly four decades have passed since its introduction, MAP therapy remains as the most effective treatment for OS (13).

This lack of new approved therapies for OS is not due to a lack of effort, as numerous approaches leveraging a wide range of mechanisms have been attempted to treat this disease. These include proteasome inhibition (14–16), immunotherapies (17,18), T cell engaging bispecific antibodies (19), anti-IL-2 monoclonal antibodies (mAb) (20), oncolytic viruses in solo (21) or in combination with another therapy (22), or modulation of innate immunity (18,23). Additionally, drugs synergistic or additive to existing MAP therapy have been evaluated, such as anti-CD47 mAb (24) or Sorafenib (25) in combination with Doxorubicin, and PPARγ agonists (26), natural products such as curcumol (27), or Eicosapentaenoic acid (28) in combination with Cisplatin.

Disease Profile

In contrast to other sarcomas, OS is not typified by a specific translocation or genetic mutation, and instead presents as an assortment of widespread chromosomal abnormalities (29). Osteosarcoma tumors can possess a large range of chromosome number, ranging from haploid all the way up to hexaploid (30,31). In lieu of gain of function mutations in oncogenes, or loss of

function mutations in tumor suppressors, OS is driven more so by changes in copy number of the genes themselves. This occurs by way of genomic amplification occurring in chromosomal regions containing oncogenes, and copy number losses occurring in regions harboring tumor suppressor genes (29).

In terms of common alterations observed in OS, these include amplification of oncogenes MYC (32–35) and mouse double minute 2 homolog (MDM2) (33,36–38) and loss of tumor suppressors tumor protein p53 (TP53) (36,37), retinoblastoma protein (RB1) (32,36,37), and cyclin-dependent kinase inhibitor 2A (CDN2A) (32,36,37). Acquisition of these genetic abnormalities in OS is likely to occur by a variety of mechanisms, such as point mutation during DNA replication (39) or aneuploidy due to errors in cell division (40,41). Additional to these canonical methods, a new mechanism, chromothripsis, has recently been identified (29). In chromothripsis, tens to hundreds of individual genomic rearrangements can occur in a single event, resulting in a genetic catastrophe for the cell (29,42). This mechanism was estimated by the authors to occur in at least 2-3% of all cancers, but in the words of the authors, is "particularly common in bone cancers", reaching a prevalence of ~25% (42).

This genomic landscape makes development of therapies for OS challenging, as the lack of *bonafide* driver mutations in OS (43) leaves few specific differences between tumor and healthy tissue which could be leveraged therapeutically. The heterogeneity of OS places it at a relative disadvantage when compared to other cancers which possess strong genetic links to disease. Salient examples of targeted therapeutics in other cancers which have utilized disease-specific mutations include imatinib (44,45) which targets the BCR-ABL fusion gene in chronic myelogenous leukemia (46), EGF/human EGFR (HER) targeting therapies such as osimertinib in

non-small cell lung cancer and breast cancer (47–49), and the wide variety of development targeting RAS mutations in many cancers (50–54).

Cancer therapeutics do not have to target a specific mutation in order to be effective, and could instead target proteins which cancer cells are highly reliant upon for survival. This has been employed to great success with the IMiD drugs Lenalidomide and Mezigdomide, which function by co-opting the ubiquitin proteasome system (UPS) to degrade Ikaros and Ailos (55–57). These two transcription factors are necessary for the growth and survival of multiple myeloma cells (58,59), and their degradation by these drugs results in the selective killing of myeloma cells. Therapeutics leveraging the UPS have been explored in OS (60), but studies on this are very limited. This relatively new modality to treat disease could provide potential in OS, however before debating between mechanisms by which to attack a target, it is of course necessary to identify a viable target in the first place.

Core Binding Factor Transcriptional Complex

RUNX2 and CBFβ Overview

RUNX2 is a member of the RUNX family of DNA-binding transcription factors, which are co-activated by interaction with another protein, CBFβ. RUNX2 is known as the master regulator of bone growth and differentiation, and has critical roles in chondrocyte maturation and osteoblast differentiation (61). Core binding factor beta (CBFβ) acts as a binding partner to the RUNX family of transcription factors, and serves as a transcriptional co-activator. When bound to CBFβ, RUNX proteins have a higher affinity for DNA (62,63).

In normal conditions, RUNX2 plays a pivotal role in the formation of bones and teeth. RUNX2-/- mice are devoid of intramembranous bones and bone collar formation (64), and RUNX2-/- calvarial cells are incapable of differentiating into osteoblasts (65). In addition to playing a pivotal role in development of the skeleton and teeth, RUNX2 is also expressed in other tissues such as the ovaries, testis, brain, and B cells in the blood (66,67). CBFβ is also crucial for skeletal development, a discovery only possible via a CBFβ-GFP 'knock-in' approach(68–70). Homozygous disruption of CBFβ is embryonic lethal in mice, with death occurring ~12 days post coitum from central nervous system hemorrhaging and disruption of liver hematopoiesis (71,72).

RUNX2 is de-regulated in OS (73), and high expression levels of RUNX2 (74,75) or CBFβ (76) are each correlated with poor response to chemotherapy, and poor overall prognosis, in OS. Additionally, many of the gene targets of RUNX2 have been linked to poor therapeutic outcome in OS (77,78), such as vascular endothelial growth factor (VEGF) (79,80), alkaline phosphatase (ALP) (81), and matrix metalloproteinase 9 (MMP-9) (82). These data brought RUNX2 and CBFβ into our focus in studying OS, and spurred questions about whether the actions of these proteins could be interrupted as a therapeutic target.

Mutations in RUNX2 and CBFβ

Mutations in the RUNX proteins and/or CBFβ can have significant consequences to health. Alterations in RUNX2 are strongly implicated in cleidocranial dysplasia (CCD) (83), a rare condition which presents as developmental difficulties in teeth and bone. CCD is predominantly caused by haploinsufficiency of RUNX2 (84–86), and mutations of RUNX2 are found in 60-70% of CCD cases (87). These mutations are commonly found in the Runt Homology Domain (RHD) (88), and typically result in inhibited binding of RUNX2 to DNA (89) or to CBFβ (83). Many

cases of CCD with no genomic alteration to RUNX2 were found to to be caused by pathogenic variants of CBFβ, underscoring how critical RUNX2 and CBFβ are in bone formation (90). Mutations in RUNX2 and CBFβ are also seen in ~25% of all *de novo* acute leukemias, and are the most commonly disrupted genes in leukemia in humans (91). RUNX1 and CBFβ are mutated in a form of acute myeloid leukemia (AML) known as CBF AML, in which chromosomal rearrangements lead to the RUNX1/RUNX1T1 and CBFβ-MYH11 (also known as CBFβ-SMMHC) fusion proteins (92). CBFβ-SMMHC is formed by the fusion of the heterodimerization domain of CBFβ to the coiled-coil domain of Smooth Muscle Myosin Heavy Chain (93,94). Expression of this fusion protein leads to dysregulation of hematopoetic development, likely resulting from CBFβ-SMMHC binding RUNX1 with higher affinity than wild-type CBFβ (93). RUNX1/2 and CBFβ are also found to be frequently mutated in breast cancer (95,96).

Therapeutic Targeting of RUNX2 and CBFβ

Efforts to target RUNX2 and CBFβ in the context of OS have generated encouraging data, as siRNA knockdown of RUNX2 in OS cells decreases colony formation and cell invasion (97), and knockdown of CBFβ in OS cells reduces cell proliferation, migration, and invasion (76). RUNX2 has been targeted therapeutically via inhibition of DNA binding by small molecule, with clinical trials currently underway (98). Inhibition of the RUNX proteins has also been proposed as a way to enhance the sensitivity of myeloma drugs which leverage the UPS (99). Ro5-3335 is an inhibitor of CBFβ-RUNX1 interaction and has shown promise *in vitro* and *in vivo* against leukemias containing translocations or inversions at CBFβ or RUNX1 genes (100), and siRNA knockdown of RUNX2 in OS cells increases sensitivity to Doxorubicin (101). Pharmacological inhibition of interaction of CBFβ with the RUNX proteins has been explored in leukemia and

breast cancer (102,103) and inhibition of CBFβ-RUNX2 interaction has been proposed as a novel therapeutic target in osteosarcoma (104).

Structural Biology of RUNX2

RUNX proteins are typified by the Runt homology domain (RHD) (105), a conserved domain key in their interaction with DNA (106). Located close to the N terminus, this domain contains the PyGPyGGTPy consensus sequence, which is essential for their binding with DNA as well as CBFβ (107). Next to the RHD is the glutamine-alanine (QA) repeat region, important in transactivation (108). The nuclear localization signal (NLS), a sequence of nine amino acids next to the RHD, governs translocation of RUNX proteins between cytoplasmic and nuclear compartments (67), and RUNX2 is predominantly found in the nucleus (109). The C-terminus of RUNX2 is also crucial in RUNX2 function, with deletion of the C-terminus phenocopying that of RUNX2 null and resulting in complete bone loss (110,111). Within the C-terminus lies the proline-serine-threonine-rich (PST) region, which possesses both transactivatory and transinhibitory functions (67,111). The matrix targeting signal (NMTS) can be found within the PST region, and works together with the NLS to govern RUNX2 nuclear localization (112). The final five amino acids within the PST region, known as VWRPY, function as a transcriptional repression domain (113,114).

Regulation of RUNX2 and CBFβ Activity

Numerous proteins and processes are implicated in regulation of RUNX2 expression and activity. In terms of expression level, RUNX2 levels are controlled by a combination of

acetylation, deacetylation, and ubiquitination (115). RUNX2 levels normally oscillate with the cell cycle, but this oscillation is disrupted in OS cells (116) due to de-regulation of proteolytic degradation (117). The regulation of RUNX2 with the cell cycle is thought to be mediated by cdc2-mediated phosphorylation of RUNX2, and RUNX2 has been implicated in entry in and exit out of cell cycle phases G2/M (118).

RUNX2 is normally degraded by the proteasome, however under stressful conditions it can also be trafficked to the lysosome by SOX9 (119). SMURF1, an E3 ligase, has been reported to regulate RUNX2 levels (120,121), and RUNX2 levels are also regulated by the CK2/HAUSP pathway (122). HDAC4/5 deacetylate RUNX2, allowing Smurf1-mediated degradation of RUNX2 to take place (115), and Akt enhances the stability of RUNX2 by regulating Smurf1 (123). WW domain-containing oxidoreductase (WWOX) has been implicated as a suppressor of RUNX2 levels and activity (124), and through this mechanism may determine the aggressive phenotype of OS (125). Hes1 stabilizes RUNX2 (126), and CBFβ has also been reported to also stabilize the RUNX proteins (127). According to published data, binding of CBFβ to RUNX proteins and subsequent protection from degradation is less pronounced in RUNX2 than in RUNX1 or RUNX3, possibly due to it binding RUNX2 with lower affinity (128). Hif-2α has been proposed to compete with CBFβ for interaction with RUNX2, and thereby downregulate RUNX2 activity via removing stabilization by CBFβ (129).

As the canonical role of CBFβ is that of a co-activator to the RUNX proteins, little is published about the regulation of CBFβ activity specifically. While RUNX2 levels oscillate during the cell cycle in healthy cells, levels of CBFβ remain more consistent (117). CBFβ can be found in both the nucleus and the cytoplasm (130), but cannot freely move between compartments on its own. CBFβ does not possess a nuclear localization signal (NLS) (131,132) and is carried into the

nucleus via piggybacking onboard the RUNX proteins (130,133). Binding of CBFβ to Filamin A prevents binding to the RUNX proteins, and thereby retains it in the cytoplasm (134). Subcellular localization of CBFβ has also been postulated to involve CRLZ-1 (also known as SAS10 or UTP3) which interacts with CBFβ (135) and may play a role in nuclear shuttling (136,137) and OS development at large (138).

As it stands today, the heterogeneity of OS patient tumors remains a significant hurdle in developing therapies to treat this population (43). In order for the wide array of mutations in OS to manifest as advantageous to cancer cells, these mutated genes must be expressed as protein. Targeting protein translation has been proposed as a way of overcoming tumor heterogeneity, as protein translation acts as a convergence point of multiple signaling pathways (139). A useful approach, in theory, would be to affect this mechanism in such a way that is preferential towards proteins implicated in cancer, so as to avoid inhibiting translation of beneficial proteins and thereby injuring healthy cells. Recently, CBFβ has been proposed to participate in protein translation (130), which may provide a new mechanism to affect protein translation in OS.

Protein Translation

Overview

Proteins are translated by two main mechanisms; cap-dependent, and cap-independent translation. Cap-independent translation relies on an internal ribosomal entry site (IRES), and is utilized under conditions where cap-dependent translation is compromised (140–142). These conditions include endoplasmic reticulum (ER) stress, hypoxia, mitosis, or nutrient limitation, and mRNAs containing IRES elements often encode proteins which are involved in recovering from

or maintaining function during these states (143). Outside of these conditions, cap-dependent translation is by far the most commonly used, and is estimated to be employed in the translation of ~95% of total cellular mRNAs (144). RUNX2, like most proteins in the cell, is expressed via cap-dependent translation under normal conditions (145), however it may rely on IRES-mediated cap-independent translation during cellular stress (146).

Cap-dependent translation is used in the expression of mRNAs with highly structured 5' un-translated regions (UTR's), as these structures must be broken down to allow ribosomes to bind to mRNA and begin protein translation (147,148). During cap-dependent translation initiation, Eukaryotic Translation Initiation Factor 4E (eIF4E) binds to the 7-methylguanosine (m7G) cap of mRNA's and initiates assembly of the translation initiation complex and subsequent direction of ribosomes to mRNA. Following binding of eIF4E, eIF4G binds and stabilizes eIF4E at the 5' cap (149). This is followed by binding of eIF4A, a helicase which unwinds 5' UTR structures (150). Together, these proteins comprise the eIF4F translation initiation complex (TIC). Although least abundant of the translation initiation factors, eIF4E is indispensable to this process as recruitment of complex proteins to the m7G cap is the rate-limiting step of the translation process (151).

Also important in cap-dependent translation are eIF4E binding proteins (4E-BPs), proteins which bind to eIF4E and function to inhibit protein translation (149,152). 4E-BPs are regulated by the mechanistic target of rapamycin complex 1 (mTORC1), which causes their phosphorylation. These proteins compete with eIF4G for a binding site on eIF4E, and phosphorylation of 4E-BPs prevents their interaction with eIF4E (152). 4E-BPs are important in translational regulation, and some repress translation of a large range of transcripts while others are restricted to smaller subsets of mRNAs by also associating with RNA binding proteins (153).

Cap-Dependent Translation in Cancer

Cap-dependent translation has garnered interest in the context of cancer, and is employed in the translation of many oncogenes implicated in OS such as MYC, Fibroblast Growth Factor 2 (FGF-2), Platelet Derived Growth Factor (PDGF), Vascular Endothelial Growth Factor (VEGF), Survivin and cyclins (154). In fact, nearly all potentially oncogenic pathways intersect at the eIF4F complex (155,156), and cap-dependent translation is commonly upregulated in most human malignancies (147). In addition to the machinery of the cap-dependent complex being essential to synthesis of many identified oncogenes (154), de-regulated expression patterns in the translation components themselves have also been implicated in OS, and cancer in general.

eIF4E expression is elevated in OS cell lines and patient samples compared to nonmalignant control cell lines and healthy bone tissue (157,158), and is further elevated in OS patients harboring distant metastases compared to those with local disease (158). This correlation between eIF4E expression and poor outcome was challenged by another study (159), although these data relied upon a four point scale of expression level rather than a more quantitative metric such as western blotting or qRT-PCR. As eIF4E is expressed at a low level, and this protein is the rate-limiting factor for translation initiation, a small shift in its expression could have drastic effects on translation activity. Importantly, an increase in quantity or activity of eIF4E does not necessarily lead to globally elevated protein translation, but rather an increase in translation of a subset of mRNAs (153). This subset includes mRNAs possessing extensive secondary structure (160) and oncogenes of particular interest in OS such as MYC, FGF and VEGF (161,162). Additionally, 4E-BPs, the negative regulators of eIF4E and therefore protein translation, are reported to exert tumor suppressive activity (163), further implicating the EIF4F complex in cancer.

Therapeutic targeting of members of the cap-dependent translational complex has shown encouraging results in OS, although the total number of studies are limited. When used in conjunction with conventional chemotherapeutics or as solo therapies, small molecule inhibitors (157) or micro RNA's (158) affecting eIF4E have shown promising data in decreasing OS cell proliferation, migration, and invasion *in vitro* and *in vivo*. Positive results have also been shown in OS by inhibitors targeting eIF4A (164,165), the helicase responsible for unwinding 5' UTR mRNA secondary structures. Additionally, use of rapamycin has demonstrated effectiveness as an inhibitor of metastasis of OS cells *in vivo* by interrupting mRNA translation (166).

Numerous papers mention that despite decades of research revealing much of the mechanism of protein translation in eukaryotes, our understanding of this process as a whole remains incomplete (167). Recently, Malik et al put forth evidence from breast cancer cells reporting that CBFβ may perform a noncanonical role, as a regulator of cap-dependent protein translation (130). CBFβ reportedly exerts this role by binding to mRNA's via hnRNPK, a multifunctional protein which participates in transcription and translation, and enhances the translation of these mRNA's through eIF4B (130). Additionally, CBFβ interaction with RUNX proteins or hnRNPK may be mutually exclusive, since cytoplasmic CBFβ did not bind to RUNX1, and nuclear CBFβ did not bind to hnRNPK, although all three proteins were present in both the nucleus and cytoplasm (130). CBFβ performs its transcriptional role in the nucleus of the cell, while this translational role is reported to occur in the cytoplasm, suggesting that shuttling of CBFβ into the nucleus by the RUNX proteins (131) could in some way alter its activity in the cytoplasm. If CBFβ also regulates cap-dependent protein translation in OS cells, this could provide a new therapeutic target to affect protein translation in OS. As protein translation acts as a convergence

point of multiple signaling pathways (168), targeting CBFβ could allow a mechanism to overcome the high degree of heterogeneity among OS patient tumors (43).

Project Rationale and Justification

OS is a highly heterogeneic cancer type, making development of targeted therapies challenging. Enhancing our understanding of mechanisms to overcome OS patient heterogeneity could greatly advance OS therapeutic development, and targeting protein translation has been put forth as one method of accomplishing this. Protein translation is an indispensable process in cells, and decades of research into this process have provided an understanding of the machinery which regulates and facilitates this process. Recent reports of CBFβ performing a non-canonical role, as a regulator of protein translation, are intriguing as they may represent a new target through which protein translation could be affected. Thus far, this noncanonical role of CBFβ has only been observed in breast cancer cells, and many questions still remain in understanding the broad and specific impacts of this role. This dissertation aims to study whether CBFβ also performs this role in OS cells, and to elucidate the significance of this role in the context of OS at large. In generating CBFβ knockout cell lines, we noticed a decrease in RUNX2 protein expression, similar to the CBFβ knockout-induced decrease in RUNX1 expression observed in breast cancer cells. We hypothesized that CBFβ may regulate RUNX2 levels in a post-transcriptional manner, and loss of CBFβ may cause alterations in protein translation within the cell. This hypothesis is tested in **Chapter 2 (CBFβ regulates RUNX2 protein levels in osteosarcoma cells)**. This chapter evaluates changes in RUNX2 expression induced by loss of CBFβ via qPCR and western blotting, and studies whether re-introduction of CBFβ can rescue low RUNX2 levels. Next, it utilizes western blotting coupled with proteasome and translation inhibitors to study potential changes in

RUNX2 stability brought about by loss of CBFβ. Finally, this chapter describes the influence of CBFβ loss on global protein translation, and investigates a potential interaction with hnRNPK that underpins this novel role of CBFβ in breast cancer cells.

Based upon the results obtained from Chapter 2, we next attempted to interrupt the binding of CBFβ to RUNX2. Previous data had suggested stabilization of RUNX2 by interaction with CBFβ did not fully explain the reduction in RUNX2 protein level, but we could not rule stabilization out as contributing somewhat to this reduction. Additionally, as interaction of CBFβ with RUNX proteins or hnRNPK may be mutually exclusive and occur in separate cellular compartments (130), it's possible the translational and transcriptional roles of CBFβ are in some way antagonistic. Possible competition for the existing pool of CBFβ taking place between RUNX proteins and hnRNPK would make individual study of each role challenging. Furthermore, knockout of one of the RUNX proteins leads to compensatory up-regulation in other members of the RUNX family (169,170). Due to these confounding effects, we opted to generate a mutant form of CBFβ, with inhibited RUNX protein binding, and use this as a tool to further study the translational role of CBFβ. This is tested in **Chapter 3 (Mutations in the RUNX2 binding pocket of CBFβ alter its cellular activity in osteosarcoma cells)**. This chapter details recombinant protein studies used to validate residues of CBFβ key in RUNX2 interaction, and subsequently generate a mutant form of CBFβ incorporating mutations at these residues. Following this, we re-introduced our mutant back into CBFβ knockout cells, and used western blotting, cellular electro-thermal shift assay (CETSA), and nuclear and cytoplasmic fractionation to understand the influence of our mutations on the behavior of CBFβ in OS cells. We demonstrate that CBFβ residues G61, N63, and N104 are important for interaction with RUNX2, and mutation of these residues to alanine results in decreased interaction with RUNX2. Additionally, we showcase that

this reduced interaction with RUNX2 prevents shuttling of CBFβ into the nucleus. Finally, we demonstrate that re-introduction of our mutant form of CBFβ into CBFβ knockout cells was unable to recover low RUNX2 protein expression. This could be due to decreased stability of RUNX2 as a result of inhibited CBFβ binding, or perhaps that these same residues utilized for RUNX2 binding are also important for the translational role of CBFβ, and through this role CBFβ stimulates production of RUNX2 protein.

Up until this point, we had demonstrated that CBFβ regulates RUNX2 expression in a post-transcriptional manner, and loss of CBFβ leads to reduced global protein translation. Furthermore, we had validated residues of CBFβ key in interaction with RUNX2, which led to the generation of a CBFβ mutant with reduced RUNX2 binding which can be used as a tool in future studies. With encouraging data thus far, we had two main questions: 1) which proteins does CBFβ interact with in performance of this noncanonical role? and 2) which genes/proteins are under the translational purview of CBFβ? Data generation until this point had been in a targeted manner, measuring RUNX2 specifically, but in our quest to reveal the full scope of CBFβ approaches casting a wider net were needed. **Chapter 4 (Profiling the interactome and translatome of CBFβ in osteosarcoma cells)** delves into these questions, describing our findings using more comprehensive assays. We utilized immunoprecipitation mass spectrometry (IP-MS) of CBFβ, both wild-type (WT) and mutant (3xMut), to reveal specific interactors of CBFβ, and understand which of these are dependent upon G61, N63, and/or N104 residues of CBFβ for this interaction. IP-MS followed by gene ontology (GO) revealed CBFβ to potentially interact with many proteins associated with protein translation, the vast majority of which have not been previously reported. We next used direct detection of biotinylated proteins (DiDBiT) and Ribo-Seq to understand which proteins experience an increase in transcription, translation, overall production, and translational

buffering in the presence of CBFβ. Encouragingly, not only did these assays identify a multitude of proteins under the translational purview of CBFβ, these proteins demonstrated high enrichment of terms and pathways linked to cancer such as Rho GTPase-associated proteins, VEGF signaling, PD-L1 and MAPK, as well as enrichment of the specific term “pathways in cancer”.

This dissertation has two main goals: the first is to expand our understanding of the interplay between loss of CBFβ and reduction in RUNX2 protein expression, and whether this suggests CBFβ involvement in a post-transcriptional mechanism. The second goal is to investigate this post-transcriptional mechanism, and gain insight into what proteins CBFβ interacts with, and regulates, in OS cells.

References

1. Hagleitner MM, De Bont ESJM, Te Loo DMWM. Survival Trends and Long-Term Toxicity in Pediatric Patients with Osteosarcoma. Sarcoma. 2012;2012:1–5.
2. Mirabello L, Troisi RJ, Savage SA. Osteosarcoma incidence and survival rates from 1973 to 2004: Data from the Surveillance, Epidemiology, and End Results Program. Cancer. 2009 Apr;115(7):1531–43.
3. Duggan MA, Anderson WF, Altekruse S, Penberthy L, Sherman ME. The Surveillance, Epidemiology, and End Results (SEER) Program and Pathology: Toward Strengthening the Critical Relationship. American Journal of Surgical Pathology. 2016 Dec;40(12):e94–102.
4. Ottaviani G, Jaffe N. The Epidemiology of Osteosarcoma. In: Jaffe N, Bruland OS, Bielack S, editors. Pediatric and Adolescent Osteosarcoma [Internet]. Boston, MA: Springer US; 2010. p. 3–13. Available from: https://doi.org/10.1007/978-1-4419-0284-9_1
5. Bhattasali O, Vo AT, Roth M, Geller D, Randall RL, Gorlick R, et al. Variability in the reported management of pulmonary metastases in osteosarcoma. Cancer Medicine. 2015;4(4):523–31.
6. Hagleitner MM, De Bont ESJM, Te Loo DMWM. Survival trends and long-term toxicity in pediatric patients with osteosarcoma. Sarcoma. 2012;2012.
7. Bruland ØS, Høifødt H, Sæter G, Smeland S, Fodstad Ø. Hematogenous Micrometastases in Osteosarcoma Patients. Clinical Cancer Research. 2005 Jul 1;11(13):4666–73.
8. Meyers PA, Schwartz CL, Krailo M, Kleinerman ES, Betcher D, Bernstein ML, et al. Osteosarcoma: A randomized, prospective trial of the addition of ifosfamide and/or muramyl tripeptide to cisplatin, doxorubicin, and high-dose methotrexate. Journal of Clinical Oncology. 2005;23(9):2004–11.
9. Mialou V, Philip T, Kalifa C, Perol D, Gentet JC, Marec-Berard P, et al. Metastatic osteosarcoma at diagnosis: Prognostic factors and long-term outcome - The French pediatric experience. Cancer. 2005;104(5):1100–9.
10. Jaffe N, Puri A, Gelderblom H. Osteosarcoma: Evolution of treatment paradigms. Sarcoma. 2013;2013.
11. Eilber F, Giuliano A, Eckardt J, Patterson K, Moseley S, Goodnight J. Adjuvant chemotherapy for osteosarcoma: a randomized prospective trial. J Clin Oncol. 1987 Jan;5(1):21–6.
12. Marcove RC, Miké V, Hajek JV, Levin AG, Hutter RV. Osteogenic sarcoma under the age of twenty-one. A review of one hundred and forty-five operative cases. J Bone Joint Surg Am. 1970 Apr;52(3):411–23.
13. Yu D, Zhang S, Feng A, Xu D, Zhu Q, Mao Y, et al. Methotrexate, doxorubicin, and cisplatinum regimen is still the preferred option for osteosarcoma chemotherapy: A meta-analysis and clinical observation. Medicine. 2019 May;98(19):e15582.
14. Patatsos K, Shekhar TM, Hawkins CJ. Pre-clinical evaluation of proteasome inhibitors for canine and human osteosarcoma. Veterinary and Comparative Oncology. 2018;16(4):544–53.
15. Chen Y, Chen H, Xie H, Yuan S, Gao C, Yu L, et al. Non-covalent proteasome inhibitor PI-1840 induces apoptosis and autophagy in osteosarcoma cells. Oncol Rep [Internet]. 2019 Mar 1 [cited 2024 Mar 31]; Available from: http://www.spandidos-publications.com/10.3892/or.2019.7040
16. Shapovalov Y, Benavidez D, Zuch D, Eliseev RA. Proteasome inhibition with bortezomib suppresses growth and induces apoptosis in osteosarcoma. Intl Journal of Cancer. 2010 Jul;127(1):67–76.

17. Lu Y, Zhang J, Chen Y, Kang Y, Liao Z, He Y, et al. Novel Immunotherapies for Osteosarcoma. Front Oncol. 2022 Apr 1;12:830546.
18. Kager L, Pötschger, Bielack. Review of mifamurtide in the treatment of patients with osteosarcoma. TCRM. 2010 Jun;279.
19. Park JA, Cheung NKV. GD2 or HER2 targeting T cell engaging bispecific antibodies to treat osteosarcoma. J Hematol Oncol. 2020 Dec;13(1):172.
20. Kohyama K, Sugiura H, Kozawa E, Wasa J, Yamada K, Nishioka A, et al. Antitumor Activity of an Interleukin-2 Monoclonal Antibody in a Murine Osteosarcoma Transplantation Model. ANTICANCER RESEARCH. 2012;
21. Domingo-Musibay E, Allen C, Kurokawa C, Hardcastle JJ, Aderca I, Msaouel P, et al. Measles Edmonston vaccine strain derivatives have potent oncolytic activity against osteosarcoma. Cancer Gene Ther. 2014 Nov;21(11):483–90.
22. Mochizuki Y, Tazawa H, Demiya K, Kure M, Kondo H, Komatsubara T, et al. Telomerase-specific oncolytic immunotherapy for promoting efficacy of PD-1 blockade in osteosarcoma. Cancer Immunol Immunother. 2021 May;70(5):1405–17.
23. Nastasi N, Pasha A, Bruno G, Subbiani A, Pietrovito L, Leo A, et al. Blockade of IL-10 Signaling Ensures Mifamurtide Efficacy in Metastatic Osteosarcoma. Cancers. 2023 Sep 27;15(19):4744.
24. Mohanty S, Aghighi M, Yerneni K, Theruvath JL, Daldrup-Link HE. Improving the efficacy of osteosarcoma therapy: combining drugs that turn cancer cell 'don't eat me' signals off and 'eat me' signals on. Molecular Oncology. 2019 Oct;13(10):2049–61.
25. Wang J, Hu F, Yu P, Wang J, Liu Z, Bao Q, et al. Sorafenib inhibits doxorubicin-induced PD-L1 upregulation to improve immunosuppressive microenvironment in Osteosarcoma. J Cancer Res Clin Oncol. 2023 Jul;149(8):5127–38.
26. Higuchi T, Yamamoto J, Sugisawa N, Tashiro Y, Nishino H, Yamamoto N, et al. PPARγ Agonist Pioglitazone in Combination With Cisplatinum Arrests a Chemotherapy-resistant Osteosarcoma PDOX Model. Cancer Genomics Proteomics. 2020;17(1):35–40.
27. Wang J, Jin J, Chen T, Zhou Q. Curcumol Synergizes with Cisplatin in Osteosarcoma by Inhibiting M2-like Polarization of Tumor-Associated Macrophages. Molecules. 2022 Jul 6;27(14):4345.
28. Zhang Y, Shen G, Meng T, Lv Z, Li X, Li J, et al. Eicosapentaenoic acid enhances the sensitivity of osteosarcoma to cisplatin by inducing ferroptosis through the DNA-PKcs/AKT/NRF2 pathway and reducing PD-L1 expression to attenuate immune evasion. International Immunopharmacology. 2023 Dec;125:111181.
29. Morrow JJ, Khanna C. Osteosarcoma Genetics and Epigenetics: Emerging Biology and Candidate Therapies. Crit Rev Oncog. 2015;20(3–4):173–97.
30. Sandberg AA, Bridge JA. Updates on the cytogenetics and molecular genetics of bone and soft tissue tumors: osteosarcoma and related tumors. Cancer Genet Cytogenet. 2003 Aug;145(1):1–30.
31. Helman LJ, Meltzer P. Mechanisms of sarcoma development. Nat Rev Cancer. 2003 Sep;3(9):685–94.
32. Spraker-Perlman HL, Barkauskas DA, Krailo MD, Meyers PA, Schwartz CL, Doski J, et al. Factors influencing survival after recurrence in osteosarcoma: A report from the Children's Oncology Group. Pediatr Blood Cancer. 2019 Jan;66(1):e27444.
33. Ferrari S, Briccoli A, Mercuri M, Bertoni F, Cesari M, Longhi A, et al. Late relapse in osteosarcoma. J Pediatr Hematol Oncol. 2006 Jul;28(7):418–22.

34. Bacci G, Briccoli A, Longhi A, Ferrari S, Mercuri M, Faggioli F, et al. Treatment and outcome of recurrent osteosarcoma: experience at Rizzoli in 235 patients initially treated with neoadjuvant chemotherapy. Acta Oncol. 2005;44(7):748–55.
35. De Noon S, Ijaz J, Coorens TH, Amary F, Ye H, Strobl A, et al. MYC amplifications are common events in childhood osteosarcoma. J Pathol Clin Res. 2021 Sep;7(5):425–31.
36. Gelderblom H, Jinks RC, Sydes M, Bramwell VHC, van Glabbeke M, Grimer RJ, et al. Survival after recurrent osteosarcoma: data from 3 European Osteosarcoma Intergroup (EOI) randomized controlled trials. Eur J Cancer. 2011 Apr;47(6):895–902.
37. Hauben EI, Bielack S, Grimer R, Jundt G, Reichardt P, Sydes M, et al. Clinico-histologic parameters of osteosarcoma patients with late relapse. Eur J Cancer. 2006 Mar;42(4):460–6.
38. Kempf-Bielack B, Bielack SS, Jürgens H, Branscheid D, Berdel WE, Exner GU, et al. Osteosarcoma relapse after combined modality therapy: an analysis of unselected patients in the Cooperative Osteosarcoma Study Group (COSS). J Clin Oncol. 2005 Jan 20;23(3):559–68.
39. Hoeijmakers JH. Genome maintenance mechanisms for preventing cancer. Nature. 2001 May 17;411(6835):366–74.
40. Compton DA. Mechanisms of aneuploidy. Curr Opin Cell Biol. 2011 Feb;23(1):109–13.
41. Kops GJPL, Weaver BAA, Cleveland DW. On the road to cancer: aneuploidy and the mitotic checkpoint. Nat Rev Cancer. 2005 Oct;5(10):773–85.
42. Stephens PJ, Greenman CD, Fu B, Yang F, Bignell GR, Mudie LJ, et al. Massive Genomic Rearrangement Acquired in a Single Catastrophic Event during Cancer Development. Cell. 2011 Jan;144(1):27–40.
43. Schiavone K, Garnier D, Heymann MF, Heymann D. The Heterogeneity of Osteosarcoma: The Role Played by Cancer Stem Cells. In: Birbrair A, editor. Stem Cells Heterogeneity in Cancer [Internet]. Cham: Springer International Publishing; 2019 [cited 2022 Nov 9]. p. 187–200. (Advances in Experimental Medicine and Biology; vol. 1139). Available from: https://link.springer.com/10.1007/978-3-030-14366-4_11
44. Hochhaus A, Larson RA, Guilhot F, Radich JP, Branford S, Hughes TP, et al. Long-Term Outcomes of Imatinib Treatment for Chronic Myeloid Leukemia. N Engl J Med. 2017 Mar 9;376(10):917–27.
45. Kantarjian H, Sawyers C, Hochhaus A, Guilhot F, Schiffer C, Gambacorti-Passerini C, et al. Hematologic and cytogenetic responses to imatinib mesylate in chronic myelogenous leukemia. N Engl J Med. 2002 Feb 28;346(9):645–52.
46. Kurzrock R, Gutterman JU, Talpaz M. The molecular genetics of Philadelphia chromosome-positive leukemias. N Engl J Med. 1988 Oct 13;319(15):990–8.
47. Ramalingam SS, Vansteenkiste J, Planchard D, Cho BC, Gray JE, Ohe Y, et al. Overall Survival with Osimertinib in Untreated, EGFR-Mutated Advanced NSCLC. N Engl J Med. 2020 Jan 2;382(1):41–50.
48. Soria JC, Ohe Y, Vansteenkiste J, Reungwetwattana T, Chewaskulyong B, Lee KH, et al. Osimertinib in Untreated EGFR-Mutated Advanced Non-Small-Cell Lung Cancer. N Engl J Med. 2018 Jan 11;378(2):113–25.
49. Park CL, Moria F, Saleh RR. Combination of Osimertinib with Concurrent Chemotherapy and Hormonal Therapy for Synchronous NSCLC, Hormone Receptor-Positive Breast Cancer, and Triple-Negative Breast Cancer: Case Report. Case Rep Oncol. 2023 Dec;16(1):1080–6.
50. Ho AL, Brana I, Haddad R, Bauman J, Bible K, Oosting S, et al. Tipifarnib in Head and Neck Squamous Cell Carcinoma With HRAS Mutations. J Clin Oncol. 2021 Jun 10;39(17):1856–64.

51. Hong DS, Fakih MG, Strickler JH, Desai J, Durm GA, Shapiro GI, et al. KRAS(G12C) Inhibition with Sotorasib in Advanced Solid Tumors. N Engl J Med. 2020 Sep 24;383(13):1207–17.
52. Ostrem JM, Peters U, Sos ML, Wells JA, Shokat KM. K-Ras(G12C) inhibitors allosterically control GTP affinity and effector interactions. Nature. 2013 Nov 28;503(7477):548–51.
53. Hallin J, Engstrom LD, Hargis L, Calinisan A, Aranda R, Briere DM, et al. The KRAS(G12C) Inhibitor MRTX849 Provides Insight toward Therapeutic Susceptibility of KRAS-Mutant Cancers in Mouse Models and Patients. Cancer Discov. 2020 Jan;10(1):54–71.
54. Welsch ME, Kaplan A, Chambers JM, Stokes ME, Bos PH, Zask A, et al. Multivalent Small-Molecule Pan-RAS Inhibitors. Cell. 2017 Feb 23;168(5):878-889.e29.
55. Krönke J, Udeshi ND, Narla A, Grauman P, Hurst SN, McConkey M, et al. Lenalidomide Causes Selective Degradation of IKZF1 and IKZF3 in Multiple Myeloma Cells. Science. 2014 Jan 17;343(6168):301–5.
56. Lu G, Middleton RE, Sun H, Naniong M, Ott CJ, Mitsiades CS, et al. The Myeloma Drug Lenalidomide Promotes the Cereblon-Dependent Destruction of Ikaros Proteins. Science. 2014 Jan 17;343(6168):305–9.
57. Hansen JD, Correa M, Nagy MA, Alexander M, Plantevin V, Grant V, et al. Discovery of CRBN E3 Ligase Modulator CC-92480 for the Treatment of Relapsed and Refractory Multiple Myeloma. J Med Chem. 2020 Jul 9;63(13):6648–76.
58. Chapman MA, Lawrence MS, Keats JJ, Cibulskis K, Sougnez C, Schinzel AC, et al. Initial genome sequencing and analysis of multiple myeloma. Nature. 2011 Mar 24;471(7339):467–72.
59. Lohr JG, Stojanov P, Carter SL, Cruz-Gordillo P, Lawrence MS, Auclair D, et al. Widespread genetic heterogeneity in multiple myeloma: implications for targeted therapy. Cancer Cell. 2014 Jan 13;25(1):91–101.
60. Shi C, Zhang H, Wang P, Wang K, Xu D, Wang H, et al. PROTAC induced-BET protein degradation exhibits potent anti-osteosarcoma activity by triggering apoptosis. Cell Death Dis. 2019 Oct 25;10(11):815.
61. Wysokinski D, Pawlowska E, Blasiak J. RUNX2: A Master Bone Growth Regulator That May Be Involved in the DNA Damage Response. DNA and Cell Biology. 2015 May;34(5):305–15.
62. Adya N, Castilla LH, Liu PP. Function of CBFβ/Bro proteins. Seminars in Cell & Developmental Biology. 2000 Oct;11(5):361–8.
63. Kagoshima H, Shigesada K, Satake M, Ito Y, Miyoshi H, Ohki M, et al. The Runt domain identifies a new family of heteromeric transcriptional regulators. Trends Genet. 1993 Oct;9(10):338–41.
64. Komori T, Yagi H, Nomura S, Yamaguchi A, Sasaki K, Deguchi K, et al. Targeted Disruption of Cbfa1 Results in a Complete Lack of Bone Formation owing to Maturational Arrest of Osteoblasts.
65. Kobayashi H, Gao Y hao, Ueta C, Yamaguchi A, Komori T. Multilineage Differentiation of Cbfa1-Deficient Calvarial Cells in Vitro. Biochemical and Biophysical Research Communications. 2000 Jul;273(2):630–6.
66. Jeong J, Jin J, Kim H, Kang S, Liu JC, Lengner CJ, et al. Expression of Runx2 transcription factor in non-skeletal tissues, sperm and brain. Journal Cellular Physiology. 2008 Nov;217(2):511–7.

67. Cohen Jr. MM. Perspectives on RUNX genes: An update. American J of Med Genetics Pt A. 2009 Dec;149A(12):2629–46.
68. Warren AJ, Williams RL, Rabbitts TH. Structural basis for the heterodimeric interaction between the acute leukaemia-associated transcription factors AML1 and CBFb.
69. Yoshida CA, Furuichi T, Fujita T, Fukuyama R, Kanatani N, Kobayashi S, et al. Core-binding factor β interacts with Runx2 and is required for skeletal development. Nat Genet. 2002 Dec;32(4):633–8.
70. Kundu M, Javed A, Jeon JP, Horner A, Shum L, Eckhaus M, et al. Cbfβ interacts with Runx2 and has a critical role in bone development. Nat Genet. 2002 Dec;32(4):639–44.
71. Sasaki K, Yagi H, Bronson RT, Tominaga K, Matsunashi T, Deguchi K, et al. Absence of fetal liver hematopoiesis in mice deficient in transcriptional coactivator core binding factor beta. Proc Natl Acad Sci U S A. 1996 Oct 29;93(22):12359–63.
72. Wang Q, Stacy T, Miller JD, Lewis AF, Gu TL, Huang X, et al. The CBFbeta subunit is essential for CBFalpha2 (AML1) function in vivo. Cell. 1996 Nov 15;87(4):697–708.
73. Martin JW, Zielenska M, Stein GS, Van Wijnen AJ, Squire JA. The Role of RUNX2 in Osteosarcoma Oncogenesis. Sarcoma. 2011;2011:1–13.
74. Nathan SS, Pereira BP, Zhou Y fang, Gupta A, Dombrowski C, Soong R, et al. Elevated expression of Runx2 as a key parameter in the etiology of osteosarcoma. Mol Biol Rep. 2009 Jan;36(1):153–8.
75. Sadikovic B, Thorner P, Chilton-MacNeill S, Martin JW, Cervigne NK, Squire J, et al. Expression analysis of genes associated with human osteosarcoma tumors shows correlation of RUNX2 overexpression with poor response to chemotherapy. BMC Cancer. 2010 Dec;10(1):202.
76. Feng Y, Liao Y, Zhang J, Shen J, Shao Z, Hornicek F, et al. Transcriptional activation of CBFβ by CDK11p110 is necessary to promote osteosarcoma cell proliferation. Cell Commun Signal. 2019 Dec;17(1):125.
77. Bajpai J, Sharma M, Sreenivas V, Kumar R, Gamnagatti S, Khan SA, et al. VEGF expression as a prognostic marker in osteosarcoma. Pediatric Blood & Cancer. 2009 Dec;53(6):1035–9.
78. Han J, Yong B, Luo C, Tan P, Peng T, Shen J. High serum alkaline phosphatase cooperating with MMP-9 predicts metastasis and poor prognosis in patients with primary osteosarcoma in Southern China. World J Surg Onc. 2012 Dec;10(1):37.
79. Zelzer E, Glotzer DJ, Hartmann C, Thomas D, Fukai N, Soker S, et al. Tissue specific regulation of VEGF expression during bone development requires Cbfa1/Runx2. Mechanisms of Development. 2001;
80. Kwon TG, Zhao X, Yang Q, Li Y, Ge C, Zhao G, et al. Physical and functional interactions between Runx2 and HIF-1α induce vascular endothelial growth factor gene expression. J Cell Biochem. 2011 Dec;112(12):3582–93.
81. Weng J jie, Su Y. Nuclear matrix-targeting of the osteogenic factor Runx2 is essential for its recognition and activation of the alkaline phosphatase gene. Biochimica et Biophysica Acta (BBA) - General Subjects. 2013 Mar;1830(3):2839–52.
82. Pratap J, Javed A, Languino LR, Van Wijnen AJ, Stein JL, Stein GS, et al. The Runx2 Osteogenic Transcription Factor Regulates Matrix Metalloproteinase 9 in Bone Metastatic Cancer Cells and Controls Cell Invasion. Molecular and Cellular Biology. 2005 Oct 1;25(19):8581–91.

83. Matheny CJ, Speck ME, Cushing PR, Zhou Y, Corpora T, Regan M, et al. Disease mutations in RUNX1 and RUNX2 create nonfunctional, dominant-negative, or hypomorphic alleles. EMBO J. 2007 Feb 21;26(4):1163–75.
84. Jensen BL, Kreiborg S. Development of the dentition in cleidocranial dysplasia. J Oral Pathol Med. 1990 Feb;19(2):89–93.
85. Feldman GJ, Robin NH, Brueton LA, Robertson E, Thompson EM, Siegel-Bartelt J, et al. A gene for cleidocranial dysplasia maps to the short arm of chromosome 6. Am J Hum Genet. 1995 Apr;56(4):938–43.
86. Liu D, Liu Y, Zhang X, Wang Y, Zhang C, Zheng S. An Exploration of Mutagenesis in a Family with Cleidocranial Dysplasia without RUNX2 Mutation. Front Genet. 2021 Oct 19;12:748111.
87. Motaei J, Salmaninejad A, Jamali E, Khorsand I, Ahmadvand M, Shabani S, et al. Molecular Genetics of Cleidocranial Dysplasia. Fetal and Pediatric Pathology. 2021 Oct 6;40(5):442–54.
88. Berkay EG, Elkanova L, Kalaycı T, Uludağ Alkaya D, Altunoğlu U, Cefle K, et al. Skeletal and molecular findings in 51 Cleidocranial dysplasia patients from Turkey. Am J Med Genet A. 2021 Aug;185(8):2488–95.
89. Han M, Kim H, Wee H, Lim K, Park N, Bae S, et al. The cleidocranial dysplasia-related R131G mutation in the Runt-related transcription factor RUNX2 disrupts binding to DNA but not CBF-β. J of Cellular Biochemistry. 2010 May;110(1):97–103.
90. Beyltjens T, Boudin E, Revencu N, Boeckx N, Bertrand M, Schütz L, et al. Heterozygous pathogenic variants involving CBFB cause a new skeletal disorder resembling cleidocranial dysplasia. J Med Genet. 2023 May;60(5):498–504.
91. Rubnitz JE, Pui CH. Molecular diagnostics in the treatment of leukemia. Curr Opin Hematol. 1999 Jul;6(4):229–35.
92. Duployez N, Marceau-Renaut A, Boissel N, Petit A, Bucci M, Geffroy S, et al. Comprehensive mutational profiling of core binding factor acute myeloid leukemia. Blood. 2016 May 19;127(20):2451–9.
93. Lukasik SM, Zhang L, Corpora T, Tomanicek S, Li Y, Kundu M, et al. Altered affinity of CBFβ-SMMHC for Runx1 explains its role in leukemogenesis. Nat Struct Biol. 2002 Sep;9(9):674–9.
94. Liu P, Tarlé SA, Hajra A, Claxton DF, Marlton P, Freedman M, et al. Fusion between transcription factor CBF beta/PEBP2 beta and a myosin heavy chain in acute myeloid leukemia. Science. 1993 Aug 20;261(5124):1041–4.
95. Ellis MJ, Ding L, Shen D, Luo J, Suman VJ, Wallis JW, et al. Whole-genome analysis informs breast cancer response to aromatase inhibition. Nature. 2012 Jun;486(7403):353–60.
96. Banerji S, Cibulskis K, Rangel-Escareno C, Brown KK, Carter SL, Frederick AM, et al. Sequence analysis of mutations and translocations across breast cancer subtypes. Nature. 2012 Jun 21;486(7403):405–9.
97. Zeng H, Xu X. RUNX2 RNA interference inhibits the invasion of osteosarcoma. Oncology Letters. 2015 Jun;9(6):2455–8.
98. Kim MS, Gernapudi R, Choi EY, Lapidus RG, Passaniti A. Characterization of CADD522, a small molecule that inhibits RUNX2-DNA binding and exhibits antitumor activity. Oncotarget. 2017 Sep 19;8(41):70916–40.

99. Zhou N, Gutierrez-Uzquiza A, Zheng XY, Chang R, Vogl DT, Garfall AL, et al. RUNX proteins desensitize multiple myeloma to lenalidomide via protecting IKZFs from degradation. Leukemia. 2019 Aug;33(8):2006–21.
100. Cunningham L, Finckbeiner S, Hyde RK, Southall N, Marugan J, Yedavalli VRK, et al. Identification of benzodiazepine Ro5-3335 as an inhibitor of CBF leukemia through quantitative high throughput screen against RUNX1–CBFβ interaction. Proc Natl Acad Sci USA. 2012 Sep 4;109(36):14592–7.
101. Roos A, Satterfield L, Zhao S, Fuja D, Shuck R, Hicks MJ, et al. Loss of Runx2 sensitises osteosarcoma to chemotherapy-induced apoptosis. Br J Cancer. 2015 Nov;113(9):1289–97.
102. Illendula A, Gilmour J, Grembecka J, Tirumala VSS, Boulton A, Kuntimaddi A, et al. Small Molecule Inhibitor of CBFβ-RUNX Binding for RUNX Transcription Factor Driven Cancers. EBioMedicine. 2016 Jun;8:117–31.
103. Mendoza-Villanueva D, Deng W, Lopez-Camacho C, Shore P. The Runx transcriptional co-activator, CBFβ, is essential for invasion of breast cancer cells. Mol Cancer. 2010 Dec;9(1):171.
104. Alegre F, Ormonde AR, Godinez DR, Illendula A, Bushweller JH, Wittenburg LA. The interaction between RUNX2 and core binding factor beta as a potential therapeutic target in canine osteosarcoma. Vet Comparative Oncology. 2020 Mar;18(1):52–63.
105. Braun T, Woollard A. RUNX factors in development: Lessons from invertebrate model systems. Blood Cells, Molecules, and Diseases. 2009 Jul;43(1):43–8.
106. Gergen JP, Butler BA. Isolation of the Drosophila segmentation gene runt and analysis of its expression during embryogenesis. Genes Dev. 1988 Sep;2(9):1179–93.
107. Chuang LSH, Ito K, Ito Y. RUNX family: Regulation and diversification of roles through interacting proteins. Intl Journal of Cancer. 2013 Mar 15;132(6):1260–71.
108. Zeng L, Wei J, Zhao N, Sun S, Wang Y, Feng H. A novel 18-bp in-frame deletion mutation in RUNX2 causes cleidocranial dysplasia. Arch Oral Biol. 2018 Dec;96:243–8.
109. Lu J, Maruyama M, Satake M, Bae SC, Ogawa E, Kagoshima H, et al. Subcellular Localization of the a and b Subunits of the Acute Myeloid Leukemia-Linked Transcription Factor PEBP2/CBF. MOL CELL BIOL. 1995;15.
110. Komori T. Roles of Runx2 in Skeletal Development. Adv Exp Med Biol. 2017;962:83–93.
111. Liu TM, Lee EH. Transcriptional regulatory cascades in Runx2-dependent bone development. Tissue Eng Part B Rev. 2013 Jun;19(3):254–63.
112. Young DW, Zaidi SK, Furcinitti PS, Javed A, Van Wijnen AJ, Stein JL, et al. Quantitative signature for architectural organization of regulatory factors using intranuclear informatics. Journal of Cell Science. 2004 Oct 1;117(21):4889–96.
113. Aronson BD, Fisher AL, Blechman K, Caudy M, Gergen JP. Groucho-Dependent and -Independent Repression Activities of Runt Domain Proteins. Molecular and Cellular Biology. 1997 Sep 1;17(9):5581–7.
114. Imai Y, Kurokawa M, Tanaka K, Friedman AD, Ogawa S, Mitani K, et al. TLE, the Human Homolog of Groucho, Interacts with AML1 and Acts as a Repressor of AML1-Induced Transactivation. Biochemical and Biophysical Research Communications. 1998 Nov;252(3):582–9.
115. Jeon EJ, Lee KY, Choi NS, Lee MH, Kim HN, Jin YH, et al. Bone Morphogenetic Protein-2 Stimulates Runx2 Acetylation. Journal of Biological Chemistry. 2006 Jun;281(24):16502–11.
116. Galindo M, Pratap J, Young DW, Hovhannisyan H, Im HJ, Choi JY, et al. The Bone-specific Expression of Runx2 Oscillates during the Cell Cycle to Support a G1-related

Antiproliferative Function in Osteoblasts. Journal of Biological Chemistry. 2005 May;280(21):20274–85.
117. San Martin IA, Varela N, Gaete M, Villegas K, Osorio M, Tapia JC, et al. Impaired cell cycle regulation of the osteoblast-related heterodimeric transcription factor Runx2-Cbfβ in osteosarcoma cells. Journal of Cellular Physiology. 2009;221(3):560–71.
118. Qiao M, Shapiro P, Fosbrink M, Rus H, Kumar R, Passaniti A. Cell Cycle-dependent Phosphorylation of the RUNX2 Transcription Factor by cdc2 Regulates Endothelial Cell Proliferation. Journal of Biological Chemistry. 2006 Mar;281(11):7118–28.
119. Cheng A, Genever PG. SOX9 determines RUNX2 transactivity by directing intracellular degradation. Journal of Bone and Mineral Research. 2010 Dec 1;25(12):2680–9.
120. Shimazu J, Wei J, Karsenty G. Smurf1 Inhibits Osteoblast Differentiation, Bone Formation, and Glucose Homeostasis through Serine 148. Cell Reports. 2016 Apr;15(1):27–35.
121. Zhao M, Qiao M, Oyajobi BO, Mundy GR, Chen D. E3 Ubiquitin Ligase Smurf1 Mediates Core-binding Factor α1/Runx2 Degradation and Plays A Specific Role in Osteoblast Differentiation. Journal of Biological Chemistry. 2003 Jul;278(30):27939–44.
122. Kim JM, Yang YS, Park KH, Ge X, Xu R, Li N, et al. A RUNX2 stabilization pathway mediates physiologic and pathologic bone formation. Nat Commun. 2020 May 8;11(1):2289.
123. Choi YH, Kim YJ, Jeong HM, Jin YH, Yeo CY, Lee KY. Akt enhances Runx2 protein stability by regulating Smurf2 function during osteoblast differentiation. FEBS J. 2014 Aug;281(16):3656–66.
124. Kurek KC, Del Mare S, Salah Z, Abdeen S, Sadiq H, Lee S hee, et al. Frequent Attenuation of the WWOX Tumor Suppressor in Osteosarcoma Is Associated with Increased Tumorigenicity and Aberrant RUNX2 Expression. Cancer Research. 2010 Jul 1;70(13):5577–86.
125. Del Mare S, Aqeilan RI. Tumor Suppressor WWOX inhibits osteosarcoma metastasis by modulating RUNX2 function. Sci Rep. 2015 Oct;5(1):12959.
126. Suh JH, Lee HW, Lee JW, Kim JB. Hes1 stimulates transcriptional activity of Runx2 by increasing protein stabilization during osteoblast differentiation. Biochemical and Biophysical Research Communications. 2008 Feb;367(1):97–102.
127. Dimerization with PEBP2β protects RUNX1/AML1 from ubiquitin–proteasome-mediated degradation [Internet]. [cited 2024 Mar 31]. Available from: https://www.embopress.org/doi/epdf/10.1093/emboj/20.4.723
128. Qin X, Jiang Q, Matsuo Y, Kawane T, Komori H, Moriishi T, et al. Cbfb Regulates Bone Development by Stabilizing Runx Family Proteins. Journal of Bone and Mineral Research. 2015 Apr 1;30(4):706–14.
129. Che X, Park N, Jin X, Jung Y, Han M, Park CY, et al. Hypoxia-inducible factor 2α is a novel inhibitor of chondrocyte maturation. Journal Cellular Physiology. 2021 Oct;236(10):6963–73.
130. Malik N, Yan H, Moshkovich N, Palangat M, Yang H, Sanchez V, et al. The transcription factor CBFB suppresses breast cancer through orchestrating translation and transcription. Nat Commun. 2019 May 6;10(1):2071.
131. Wang Q, Stacy T, Miller JD, Lewis AF, Gu TL, Huang X, et al. The CBFᴺᒐ Subunit Is Essential for CBF⎵2 (AML1) Function In Vivo.
132. Tahirov TH, Inoue-Bungo T, Morii H, Fujikawa A, Sasaki M, Kimura K, et al. Structural Analyses of DNA Recognition by the AML1/Runx-1 Runt Domain and Its Allosteric Control by CBFᴺᒐ. :13.

133. Khan A, Campbell K, Cameron E, Blyth K. The RUNX/CBFβ Complex in Breast Cancer: A Conundrum of Context. Cells. 2023 Feb 16;12(4):641.
134. Yoshida N, Ogata T, Tanabe K, Li S, Nakazato M, Kohu K, et al. Filamin A-Bound PEBP2␣/CBF␣ Is Retained in the Cytoplasm and Prevented from Functioning as a Partner of the Runx1 Transcription Factor. MOL CELL BIOL. 2005;25:11.
135. Sakuma T, Li QL, Jin Y, Choi LW, Kim EG, Ito K, et al. Cloning and expression pattern of a novel PEBP2b-binding protein (charged amino acid rich leucine zipper-1 [Crl-1]) in the mouse. Mechanisms of Development. 2001;
136. Park SK, Lim JH, Kang CJ. Crlz1 activates transcription by mobilizing cytoplasmic CBFβ into the nucleus. Biochimica et Biophysica Acta (BBA) - Gene Regulatory Mechanisms. 2009 Nov;1789(11–12):702–8.
137. Choi SY, Pi JH, Park SK, Kang CJ. Crlz-1 Controls Germinal Center Reaction by Relaying a Wnt Signal to the Bcl-6 Expression in Centroblasts during Humoral Immune Responses. JI. 2019 Nov 15;203(10):2630–43.
138. Liu B, Zhang Z, Dai EN, Tian JX, Xin JZ, Xu L. Modeling osteosarcoma progression by measuring the connectivity dynamics using an inference of multiple differential modules algorithm. Molecular Medicine Reports. 2017 Feb;16(2):1047–54.
139. Polunovsky VA, Bitterman PB. The Cap-Dependent Translation Apparatus Integrates and Amplifies Cancer Pathways. RNA Biology. 2006 Jan;3(1):10–7.
140. Hellen CUT, Sarnow P. Internal ribosome entry sites in eukaryotic mRNA molecules. Genes Dev. 2001 Jul 1;15(13):1593–612.
141. Balvay L, Rifo RS, Ricci EP, Decimo D, Ohlmann T. Structural and functional diversity of viral IRESes. Biochimica et Biophysica Acta (BBA) - Gene Regulatory Mechanisms. 2009 Sep;1789(9–10):542–57.
142. Jackson RJ, Hellen CUT, Pestova TV. The mechanism of eukaryotic translation initiation and principles of its regulation. Nat Rev Mol Cell Biol. 2010 Feb;11(2):113–27.
143. Mokrejš M, Mašek T, Vopálenský V, Hlubuček P, Delbos P, Pospíšek M. IRESite—a tool for the examination of viral and cellular internal ribosome entry sites. Nucleic Acids Research. 2010 Jan;38(suppl_1):D131–6.
144. Merrick WC. Cap-dependent and cap-independent translation in eukaryotic systems. Gene. 2004 May;332:1–11.
145. Elango N, Li Y, Shivshankar P, Katz MS. Expression of RUNX2 isoforms: Involvement of cap-dependent and cap-independent mechanisms of translation. Journal of Cellular Biochemistry. 2006;99(4):1108–21.
146. Xiao ZS, Simpson LG, Quarles LD. IRES-dependent translational control of Cbfa1/Runx2 expression. Journal of Cellular Biochemistry. 2003;88(3):493–505.
147. De Benedetti A, Graff JR. eIF-4E expression and its role in malignancies and metastases. Oncogene. 2004 Apr 19;23(18):3189–99.
148. Culjkovic-Kraljacic B, Skrabanek L, Revuelta MV, Gasiorek J, Cowling VH, Cerchietti L, et al. The eukaryotic translation initiation factor eIF4E elevates steady-state m7G capping of coding and noncoding transcripts. Proc Natl Acad Sci USA. 2020 Oct 27;117(43):26773–83.
149. Mader S, Lee H, Pause A, Sonenberg N. The Translation Initiation Factor eIF-4E Binds to a Common Motif Shared by the Translation Factor eIF-4gamma and the Translational Repressors 4E-Binding Proteins. MOL CELL BIOL. 1995;15.
150. Pain VM. Initiation of protein synthesis in eukaryotic cells. European Journal of Biochemistry. 1996;236(3):747–71.

151. Duncan R, Milburn SC, Hershey JWB. Regulated Phosphorylation and Low Abundance of HeLa Cell Initiation Factor eIF-4F Suggest a Role in Translational Control. Journal of Biological Chemistry. 1987;262(1):380–8.
152. Gingras AC, Gygi SP, Raught B, Polakiewicz RD, Abraham RT, Hoekstra MF, et al. Regulation of 4E-BP1 phosphorylation: a novel two-step mechanism. Genes & Development. 1999 Jun 1;13(11):1422–37.
153. Richter JD, Sonenberg N. Regulation of cap-dependent translation by eIF4E inhibitory proteins. Nature. 2005 Feb;433(7025):477–80.
154. Bitterman PB, Polunovsky VA. Translational control of cell: Fate from integration of environmental signals to breaching anticancer defense. Cell Cycle. 2012;11(6):1097–107.
155. Robichaud N, Sonenberg N, Ruggero D, Schneider RJ. Translational Control in Cancer. Cold Spring Harb Perspect Biol. 2019 Jul;11(7):a032896.
156. Polunovsky VA, Houghton PJ, editors. mTOR Pathway and mTOR Inhibitors in Cancer Therapy [Internet]. Totowa, NJ: Humana Press; 2010 [cited 2024 Jul 22]. Available from: http://link.springer.com/10.1007/978-1-60327-271-1
157. Chen J, Xu X, Chen J. Clinically relevant concentration of anti-viral drug ribavirin selectively targets pediatric osteosarcoma and increases chemosensitivity. Biochemical and Biophysical Research Communications. 2018;506(3):604–10.
158. Qi NN, Tian S, Li X, Wang FL, Liu B. Up-regulation of microRNA-496 suppresses proliferation, invasion, migration and in vivo tumorigenicity of human osteosarcoma cells by targeting eIF4E. Biochimie. 2019;163:1–11.
159. Osborne TS, Ren L, Healey JH, Shapiro LQ, Chou AJ, Gorlick RG, et al. Evaluation of eIF4E Expression in an Osteosarcoma-Specific Tissue Microarray. Journal of Pediatric Hematology/Oncology. 2011 Oct;33(7):524–8.
160. Koromilas AE, Lazaris-Karatzas A, Sonenberg N. mRNAs containing extensive secondary structure in their 5’ non-coding region translate efficiently in cells overexpressing initiation factor elF-4E.
161. Graff JR, Zimmer SG. Translational control and metastatic progression: enhanced activity of the mRNA cap-binding protein eIF-4E selectively enhances translation of metastasis-related mRNAs. Clin Exp Metastasis. 2003;20(3):265–73.
162. Gingras AC, Raught B, Sonenberg N. eIF4 initiation factors: effectors of mRNA recruitment to ribosomes and regulators of translation. Annu Rev Biochem. 1999;68:913–63.
163. Rousseau D, Gingras AC, Pause A, Sonenberg N. The eIF4E-binding proteins 1 and 2 are negative regulators of cell growth. Oncogene. 1996 Dec 5;13(11):2415–20.
164. Chang LS, Oblinger JL, Burns SS, Huang J, Anderson LW, Hollingshead MG, et al. Targeting Protein Translation by Rocaglamide and Didesmethylrocaglamide to Treat MPNST and Other Sarcomas. Molecular cancer therapeutics. 2020;19(3):731–41.
165. Chang LS, Oblinger JL, Burns SS, Huang J, Anderson LW, Hollingshead MG, et al. Targeting Protein Translation by Rocaglamide and Didesmethylrocaglamide to Treat MPNST and Other Sarcomas. Molecular Cancer Therapeutics. 2020 Mar 1;19(3):731–41.
166. Morrow JJ, Mendoza A, Koyen A, Lizardo MM, Ren L, Waybright TJ, et al. mTOR Inhibition Mitigates Enhanced mRNA Translation Associated with the Metastatic Phenotype of Osteosarcoma Cells *In Vivo*. Clinical Cancer Research. 2016 Dec 15;22(24):6129–41.
167. Gandin V, English BP, Freeman M, Leroux LP, Preibisch S, Walpita D, et al. Cap-dependent translation initiation monitored in living cells. Nat Commun. 2022 Nov 2;13(1):6558.

168. Polunovsky VA, Bitterman PB. The cap-dependent translation apparatus integrates and amplifies cancer pathways. RNA Biology. 2006;3(1):10–7.
169. Kamikubo Y. Genetic compensation of RUNX family transcription factors in leukemia. Cancer Science. 2018 Aug;109(8):2358–63.
170. Morita K, Suzuki K, Maeda S, Matsuo A, Mitsuda Y, Tokushige C, et al. Genetic regulation of the RUNX transcription factor family has antitumor effects. Journal of Clinical Investigation. 2017 May 22;127(7):2815–28.

Chapter 2

CBFβ regulates RUNX2 protein levels in osteosarcoma cells

Abstract

Development of novel therapies to treat OS has lagged behind much of the field of cancer research, due in large part due to the heterogeneity of OS and lack of identified driver mutations. High expression of RUNX2, the master regular of bone growth and differentiation, is implicated in OS, and the transcriptional function of RUNX2 is enhanced by CBFβ. In the process of profiling a CBFβ knockout (KO) cell line developed for another project, we identified a reduction in RUNX2 expression upon loss of CBFβ. We sought to unravel the mechanism underlying this and enhance our understanding of the biology of OS at large. To this end, we evaluated the loss of CBFβ and how this effects RUNX2 mRNA and protein levels, RUNX2 stability, and global protein translation. Additionally, we assessed a protein-protein interaction between CBFβ and hnRNPK previously demonstrated in breast cancer, and proposed to be key to a putative noncanonical role performed by CBFβ. Finally, we conducted a rescue experiment reconstituting CBFβ back into CBFβ KO cells and evaluated alterations to RUNX2 levels. Loss of CBFβ caused a reduction in RUNX2 protein expression, however RUNX2 mRNA levels were unaffected. This decrease in RUNX2 protein levels was not sufficiently explained by a change in RUNX2 stability from loss of its binding partner. CBFβ was confirmed to interact with hnRNPK and loss of CBFβ resulted in a decrease in global protein translation. Lastly, reconstitution of CBFβ into CBFβ KO cells rescued low RUNX2 protein expression. These results together demonstrate that CBFβ may play a role in protein translation in OS, and could present a novel therapeutic target in treatment of this disease.

Introduction

Osteosarcoma (OS) is a highly aggressive primary bone cancer, and the most prevalent of this cancer type in humans and canines (1). OS most frequently presents early in life, affecting primarily children and adolescents (2), which places it in stark contrast to the average age of all cancer diagnoses of 66 years (3). OS Patients presenting with localized disease at time of diagnosis have an estimated 5-year survival rate of 60-80% (4), yet this plummets to ~20% for those presenting with clinically detectable metastases (5,6). Despite numerous advances in the field of cancer research as a whole, the current treatment outlook for osteosarcoma has remained essentially unchanged over the past 30 years (7). The highly aggressive nature of osteosarcoma combined with its early age of presentation and lack of therapeutic advancement represents a critical unmet need in cancer research today.

Core binding factor beta (CBFβ) functions as a binding partner to the RUNX family of DNA-binding transcription factors (RUNX1-3) and acts as a transcriptional co-activator by allosterically increasing their affinity to DNA (8,9) . RUNX2 is known as the master regular of bone growth, playing a critical role in osteoblast proliferation and differentiation (10). In the context of OS, high expression levels of RUNX2 (11,12) or CBFβ (13) have each demonstrated correlation with poor disease prognosis. siRNA knockdown of RUNX2 in OS cells increases sensitivity to Doxorubicin (14) and leads to reduced colony formation and cell invasion (15), while siRNA knockdown of CBFβ in OS cells causes reduced cell proliferation, migration, and invasion (13). RUNX2 modulates the expression of genes such as vascular endothelial growth factor (VEGF) (16,17), alkaline phosphatase (ALP) (18), and matrix metalloproteinase 9 (MMP-9) (19), all of which have also been linked to poor therapeutic outcome in OS (20,21). The array of data

implicating RUNX2 in OS, combined with CBFβ functioning as a co-activator to RUNX2, led to the proposal of the CBFβ-RUNX2 interaction as a novel therapeutic target in OS (22).

This project began in simply studying this interaction, but as additional data was gathered, the scope expanded from studying this interaction to evaluating the roles of CBFβ itself. A recent study in breast cancer proposed a novel role for CBFβ as a regulator of protein translation (23), and as we advanced in profiling our CBFβ KO cell line, our data began to corroborate this possibility in OS as well. Protein translation acts as a convergence point of multiple signaling pathways (24), and modulating this process therapeutically could provide a mechanism to target cancers with wide mutational profiles. This is especially interesting in the context of OS, being one of the most heterogeneic forms of cancer studied (25). These parallels between our data and that in breast cancer inspired us to intensify our focus on investigating if CBFβ performs this non-canonical role in OS, and if so, to what extent does this influence the malignant phenotype of OS overall.

Proteins can be translated via a cap-dependent or cap-independent mechanism, with the former garnering particular interest due to oncogenes identified in OS such as MYC, fibroblast growth factor 2 (FGF-2), platelet derived growth factor (PDGF), vascular endothelial growth factor (VEGF), survivin and cyclins being translated in this manner (26). This has led to research targeting cap-dependent translation in OS (27–29), which is the same pathway CBFβ had been suggested to regulate in breast cancer cells (23). It is important to note that the study of this novel role of CBFβ in breast cancer is still in its infancy, and the overall impact of CBFβ on breast cancer is still a point of contention. Loss of CBFβ transformed breast cancer cells and led to increased tumor formation in one study (23), while loss of CBFβ was found to inhibit formation of metastases in another study (30). While there may not be as much conflict regarding the broad impact of CBFβ

in OS, as high expression is known to correlate with poor overall survival (13,31), there is currently no data available regarding the role of CBFβ in protein translation in OS. This study represents the first of its kind interrogating this novel function, with the goal of enhancing our understanding of OS overall and potentially leading to identification of a novel therapeutic target.

Materials and Methods

Cell Lines and Culture Conditions

Parental U2OS (American Type Culture Collection [ATCC], Manassas, Virginia) and U2OS-derived cell lines were maintained in McCoy's 5A (Iwakata & Grace Modification) media supplemented with 10% FBS (Corning Inc., Glendale, Arizona) and U/mL Penicillin-Streptomycin (P/S) (Corning) at 37C in a humidified atmosphere with 5% CO2 unless otherwise specified. HEK293T cells (ATCC) were maintained in DMEM media (Corning) supplemented with 10% FBS and 1% P/S in the same atmosphere as previously listed cells. Cell populations were maintained in T75 flasks (Corning) and were split twice weekly with Trypsin (Gibco, Thermo Fisher Scientific, Waltham, Massachusetts) upon reaching 70-80% confluence and discarded after 20 passages.

Knockout Generation

CBFβ knockout (KO) cell lines were generated in the parental human U2OS wild-type (wt) cell line. Briefly, the Synthego multi-sgRNA CRISPR/Cas9 ribonucleoprotein complex (Gene Knockout Kit v2, Synthego, Redwood City, CA) was transfected into 80,000 cells with Lipofectamine CRISPRMAX (Invitrogen, Carlsbad, CA) for 24-hours. The media was replaced with fresh supplemented media and cells were incubated for two additional days. A limited dilution (0.8 cells/well) was performed in a 96-well plate format and monitored for individual cells to produced individual colonies that were selected for sequencing. DNA was isolated using a genomic DNA purification kit (Promega, Madison, WI) from each viable clone and was submitted to Genewiz (Azenta Life Sciences, South San Francisco, CA) for Sanger sequencing. Sequencing

trace files were analyzed using the Synthego Interference of CRISPR Edits (ICE) Analysis Tool (Synthego Performance Analysis, ICE Analysis. 2019. v3.0) to determine the transfection efficiency, indel size, and knockout score.

Western Blotting

Lysate Harvesting: Cells were dissociated with Trypsin then quenched by addition of normal growth media. Cell suspension was spun down 500g x 5 min and washed twice in PBS on ice. Pellets were then resuspended in varying amounts of RIPA lysis buffer (50 mM Tris pH 7.5, 150 mM NaCl, 0.1% Triton X-100, 0.50% sodium deoxycholate, 0.1% SDS) supplemented with 1x cOmplete EDTA-free protease inhibitor cocktail (Thermo Fisher Scientific), 2mM NaVO3, 5 mM NaF and 1mM phenylmethylsulfonyl fluoride (PMSF) (all sourced from Sigma-Aldrich, St. Louis, Missouri). Cells were incubated in RIPA buffer on ice for 5 min, passed through a 26 gauge syringe 6x, then vortexed 2,000 rpm for 30 min. at 4C and centrifuged 15,000g for 20 min. at 4C. The pellet was discarded and supernatant was transferred to a fresh tube for BCA analysis.

Protein Content Normalization: Protein content of harvested lysates was analyzed using Bicinchoninic Acid (BCA) Protein Assay Kit (Thermo Fisher Scientific) following manufacturer's recommendations. Assays were read using a Synergy H1 plate reader (Biotek Instruments, Winooski, Vermont) measuring excitation/emission of 560 and 590 nm, respectively. Acceptable calibration curves were defined as those with an R squared value ≥ 0.95. Protein concentration of lysates was normalized by addition of varying volumes of RIPA lysis buffer.

SDS-PAGE: Normalized samples were mixed with NuPage Laemmle Buffer (Thermo Fisher Scientific) and DTT (F. Hoffmann-La Roche AG, Basel, Switzerland) to achieve final

concentrations of 1x Laemmle Buffer and 50 mM DTT, then heated at 70°C for 10 min. with occasional vortex mixing. Samples were cooled on ice for 5 minutes and then loaded into 4-12% Bis-Tris Thermo Fisher NuPage mini gels and run at 200V constant voltage for 30-50 min using a 300V Enduro power supply (Labnet, Edison, New Jersey), then transferred to PVDF (MilliporeSigma, Burlington, Massachusetts) for 37 min. at 30V constant voltage. Running and transfer buffers used were prepared according to Thermo NuPage manufacturer's recommendations. Membranes were blocked by rocking gently with 5% non-fat dry milk (NFDM; LabScientific bioKEMIX, Danvers, Massachusetts) in Tris-Buffered Saline with Tween-20 (TBST) (Sigma-Aldrich) for 1h at room temperature. Primary antibodies (Table 1) were diluted in 5% NFDM in TBST and incubated overnight (16h) with rocking at 4°C. Membranes were washed by gently rocking 3x5 min. at room temperature with TBST. Secondary antibodies were diluted in 5% NFDM in TBST and antibody solution was incubated with blots for 1.25h with gentle rocking at room temperature. Membranes were then washed via rocking 5x5min. with TBST and developed using Pico or Femto (Thermo Fisher Scientific) developing reagents. Images were taken using ProteinSimple gel imager (Bio-Techne, Minneapolis, Minnesota).

Antibodies: Antibodies were sourced from Cell Signaling Technologies (CST)(Danvers, Massachusetts), Santa Cruz Biotechnology (SCBT)(Santa Cruz, California), Sigma Aldrich (St. Louis, Missouri) and Proteintech (Rosemont, Illinois). Antibodies were diluted in 5% NFDM in TBST as described in **Table 1**.

Table 2.1: Primary and secondary antibodies used in western blot experiments

Target	Antibody	Dilution
RUNX2	CST α-RUNX2 #D1L7F	1:1,000
CBFβ	CST α-CBFβ #D4N2N	1:1,000
GAPDH	SCBT α-GAPDH sc-166574	1:1,000
FLAG	Sigma M2 α-FLAG F1804	1:1,000
Actin	SCBT α-Actin SPM161	1:10,000
hnRNPK	SCBT α-hnRNPK sc-28380	1:1,000
Biotin	CST α-Biotin-HRP 7075	1:3,000
eIF4B	ProteinTech α- eIF4B 17917-1-AP	1:1,000
Rabbit Primary	CST Goat α-Rabbit #7076	1:1,000
Mouse Primary	CST Goat α-Mouse #7074	1:4,000

Membrane Stripping: Membranes were stripped and re-probed using Abcam (Cambridge, United Kingdom) mild western blot stripping protocol. Briefly, membranes were incubated by shaking for 10 min. with mild stripping buffer (0.2M Glycine, 0.1%SDS, 0.1% Tween-20, pH 2.2), then washed twice with PBS for 10 min. with shaking. Stripping was verified via incubation of membrane with Femto ECL developing reagent (Thermo Fisher) and imaged for residual signal. Any membranes showing residual signal were subjected to additional 5-10 min. of incubation with mild stripping buffer. Following verification of successful membrane stripping, membranes were subjected to 2x 5min. washes in TBST on a shaker at room temperature, and then blocked for 1.25h with 5% milk in TBST at room temperature. Following this, membranes were probed as described above.

Densitometry: Densitometric analysis was performed using ImageJ (32), with bands of interest selected using built-in gel analysis tool. Background subtraction using 80px diameter rolling ball was applied to select images.

Proteasome Inhibition Assay

U2OS wt and U2OS CBFβ KO cells were plated on 10 cm dishes and grown to 50% confluence, then treated with MG132 (Sigma-Aldrich, St. Louis, Missouri) 50 μM or equivalent DMSO control for 4h or 18h followed by western blot analysis as mentioned previously. In some experiments floating cells were also collected, spun down with harvested adherent cells and combined together before lysate collection. The extent of proteasome inhibition induced by MG132 was evaluated using Abcam Proteasome Activity kit according to manufacturer's recommendations.

Cycloheximide Pulse Assay

U2OS wt and U2OS CBFβ KO cells were grown in a 6-well plate to 60% confluence, then treated with McCoy's media supplemented with 10% FBS, 1% P/S, 15 mM HEPES pH 6.95 and 150 μg/mL cycloheximide (CHX) for up to 24h. Cells were all plated in the same batch and drugged in a staggered timeline resulting in all cells being collected at the same time. Following treatment, cells were collected and analyzed via western blot as described previously.

RNAseq

Sequencing: Batch 3' Tag-Seq RNA-seq data was collected and analysis was performed at the Bioinformatics Core (UC Davis Genome Center). The RNA sequencing data were preprocessed using HTStream, version 1.3.3 (https://s4hts.github.io/HTStream/) and PCR duplicates were removed using umitools, version 1.0.1 (33). Reads were aligned to GRCh38 using STAR (34). Comparison for analysis was U2OS CBFβ KO vs DMSO-treated U2OS wt control.

Differential Expression Analyses: Differentially expressed genes were identified using the limma-voom Bioconductor pipeline (limma version 3.50.1, edgeR version 3.36.0) (35). In this pipeline, the TMM method is used to obtain normalization factors and adjusted library sizes for each sample (36). These adjusted library sizes are then used to calculate counts per million reads (CPMs), using the adjusted library sizes instead of the total counts as the denominator. CPMs are log2 transformed, and voom is used to calculate variance weights for each observation, which are used in a weighted least squares model in limma (37). Empirical Bayes smoothing is used to obtain improved smoothed standard errors for log fold changes for use in hypothesis testing. The resulting p- values are adjusted for multiple testing using the Benjamini-Hochberg false discovery rate (FDR) controlling method (38).

Global Translation Assay

Global protein translation was evaluated using Thermo Fisher Click-iT OPP Alexa488 kit. Briefly, 4,500 U2OS wt and U2OS CBFβ KO cells were seeded into each well of a 96-well plate 12h before labeling. Nascent proteins were labeled for 2h with McCoy's media + 6.2 μM O-propargyl-puromycin (OPP) in DMSO, with control wells including 150 μg/mL cycloheximide (CHX) (Sigma-Aldrich) or equivalent DMSO control. Cells were fixed and permeabilized and click conjugation was conducted, all according to manufacturer's recommendations. Nuclei of fixed cells were then stained with HCS NuclearMask Stain (Thermo Fisher Scientific) diluted 1:2,000 in PBS according to manufacturer's recommendations. Images were obtained using a Jenoptik ProgRes MF Cool CCD mounted on a Leica DMI3000B microscope with a Leica HCX PL FLUOTAR L 20X/0.40na CORR objective. Samples were illuminated by a Leica EL6000

fluorescent light source, and cell counts and nascent protein signal was quantified using ImageJ. Fluorescent signal was normalized to quantity of nuclei as stained by NuclearMask.

Lentiviral Transduction

Plasmid Design: The open reading frame (ORF) for CBFβ was cloned out of OHu25418 plasmid incorporating NM_022845.3 (GenScript Biotech Corporation, Piscataway, New Jersey) using primers listed in **Table 2,** produced by Integrated DNA Technologies (IDT, Newark, NJ). CBFβ ORF was then inserted into pHIV-EGFP by use of XbaI and TspMI restriction enzymes (New England BioLabs, Ipswich, MA) to generate CBFβ_WT. *In silico* cloning simulations, primer design, and plasmid diagrams were made using SnapGene® software (from Dotmatics; available at snapgene.com). The vector was digested by both enzymes simultaneously in NEB Cutsmart 3.1 buffer according to manufacturer's recommendations, cleaned up by electrophoresis in 1% agarose gel (IBI Scientific, Dubuque, Iowa) in TBE run at 160V, and DNA was extracted from gel using GeneJET Gel Extraction Kit (Thermo Fisher Scientific) according to manufacturer's recommendations. Plasmid was eluted from GeneJET column using 30 µL nuclease free water (Ambion, Thermo Fisher Scientific). Insert and vector were combined at 7:1 stoichiometric ratio and ligated using T4 Ligase (Thermo Fisher Scientific) according to manufacturer's recommendations. Vector was transformed into NEB Stable *E. coli* according to manufacturer's recommendations, then grown overnight at 37°C on LB (Luria-Bertani) (Thermo Fisher Scientific) and Agar (Sigma-Aldrich) plates containing 100 µg/mL carbenicillin (IBI Scientific, Dubuque, Iowa). Colonies growing in presence of 100 µg/mL carbenicillin were inoculated into 5 mL of LB broth supplemented with 100 µg/mL carbenicillin and grown overnight at 37°C with 180rpm rotation. Following overnight growth, plasmid DNA was collected using

GeneJET Plasmid Miniprep Kit (Thermo Fisher Scientific) according to manufacturer's recommendations, with final elution from column accomplished with 50 μL nuclease-free water. Eight hundred (800) ng of purified plasmid was sent for Sanger sequencing verification by Genewiz using primers listed in **Table 2**.

C-terminus FLAG tagged CBFβ (denoted as CBFβ_WT_FLAG) was generated through site directed mutagenesis of the above described vector via Q5 Mutagenesis Kit (New England BioLabs) according to manufacturer's instructions, with same transformation, miniprep, and sequence verification steps as listed above, using primers in **Table 2**.

Table 2.2: Primer sequences for Lentiviral Vector Generation

Usage	**Primer Sequence**
Add XbaI restriction site and a Kozak sequence to CBFβ N-term for cloning into pHIV-EGFP F	5'-GGAGGATTCTAGAGC CACCATGCCGCGC-3'
Add TspMI restriction site and stop codon (snipping off FLAG tag in original pcDNA3.1 vector) to CBFβ C-term for cloning into pHIV-EGFP R	5'-GGAGGTCCCGGGTTATCAACG AAGTTTGAGGTCATCACCACC-3'
Mutate add C-term FLAG tag to CBFβ in pHIV-EGFP F	5'-GACGACGATAAGTGAT AACCCGGGCTAGGA-3'
Mutate add C-term FLAG tag to CBFβ in pHIV-EGFP R	5'-ATCCTTGTAATCACGAA GTTTGAGGTCATCAC-3'
Sequence T7 F	5'- TCAAGCCTCAGACAGTGGTTC-3'
Begin Sanger sequencing at elongation factor-1α promoter	5'- TCAAGCCTCAGACAGTGGTTC-3'

HEK293T Transfection: Wells of a 6-well plate were filled with 1 mL antibiotic-free 10% FBS DMEM and pre-incubated to reach 37C. Third (3rd) generation lentiviral plasmids (39,40), listed below, were mixed with jetPRIME (Polyplus, Sartorius, New York, New York) and added

to media according to manufacturer's recommendations, using 2:1 ratio of jetPRIME volume (μL) to DNA quantity (μg). Total quantity of each plasmid used for co-transfection is listed in **Table 3.**

Table 2.3: Plasmids and their source used in HEK293T transfection experiments

Plasmid	**Source**	**DNA (μg)**
pHIV-EGFP	Addgene #21373	0.87
pMDLg/pRRE	Addgene #12251	0.44
pRSV/REV	Addgene #12253	0.22
pMD2.G	Addgene #12259	0.22

1.4 million HEK293T cells per well were then plated on top of 1 mL media + transfection reagents + plasmids, and cells were incubated in presence of transfection reagents for 18h. Media was changed and lentiviral particles were harvested as described below.

Harvesting of Lentiviral Particles: Viral supernatant was then removed and fresh antibiotic-free DMEM supplemented with 10% FBS was added. Supernatant containing lentiviral particles was collected 48h and 72h post-transfection and pooled. Supernatant was then cleared by centrifugation at 500g for 10 min and sterilized by passing through a 0.2 μm nylon filter (Sigma-Aldrich) and stored at -80C until lentiviral transduction.

Infection of Target Cells: Fifty-one thousand U2OS CBFβ KO cells were seeded into each well of a 24- well plate and grown at 37°C for 16h prior to transduction. Previously harvested lentiviral particles were thawed at 4°C and diluted 20x, 50x, 125x, 313x, 781x, and 1953x in normal media supplemented with 4 μg/mL Polybrene (Sigma-Aldrich) and added to target cells. Infection was allowed to continue for 3 days at 37°C, after which cells were split into 6-well plates and inspected for fluorescence using a Leica DMI3000B microscope with a Leica EL6000 fluorescent light source. The cell population from each infection used for harvesting via trypsin

and outgrowth in T75 flask was chosen based on <5% EGFP+ cells. This was done to reduce risk of double integration from lentivirus. Dilution factors of lentiviral particles in cell populations selected for outgrowth are shown in **Table 4**:

Table 2.4: Lentiviral inserts and dilution factors utilized for transduction experiments

Lentiviral Insert	Dilution
Empty vector pHIV-EGFP	125x
pHIV-EGFP with CBFβ (wt)	313x
pHIV-EGFP with CBFβ_FLAG (wt)	781x

FACS Sorting of Monoclonal Cell Lines: Ten million cells from each lentiviral insert-containing population were harvested via trypsin, washed 2x with PBS, then resuspended in PBS supplemented with 1% FBS and 2% P/S. Cells were passed through a sterile 40 μm nylon mesh (Sigma-Aldrich) just before sorting. Single cells were separated into individual wells of 96 well culture plates for subsequent expansion using a 4-laser, 18-color Astrios EQ cell sorter (Beckman Coulter, Brea, CA). The Astrios was configured with its 70μm nozzle at 60psi to quickly and accurately deposit single EGFP+ cells into 96 well plates prefilled with McCoy's media supplemented with 10% FBS and 1% P/S. Each 96 well plate was pre-chilled to ~4C to preserve cell vitality during sorting. Following sorting into 96-well plates, media was regularly changed and cells were harvested via trypsin and transferred to successively larger vessels upon reaching ~50% confluence in each. Vessel order was: 96-well plate, 24-well plate, 6-well plate, and finally cells were seeded into a T75 flask. 5 different clonal cell lines from each of 4 different lentiviral inserts were generated.

RNA Collection

U2OS wt and U2OS CBFβ KO cells were grown to 70% confluence on 10 cm plates in 10% FBS 1% P/S McCoy's. Cells were washed 2x with PBS then lysed with 1 mL TRIzol (Ambion, Thermo Fisher Scientific) per plate, which was transferred to a 1.5 mL tube, 200 µL of Chloroform (Thermo Fisher Scientific) was added, and tubes were mixed and centrifuged at 4°C 12,000g for 15 min. The aqueous layer (top) was transferred to a fresh tube, 500 µL of 2-propanol (Thermo Fisher Scientific) was added, and samples were mixed and allowed to sit at room temp for 5 min. Sample was pelleted at 4°C 12,000g for 10 min, supernatant was removed, and pellet was washed with 1 mL 75% ethanol (Decon Labs, King of Prussia, Pennsylvania) in water, w/v, centrifuged, washed, and centrifuged again. Supernatant was removed and pellet was dried for 10 min. and re-solvated in 30 µL nuclease-free water and vortex mixed at 300 rpm at 55°C for 10 min. to facilitate dissolution. RNA samples were stored -80C until further analysis.

Quantitative real-time PCR (qRT-PCR)

cDNA synthesis and gDNA wipeout was performed using QuantiTect Reverse Transcription Kit (Qiagen, Hilden, Germany). Briefly, RNA was thawed on ice and all kit solutions were thawed at room temperature. gDNA wipeout and following cDNA synthesis reactions were performed per manufacturer's recommendations, using 1 µg RNA as starting material. qRT-PCR was performed by creating a master mix comprised of: 6.5 µL nuclease-free water, 1 µL forward primer (2.5 µM stock), 3 µL reverse primer (2.5 µM stock) and 12.5 µL SYBR green per reaction. Twenty three (23) µL of master mix was added to each well of a 96-well PCR plate, and 2 µL of 5ng/µL cDNA was spiked into each well. qRT-PCR reaction was promptly started, with gradient

conditions of 5 min. at 95°C followed by 45 cycles of 10s at 95C and 30s at 60°C. qRT-PCR was performed on an AriaMx Real-Time PCR System (Agilent Technologies, Santa Clara, CA). Threshold was set to region of sigmoid where amplification became linear.

Table 2.5: Primers utilized for quantitative real time RT-PCR of RUNX2.

Usage	Primer Sequence
qPCR HPRT F	5'- CCTGGCGTCGTGATTAGTGA -3'
qPCR HPRT R	5'- CGAGCAAGACGTTCAGTCCT -3'
qPCR RUNX2 F	5'- TAGGCGCATTTCAGGTGCTT -3'
qPCR RUNX2 R	5'- GGTGTGGTAGTGAGTGGTGG -3'

CBFβ-hnRNPK Co-Immunoprecipitation

Pulldown of CBFβ: U2OS cells were grown in 15% FBS 1% Pen-Strep McCoy's media on 2x 10 cm plates until 70% confluent. Cells were lysed according to western blot lysate collection protocol outlined above, except cells were lysed in modified RIPA buffer (50 mM Tris pH 7.5, 150 mM NaCl, 1% NP40, 0.25% sodium deoxycholate) supplemented with 1x cOmplete EDTA-free protease inhibitor cocktail, 2mM NaVO3, NaF 5 mM and 1mM PMSF. CBFβ was immunoprecipitated from cell lysates using anti-CBFβ antibody A303-547A (Bethyl Labs, Montgomery, Texas) and Protein A Sepharose CL-4B beads (GE Healthcare, Chicago, IL) as follows: cell lysates were normalized to 1.00 mg/mL protein concentration, adjusted to a final volume 300 µL, and 3 µg anti-CBFβ antibody was added to lysates and rotated overnight at 4C. The following day agarose beads were re-hydrated and washed 3x with PBS, then finally resuspended in lysis buffer and added to samples, and rotated for 4h at 4°C. Following this, agarose beads were spun down and washed twice with lysis buffer, then twice with wash buffer (50 mM Tris pH 7.5, 0.1% NP40, 0.05% sodium deoxycholate). Washes were removed and protein was extracted from beads by heating at 70°C for 10 min. in the presence of 1x Laemmle buffer and 50

mM DTT. The eluted protein was then analyzed by western blot as described above. Membranes were stored in TBS at 4°C between antibody detection.

Pulldown of hnRNPK: Experiment was conducted the same as above except hnRNPK was immunoprecipitated from cell lysates using anti-hnRNPK antibody (Santa Cruz Biotech SC-28380) and anti-GAPDH antibody was used as isotype control (Santa Cruz Biotech SC-166574). Antibody quantities added were the same as above.

Statistical Analyses

Figure 2.1B: Error bars are standard deviation (SD), n=9 (biological), *** = $p<0.0001$, unpaired two-tailed Welch's t-test. ***Figure 2.2A:*** Error bars are SD, n=3 (technical); **** = $p<0.0001$, two-way ANOVA with Tukey's post hoc test. ns = not significant. ***Figure 2.2C:*** Error bars are SD, n=3 (biological); * = $p<0.05$, ** = $p<0.01$, two-way ANOVA with Tukey's post hoc test. ***Figure 2.4A:*** Error bars are SD, n=3 (3 biological replicates, 3 technical replicates per run); one-way t-test. ***Figure 2.6C,D:*** Error bars are SD, n=5 (biological); * = $p<0.05$, *** = $p<0.001$, one-way ANOVA with Tukey's post hoc test.

Results

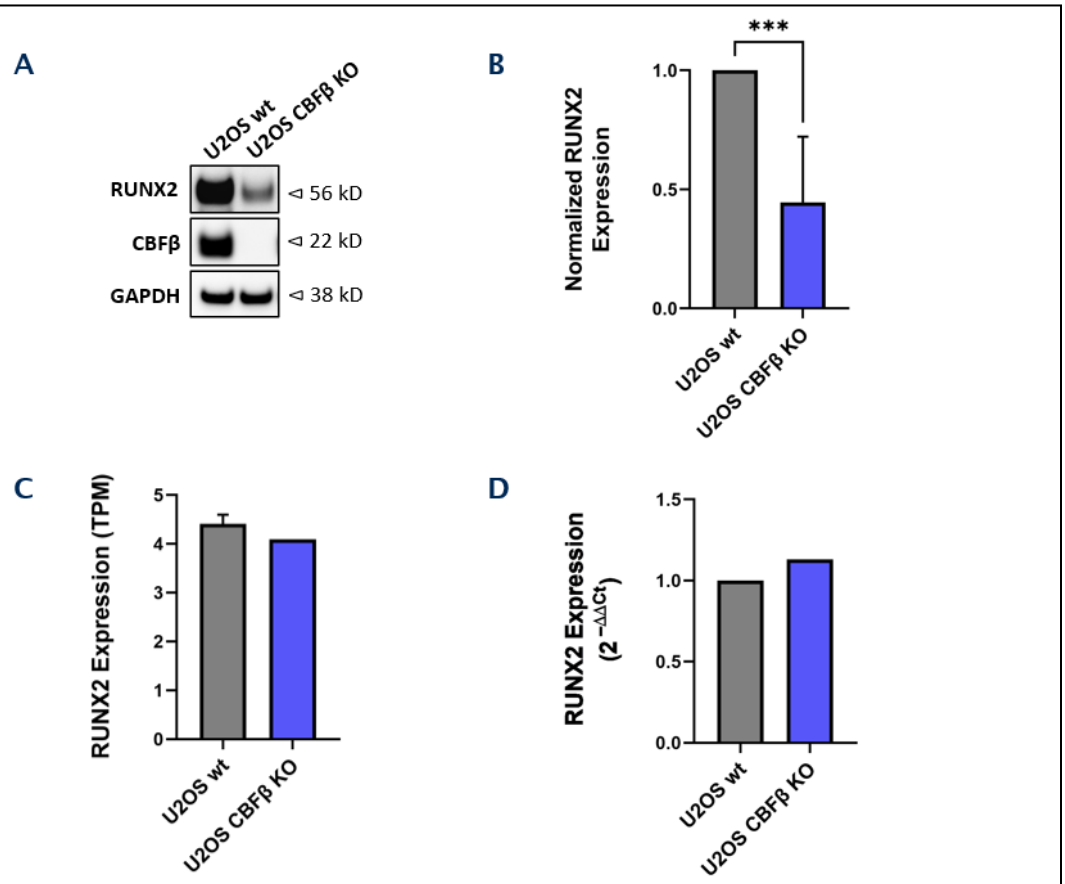

Figure 2.1 A) Representative western blot images of RUNX2, CBFβ and GAPDH expression in U2OS wt and U2OS CBFβ KO cells. B) Densitometry of RUNX2 expression in U2OS wt and U2OS CBFβ KO cells across nine different western blots, all normalized to GAPDH. C) RNAseq data of RUNX2 mRNA expression in U2OS wt and CBFβ KO cells. D) Quantitative RT-PCR analysis of RUNX2 expression in U2OS wt and CBFβ KO cells, normalized to HPRT.

Loss of CBFβ leads to reduced RUNX2 protein expression. A U2OS CBFβ KO cell line was developed using CRISPR and profiled via western blotting. When compared to U2OS wt cells, U2OS CBFβ KO cells consistently demonstrated lower RUNX2 protein expression, normalized to GAPDH. Interestingly, both cell lines demonstrated similar relative RUNX2 mRNA expression when measured by RNAseq. qRT-PCR was then conducted to validate RNAseq data, and RUNX2 mRNA expression again appeared similar between both cell lines.

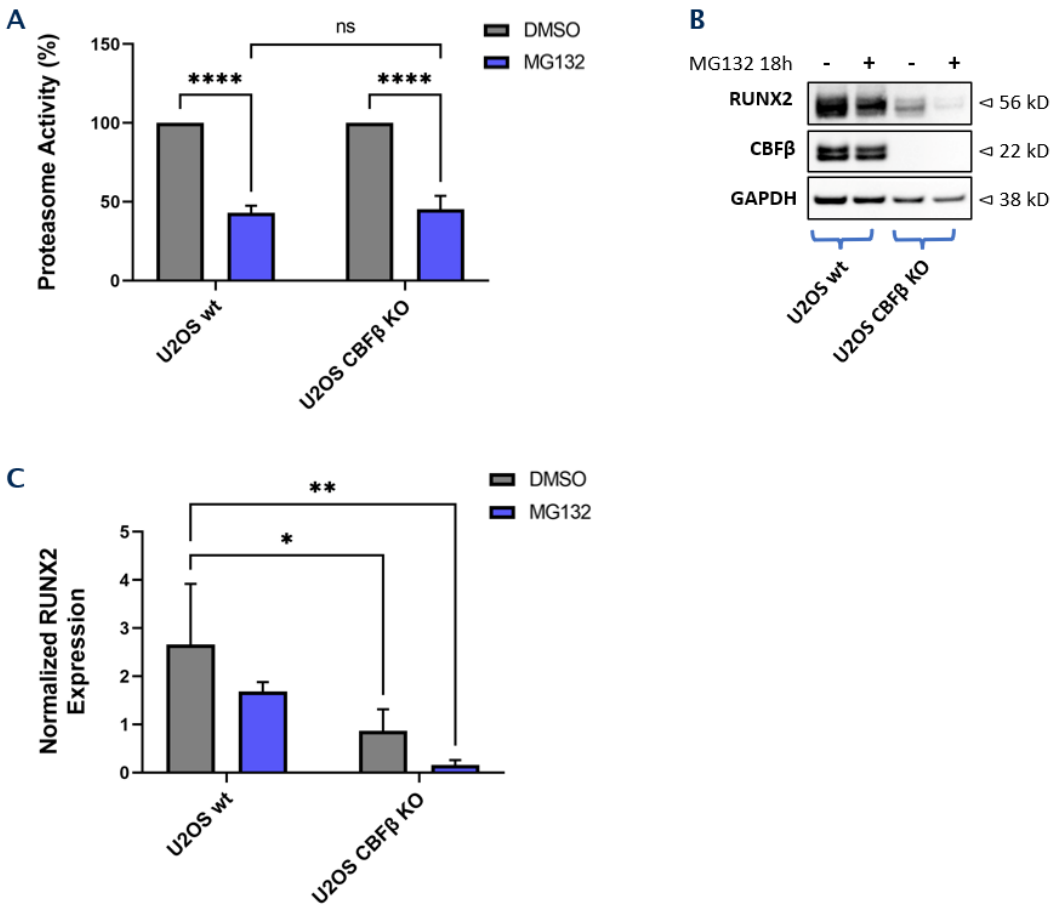

Figure 2.2 A) Readout from fluorometric proteasome activity kit proteasomal inhibition capacity of MG132 in U2OS wt and U2OS CBFβ KO cells. B) Representative western blot images of RUNX2, CBFβ, and GAPDH expression in U2OS wt and U2OS CBFβ KO cells treated with 50 μM MG132 or DMSO for 18h. C) Densitometry of RUNX2 expression in U2OS wt and U2OS CBFβ KO cells with MG132 or DMSO, normalized to GAPDH.

Reduced RUNX2 protein expression in U2OS CBFβ KO cells is not rescued by proteasomal inhibition. To assess if proteasomal degradation could explain this decrease in RUNX2 protein expression in U2OS CBFβ KO cells, we subjected our two cell lines to proteasome inhibition followed by western blotting. We first tested our proteasome inhibitor, MG132, to ensure it was capable of inhibiting the proteasome in our cell lines. Treatment of both cell lines with 50 μM MG132 resulted in ~45% proteasome inhibition in each, and we used this same treatment for our

western blotting experiments. Proteasomal inhibition did not rescue low RUNX2 protein expression in U2OS CBFβ KO cells, and instead caused RUNX2 expression to decrease further. This was observed in both cell lines, however in terms of fold change it was more pronounced in U2OS CBFβ KO cells. RUNX2 protein expression in DMSO-treated samples was again lower in CBFβ KO cells than WT U2OS cells, in accordance with previous data.

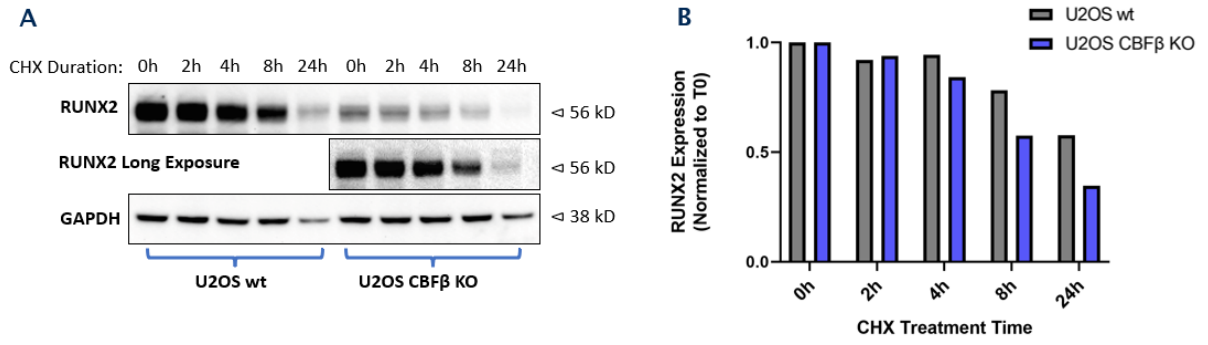

Figure 2.3 A) Representative western blot images of RUNX2 and GAPDH expression in U2OS wt and U2OS CBFβ KO cells treated with 150 µg/mL Cycloheximide (CHX) for various timepoints. B) Densitometry of blot at left, with RUNX2 expression normalized to GAPDH.

Loss of CBFβ does not drastically alter RUNX2 degradation in U2OS cells. To further evaluate if heightened degradation explains lower RUNX2 protein expression in U2OS CBFβ KO cells, we utilized an orthogonal assay involving CHX, a protein translation inhibitor. Instead of inhibiting degradation, as before, we inhibited synthesis of new protein and observed degradation itself. Following treatment with CHX, RUNX2 protein expression did decrease over time in both cell lines, which was expected. In comparing the two cell lines, we did see a small difference in terms of quantity of RUNX2 degraded over time, with RUNX2 in U2OS CBFβ KO cells seemingly having a slightly shorter half-life than that of RUNX2 in WT U2OS cells.

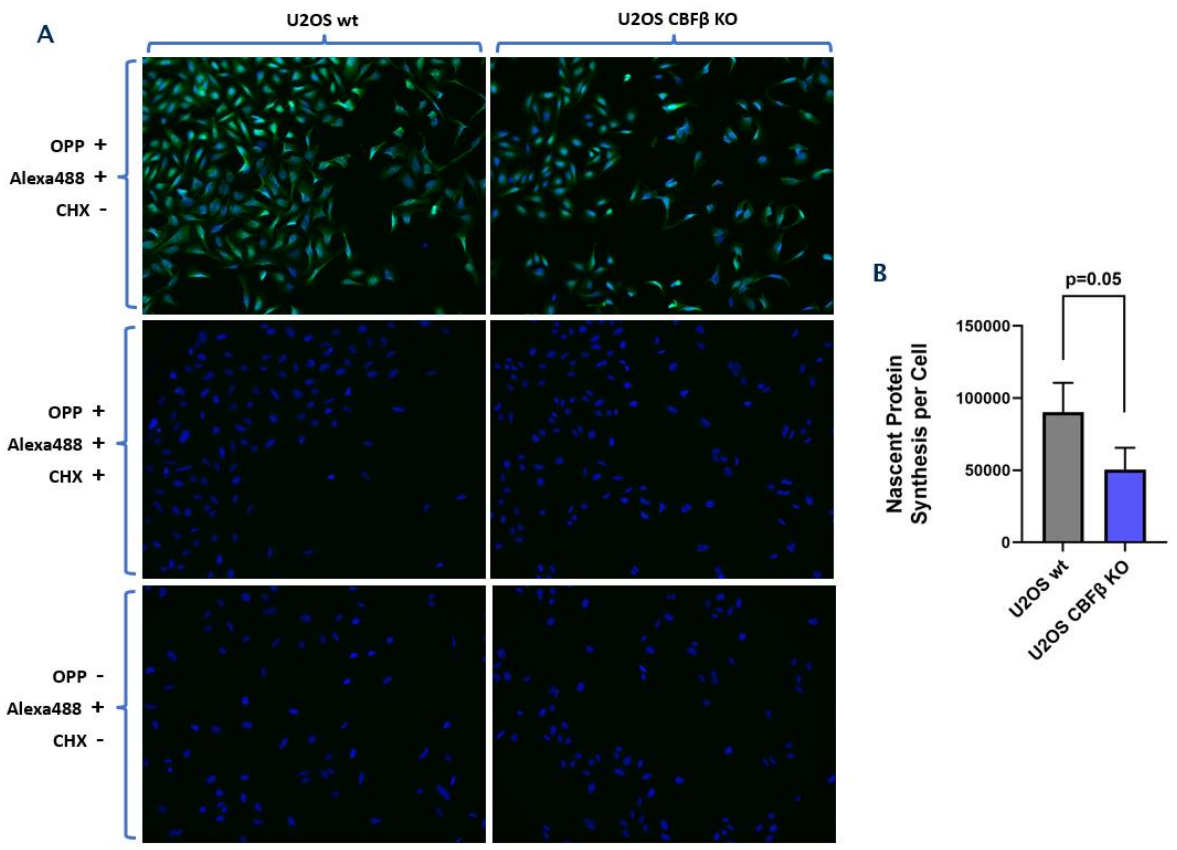

Figure 2.4 (A) Representative fluorescent microscopy images of U2OS wt and U2OS CBFβ KO cells subjected to Click-iT OPP Alexa 488 protein translation assay. Alexa488 stain of newly translated proteins is represented as green in above images, with NuclearMask™ stain represented as blue. B) Quantitation of nascent protein synthesis rates in U2OS wt and U2OS CBFβ KO cells, with protein synthesis rates normalized per cell by counting nuclei as stained with NuclearMask™.

Loss of CBFβ leads to a decrease in global protein translation in U2OS cells. In order to understand CBFβ's contribution to global protein translation, we subjected U2OS wt and U2OS CBFβ KO cells to the Click-iT OPP Alexa 488 protein translation assay. This experiment was performed in technical and biological triplicate. We observed a consistent decrease in global protein translation in U2OS CBFβ KO cells compared to U2OS WT, slightly exceeding the cutoff for statistical significance.

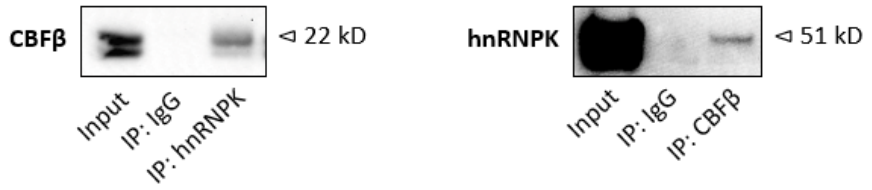

Figure 2.5 Co-IP of hnRNPK in U2OS cells followed by blotting for CBFβ, and reciprocal Co-IP pulling down CBFβ and blotting for hnRNPK.

CBFβ and hnRNPK interact in U2OS cells. Other research posited CBFβ to participate in protein translation through interaction with hnRNPK. To evaluate whether this interaction occurred in osteosarcoma cells, we subjected U2OS cells to reciprocal Co-IP's of CBFβ and hnRNPK. hnRNPK was present in CBFβ pulldown, and CBFβ was present in hnRNPK pulldown. Isotype control (IP: IgG) demonstrated no signal in either experiment.

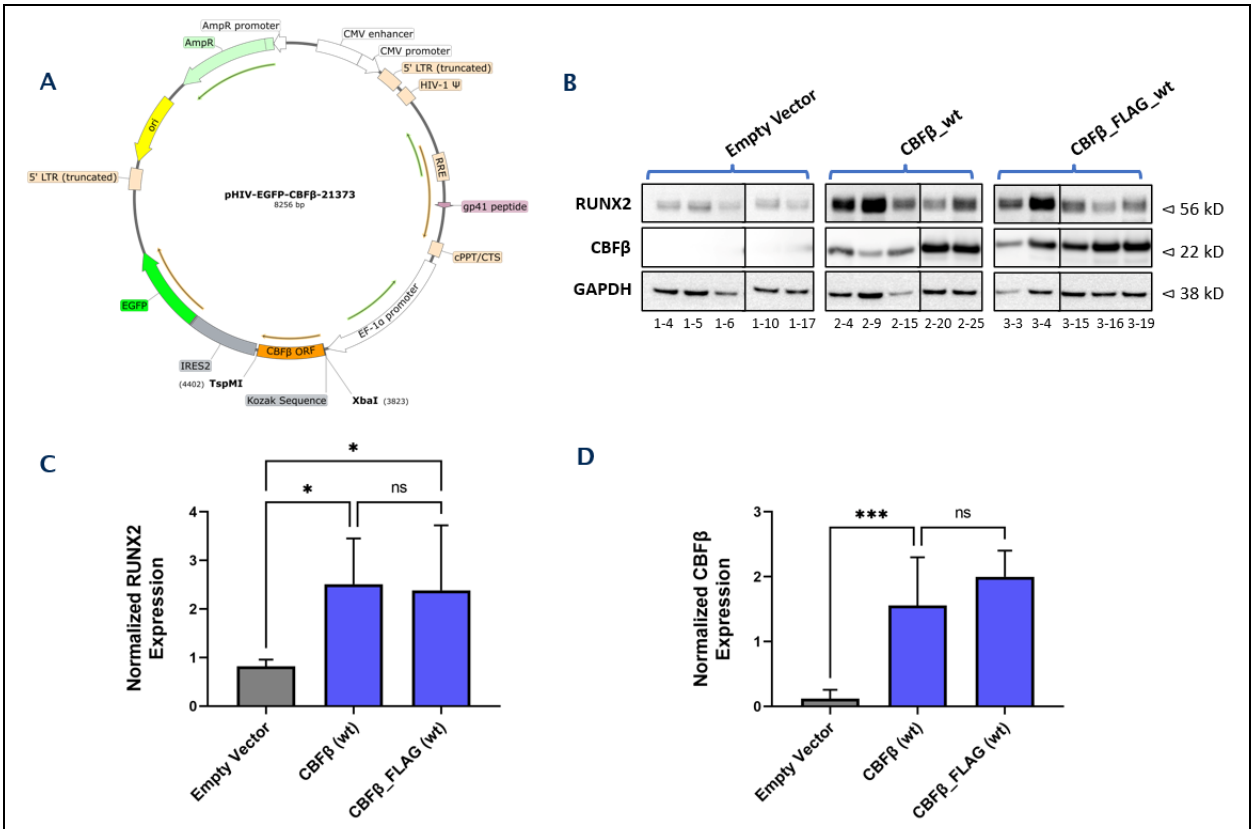

Figure 2.6 (A) Plasmid diagram showing transfer plasmid #21373 with CBFβ_wt cloned in and relevant restriction enzyme sites highlighted. B) Representative western blot images of RUNX2, CBFβ, and GAPDH expression in monoclonal cell lines generated by transducing U2OS CBFβ KO cells with either Empty Vector, wt CBFβ, or wt CBFβ with C-term 1x FLAG tag. Numbers below blots denote clone designation, with 5 clones per lentiviral insert pictured. C) Densitometry of RUNX2 protein expression relative to GAPDH, quantitated from western blot pictured in 2.5B. D) Densitometry of CBFβ expression relative to GPADH, quantitated from 2.5B.

Re-introduction of WT CBFβ rescues low RUNX2 expression in U2OS CBFβ KO cells. To evaluate that we were indeed studying a CBFβ-specific effect, we used lentiviral transduction of CBFβ KO cells to generate stable cell lines expressing Empty Vector, CBFβ_WT, or CBFβ_WT_FLAG. Transduction with CBFβ_WT or CBFβ_WT_FLAG resulted in statistically significant increases in RUNX2 protein expression relative to cells transduced with Empty Vector.

Expression levels of both endogenous RUNX2 and CBFβ transgene were consistent between CBFβ_WT and CBFβ_WT_FLAG transduced cells.

Discussion

As measured by western blot, RUNX2 protein expression was consistently lower in U2OS CBFβ KO cells than in U2OS wt cells (**Figure 2.1)**. This was not accompanied by a commensurate decrease in RUNX2 mRNA expression, implying a post-transcriptional mechanism, seemingly dependent upon CBFβ. Potential explanations to this include increased protein degradation, decreased mRNA stability, or decreased translational efficiency of RUNX2. We chose to focus our efforts on proteasomal degradation as this is the pathway governing RUNX2 turnover under normal conditions (41–44), and previous studies suggested CBFβ protects RUNX2 from proteasomal degradation (45,46). The resulting the decrease in RUNX2 levels due the loss of loss of CBFβ was not due to proteasome degradation, because treatment with MG132 was unable to rescue low RUNX2 expression observed in CBFβ KO cells (**Figure 2.2).**

It was surprising that both cell lines exhibited decreased expression of RUNX2 upon MG132 treatment, when proteasome inhibition typically causes an accumulation of proteins (47). Nevertheless, this phenomenon is not unheard of and has been observed in other studies treating U2OS cells with MG132 for a similar duration (48), as well as in other cell models (49–51). Proteasome inhibitors may lead to increased lysosomal degradation of proteins (52), and cause RUNX2 to undergo trafficking to the lysosome through interaction with SOX9 (53), which could explain the decrease in RUNX2 protein following MG132 treatment. Interestingly, RNAseq data (not shown) revealed heightened SOX9 mRNA expression in CBFβ KO cells compared to U2OS wt cells, which may underly the more severe decrease in RUNX2 protein observed in U2OS CBFβ KO cells compared to U2OS wt cells. Further studies of the significance of SOX9 and lysosomal degradation in RUNX2 stability would be necessary to delve into this further, and could entail

MG132 treatment in the presence of SOX9 siRNA or use of lysosomal protease inhibitors such as Bafilomycin A1 (54) or Leupeptin (55).

Treatment of our cell lines with CHX did demonstrate a slightly reduced half-life of RUNX2 in U2OS CBFβ KO cells, suggesting RUNX2 may be degraded at a slightly increased rate in the absence of CBFβ (**Figure 2.3)**. This difference in RUNX2 half-life was small in magnitude overall, and most prominent in latter timepoints. It's important to note that CHX treatment of cell lines in other studies is typically shorter in duration, as the median half-life of human proteins hovers around 8.7 h (56). In our hands, RUNX2 appeared to have a particularly long half-life in U2OS cells, necessitating a longer treatment time to observe a significant amount of degradation. Extended treatment with CHX, and therefore shutdown of nascent protein synthesis, is likely to place cells under stress and alter degradation kinetics (57), which may confound these data at the later timepoints.

Other methods are available that could allow us to delve deeper into potential alterations in the stability of RUNX2, such as immunoprecipitation (IP) of RUNX2 followed by immunoblotting for ubiquitin (58) or pulse-chase labeling of nascent proteins followed by IP of RUNX2 (59). While these methods have been used with great success in other studies, they were not feasible for us due to a myriad of issues encountered with IP of RUNX2. These are listed in further detail in the Chapter 3 discussion, but in short, this experiment was attempted ad nauseam under numerous conditions and ultimately proved insurmountable. Ultimately, we concluded that decreased stability of RUNX2 due to loss of its binding partner, CBFβ, did not sufficiently explain the discrepancy in RUNX2 levels we observed. Around the same time, similar data was reported in breast cancer cells demonstrating a reduction in RUNX1 protein upon loss of CBFβ (23), and we observed a decrease in RUNX1 in our hands as well (data not shown). The authors went on to

implicate CBFβ playing a critical role protein translation, which supports our results that pointed to a mechanism other than stabilization of RUNX2.

Utilizing a Click-iT OPP Alexa 488 protein translation assay, we assessed global protein translation rates of U2OS wt and U2OS CBFβ KO cells. In all three biological replicates performed, U2OS CBFβ KO cells consistently registered lower global protein translation rates than U2OS wt cells (**Figure 2.4)**. While our result did not quite meet the criteria for statistical significance ($p=0.05$, not $p<0.05$), it's important to note that this assay evaluates translation rates of all cellular proteins collectively rather than on a case-by-case basis. The influence of CBFβ on protein translation might not be broad enough to significantly skew global protein synthesis, but may strongly influence the translation of a subset of proteins within OS cells, particularly those reliant on cap-dependent translation. This consistent reduction in global protein synthesis rates between our cell lines was encouraging enough for us to move forward studying protein translation in latter, more specific assays.

Previous work postulated that the role of CBFβ in protein translation is accomplished by binding to mRNA via hnRNPK, and CBFβ modulates translation through binding to eIF4B, a member of the eIF4 translational complex (23). We next conducted co-IP experiments to assess if this CBFβ-hnRNPK interaction also occurs in OS cells. Reciprocal Co-IP demonstrated an interaction between hnRNPK and CBFβ in U2OS cells, as evidenced by CBFβ being present in the pulldown of hnRNPK, and vice versa (**Figure 2.5)**. We did not see strong enrichment of either protein in our pulldowns, possibly due to weak CBFβ-hnRNPK interaction, or a low fraction of total CBFβ and hnRNPK bound to each other at any point in time. Nevertheless, our pulldown was specific and demonstrated CBFβ and hnRNPK do interact in U2OS cells as neither protein was present in IgG isotype samples.

Taken together, our results were supportive of a non-canonical role for CBFβ in protein translation in OS cells. To further support this claim, it was necessary to confirm our conclusions weren't misled by off-target CRISPR activity (60) in our starting CBFβ KO cell line. To this end, we conducted a rescue experiment reconstituting wt CBFβ back into CBFβ KO cells. Transient transfection was first attempted, but U2OS CBFβ KO cells proved resistant to multiple transfection reagents and optimization panels, yielding a maximum transfection efficiency of 16%. This low efficiency precluded measure of changes in RUNX2 brought about by CBFβ, as any shifts in RUNX2 expression are blunted by the abundance of un-transfected cells. Furthermore, RUNX2 demonstrated slow degradation in our previous studies, meaning its synthesis rate was commensurately slow as well (61). Transient transfection results in transgene expression lasting just a few days, which we reasoned might not be enough time for reconstituted CBFβ to drive appreciable changes in RUNX2 levels.

In order to interrogate this system over a longer time period, we opted to reconstitute CBFβ through lentiviral transduction. The cytomegalovirus (CMV) promoter is commonly chosen for driving transgene expression in transduced cells, however reports of it causing inconsistent expression over time are numerous (62–64). We instead selected the EF-1α promoter due to its lauded capability to drive stable, long-term transgene expression (63,65). Cells were transduced with CBFβ_WT as well as CBFβ_WT incorporating a 1xFLAG tag. The FLAG tag was cloned in at the C-terminus, as the N-terminus of CBFβ is key in CBFβ-RUNX2 interaction (66) and RUNX protein binding would have been blocked by a FLAG tag at this location (23,67).

Lentiviral particles with transfer plasmids containing either Empty Vector, CBFβ_WT, or CBFβ_WT_FLAG were generated and used to infect U2OS CBFβ KO cells, and multiple monoclonal cell lines for each insert were generated. RUNX2 expression in these resultant cell

lines was then evaluated via western blotting (**Figure 2.6)**. We observed a statistically significant increase in RUNX2 protein expression in our CBFβ-expressing transductants, indicating that CBFβ alone was both necessary, and sufficient, to rescue low RUNX2 protein levels in U2OS CBFβ KO cells. RUNX2 and CBFβ expression was consistent between cell lines transduced with either untagged CBFβ or our FLAG-tagged variant, demonstrating that our affinity tag did not alter transgene expression or hamper CBFβ-mediated rescue of RUNX2.

In conclusion, we have demonstrated that loss of CBFβ in U2OS cells leads to a reduction in RUNX2 protein expression while RUNX2 mRNA levels are unaffected, implying a post-transcriptional mechanism. This reduction in RUNX2 protein expression is specific to loss of CBFβ, as reconstitution of wt CBFβ restores low RUNX2 protein expression. The observed reduction in RUNX2 protein expression upon loss of CBFβ is not fully explained by a decrease in the stability of RUNX2, and may be explained by CBFβ playing a role in protein translation. This noncanonical role of CBFβ has been reported in breast cancer, and, in that setting, occurs via interaction with hnRNPK. Indeed, we observed a reduction in global protein translation upon loss of CBFβ, and confirmed CBFβ and hnRNPK do interact in osteosarcoma cells. Further study is needed to unravel more about the significance of this noncanonical OS, and reveal which proteins or pathways may be under the purview of CBFβ.

Acknowledgements

We would like to thank Dr. Dayn Godinez for generating the U2OS CBFβ KO cells which were seminal to this study. We would also like to thank Dr. Chris Lucchesi for his mentorship in molecular cloning which made the lentiviral transduction experiment possible, and Dr. Xinbin Chen for providing the lab space in which the mentoring took place. Additionally, we would like to thank Dr. Daniel York for his advice in growing up monoclonal cell lines, which helped greatly with generation of stably transduced cell lines.

pMDLg/pRRE, pRSV-Rev, and pMD2.G were gifts from Didier Trono (Addgene plasmid # 12251 ; http://n2t.net/addgene:12251; RRID:Addgene_12251), (Addgene plasmid # 12253 ; http://n2t.net/addgene:12253; RRID:Addgene_12253), (Addgene plasmid # 12259 ; http://n2t.net/addgene:12259; RRID:Addgene_12259). pHIV-EGFP was a gift from Bryan Welm & Zena Werb (Addgene plasmid # 21373; http://n2t.net/addgene:21373; RRID:Addgene_21373).

This project was supported by the University of California Davis Flow Cytometry Shared Resource Laboratory with funding from the NCI P30 CA093373 (Comprehensive Cancer Center), and S10 OD018223 (Astrios Cell Sorter) grants, with technical assistance from Ms. Bridget McLaughlin and Mr. Jonathan Van Dyke.

This project was supported in part by NIH K01OD026526, NIH R03OD031958, and startup funds provided to Dr. Wittenburg through the UC Davis Comprehensive Cancer Center.

References

1. Hagleitner MM, De Bont ESJM, Te Loo DMWM. Survival Trends and Long-Term Toxicity in Pediatric Patients with Osteosarcoma. Sarcoma. 2012;2012:1–5.
2. Fletcher CDM, World Health Organization, International Agency for Research on Cancer, editors. WHO classification of tumours of soft tissue and bone. 4th ed. Lyon: IARC Press; 2013. 468 p. (World Health Organization classification of tumours).
3. Duggan MA, Anderson WF, Altekruse S, Penberthy L, Sherman ME. The Surveillance, Epidemiology, and End Results (SEER) Program and Pathology: Toward Strengthening the Critical Relationship. American Journal of Surgical Pathology. 2016 Dec;40(12):e94–102.
4. Meyers PA, Schwartz CL, Krailo M, Kleinerman ES, Betcher D, Bernstein ML, et al. Osteosarcoma: A randomized, prospective trial of the addition of ifosfamide and/or muramyl tripeptide to cisplatin, doxorubicin, and high-dose methotrexate. Journal of Clinical Oncology. 2005;23(9):2004–11.
5. Hagleitner MM, De Bont ESJM, Te Loo DMWM. Survival trends and long-term toxicity in pediatric patients with osteosarcoma. Sarcoma. 2012;2012.
6. Mialou V, Philip T, Kalifa C, Perol D, Gentet JC, Marec-Berard P, et al. Metastatic osteosarcoma at diagnosis: Prognostic factors and long-term outcome - The French pediatric experience. Cancer. 2005;104(5):1100–9.
7. Jaffe N, Puri A, Gelderblom H. Osteosarcoma: Evolution of treatment paradigms. Sarcoma. 2013;2013.
8. Adya N, Castilla LH, Liu PP. Function of CBFβ/Bro proteins. Seminars in Cell & Developmental Biology. 2000 Oct;11(5):361–8.
9. Kagoshima H, Shigesada K, Satake M, Ito Y, Miyoshi H, Ohki M, et al. The Runt domain identifies a new family of heteromeric transcriptional regulators. Trends Genet. 1993 Oct;9(10):338–41.
10. Wysokinski D, Pawlowska E, Blasiak J. RUNX2: A Master Bone Growth Regulator That May Be Involved in the DNA Damage Response. DNA and Cell Biology. 2015 May;34(5):305–15.
11. Nathan SS, Pereira BP, Zhou Y fang, Gupta A, Dombrowski C, Soong R, et al. Elevated expression of Runx2 as a key parameter in the etiology of osteosarcoma. Mol Biol Rep. 2009 Jan;36(1):153–8.
12. Sadikovic B, Thorner P, Chilton-MacNeill S, Martin JW, Cervigne NK, Squire J, et al. Expression analysis of genes associated with human osteosarcoma tumors shows correlation of RUNX2 overexpression with poor response to chemotherapy. BMC Cancer. 2010 Dec;10(1):202.
13. Feng Y, Liao Y, Zhang J, Shen J, Shao Z, Hornicek F, et al. Transcriptional activation of CBFβ by CDK11p110 is necessary to promote osteosarcoma cell proliferation. Cell Commun Signal. 2019 Dec;17(1):125.
14. Roos A, Satterfield L, Zhao S, Fuja D, Shuck R, Hicks MJ, et al. Loss of Runx2 sensitises osteosarcoma to chemotherapy-induced apoptosis. Br J Cancer. 2015 Nov;113(9):1289–97.
15. Zeng H, Xu X. RUNX2 RNA interference inhibits the invasion of osteosarcoma. Oncology Letters. 2015 Jun;9(6):2455–8.
16. Zelzer E, Glotzer DJ, Hartmann C, Thomas D, Fukai N, Soker S, et al. Tissue specific regulation of VEGF expression during bone development requires Cbfa1/Runx2. Mechanisms of Development. 2001;

17. Kwon TG, Zhao X, Yang Q, Li Y, Ge C, Zhao G, et al. Physical and functional interactions between Runx2 and HIF-1α induce vascular endothelial growth factor gene expression. J Cell Biochem. 2011 Dec;112(12):3582–93.
18. Weng J jie, Su Y. Nuclear matrix-targeting of the osteogenic factor Runx2 is essential for its recognition and activation of the alkaline phosphatase gene. Biochimica et Biophysica Acta (BBA) - General Subjects. 2013 Mar;1830(3):2839–52.
19. Pratap J, Javed A, Languino LR, Van Wijnen AJ, Stein JL, Stein GS, et al. The Runx2 Osteogenic Transcription Factor Regulates Matrix Metalloproteinase 9 in Bone Metastatic Cancer Cells and Controls Cell Invasion. Molecular and Cellular Biology. 2005 Oct 1;25(19):8581–91.
20. Bajpai J, Sharma M, Sreenivas V, Kumar R, Gamnagatti S, Khan SA, et al. VEGF expression as a prognostic marker in osteosarcoma. Pediatric Blood & Cancer. 2009 Dec;53(6):1035–9.
21. Han J, Yong B, Luo C, Tan P, Peng T, Shen J. High serum alkaline phosphatase cooperating with MMP-9 predicts metastasis and poor prognosis in patients with primary osteosarcoma in Southern China. World J Surg Onc. 2012 Dec;10(1):37.
22. Alegre F, Ormonde AR, Godinez DR, Illendula A, Bushweller JH, Wittenburg LA. The interaction between RUNX2 and core binding factor beta as a potential therapeutic target in canine osteosarcoma. Vet Comparative Oncology. 2020 Mar;18(1):52–63.
23. Malik N, Yan H, Moshkovich N, Palangat M, Yang H, Sanchez V, et al. The transcription factor CBFB suppresses breast cancer through orchestrating translation and transcription. Nat Commun. 2019 May 6;10(1):2071.
24. Polunovsky VA, Bitterman PB. The Cap-Dependent Translation Apparatus Integrates and Amplifies Cancer Pathways. RNA Biology. 2006 Jan;3(1):10–7.
25. Schiavone K, Garnier D, Heymann MF, Heymann D. The Heterogeneity of Osteosarcoma: The Role Played by Cancer Stem Cells. In: Birbrair A, editor. Stem Cells Heterogeneity in Cancer [Internet]. Cham: Springer International Publishing; 2019 [cited 2022 Nov 9]. p. 187–200. (Advances in Experimental Medicine and Biology; vol. 1139). Available from: https://link.springer.com/10.1007/978-3-030-14366-4_11
26. Bitterman PB, Polunovsky VA. Translational control of cell fate: From integration of environmental signals to breaching anticancer defense. Cell Cycle. 2012 Mar 15;11(6):1097–107.
27. Chen J, Xu X, Chen J. Clinically relevant concentration of anti-viral drug ribavirin selectively targets pediatric osteosarcoma and increases chemosensitivity. Biochemical and Biophysical Research Communications. 2018 Nov;506(3):604–10.
28. Qi NN, Tian S, Li X, Wang FL, Liu B. Up-regulation of microRNA-496 suppresses proliferation, invasion, migration and in vivo tumorigenicity of human osteosarcoma cells by targeting eIF4E. Biochimie. 2019 Aug;163:1–11.
29. Chang LS, Oblinger JL, Burns SS, Huang J, Anderson LW, Hollingshead MG, et al. Targeting Protein Translation by Rocaglamide and Didesmethylrocaglamide to Treat MPNST and Other Sarcomas. Molecular Cancer Therapeutics. 2020 Mar 1;19(3):731–41.
30. Ran R, Harrison H, Syamimi Ariffin N, Ayub R, Pegg HJ, Deng W, et al. A role for CBFβ in maintaining the metastatic phenotype of breast cancer cells. Oncogene. 2020 Mar 19;39(12):2624–37.

31. Tang Z, Kang B, Li C, Chen T, Zhang Z. GEPIA2: an enhanced web server for large-scale expression profiling and interactive analysis. Nucleic Acids Research. 2019 Jul 2;47(W1):W556–60.
32. Schneider CA, Rasband WS, Eliceiri KW. NIH Image to ImageJ: 25 years of image analysis. Nat Methods. 2012 Jul;9(7):671–5.
33. Smith T, Heger A, Sudbery I. UMI-tools: modeling sequencing errors in Unique Molecular Identifiers to improve quantification accuracy. Genome Res. 2017 Mar;27(3):491–9.
34. Dobin A, Davis CA, Schlesinger F, Drenkow J, Zaleski C, Jha S, et al. STAR: ultrafast universal RNA-seq aligner. Bioinformatics. 2013 Jan 1;29(1):15–21.
35. Ritchie ME, Phipson B, Wu D, Hu Y, Law CW, Shi W, et al. limma powers differential expression analyses for RNA-sequencing and microarray studies. Nucleic Acids Research. 2015 Apr 20;43(7):e47–e47.
36. Robinson MD, Oshlack A. A scaling normalization method for differential expression analysis of RNA-seq data. Genome Biol. 2010;11(3):R25.
37. Law CW, Chen Y, Shi W, Smyth GK. voom: precision weights unlock linear model analysis tools for RNA-seq read counts. Genome Biol. 2014;15(2):R29.
38. Smyth GK. Linear Models and Empirical Bayes Methods for Assessing Differential Expression in Microarray Experiments. Statistical Applications in Genetics and Molecular Biology. 2004 Jan 12;3(1):1–25.
39. Welm BE, Dijkgraaf GJP, Bledau AS, Welm AL, Werb Z. Lentiviral Transduction of Mammary Stem Cells for Analysis of Gene Function during Development and Cancer. Cell Stem Cell. 2008 Jan;2(1):90–102.
40. Dull T, Zufferey R, Kelly M, Mandel RJ, Nguyen M, Trono D, et al. A Third-Generation Lentivirus Vector with a Conditional Packaging System. J Virol. 1998 Nov 1;72(11):8463–71.
41. Shen R, Wang X, Drissi H, Liu F, O'Keefe RJ, Chen D. Cyclin D1-Cdk4 Induce Runx2 Ubiquitination and Degradation. Journal of Biological Chemistry. 2006 Jun;281(24):16347–53.
42. Choi YH, Kim YJ, Jeong HM, Jin YH, Yeo CY, Lee KY. Akt enhances Runx2 protein stability by regulating Smurf2 function during osteoblast differentiation. FEBS J. 2014 Aug;281(16):3656–66.
43. Shimazu J, Wei J, Karsenty G. Smurf1 Inhibits Osteoblast Differentiation, Bone Formation, and Glucose Homeostasis through Serine 148. Cell Reports. 2016 Apr;15(1):27–35.
44. Zhao M, Qiao M, Oyajobi BO, Mundy GR, Chen D. E3 Ubiquitin Ligase Smurf1 Mediates Core-binding Factor α1/Runx2 Degradation and Plays A Specific Role in Osteoblast Differentiation. Journal of Biological Chemistry. 2003 Jul;278(30):27939–44.
45. Qin X, Jiang Q, Matsuo Y, Kawane T, Komori H, Moriishi T, et al. Cbfb Regulates Bone Development by Stabilizing Runx Family Proteins. Journal of Bone and Mineral Research. 2015 Apr 1;30(4):706–14.
46. Lim KE, Park NR, Che X, Han MS, Jeong JH, Kim SY, et al. Core Binding Factor β of Osteoblasts Maintains Cortical Bone Mass via Stabilization of Runx2 in Mice. Journal of Bone and Mineral Research. 2015 Apr 1;30(4):715–22.
47. Kim W, Bennett EJ, Huttlin EL, Guo A, Li J, Possemato A, et al. Systematic and Quantitative Assessment of the Ubiquitin-Modified Proteome. Molecular Cell. 2011 Oct;44(2):325–40.
48. Lee HK, Park SH, Nam MJ. Proteasome inhibitor MG132 induces apoptosis in human osteosarcoma U2OS cells. Hum Exp Toxicol. 2021 Nov;40(11):1985–97.

49. Mou D, Yang X, Li S, Zhao W, Li M, Zhao M, et al. MG132 inhibits the expression of PBX3 through miRNAs by targeting Argonaute2 in hepatoma cells. Saudi Journal of Biological Sciences. 2020 Aug;27(8):2157–63.
50. Han L, Zhu B, Chen H, Jin Y, Liu J, Wang W. Proteasome inhibitor MG132 inhibits the process of renal interstitial fibrosis. Exp Ther Med [Internet]. 2019 Feb 28 [cited 2024 Mar 27]; Available from: http://www.spandidos-publications.com/10.3892/etm.2019.7329
51. You J, Lee E, Bonilla L, Francis J, Koh J, Block J, et al. Treatment with the Proteasome Inhibitor MG132 during the End of Oocyte Maturation Improves Oocyte Competence for Development after Fertilization in Cattle. Singh SR, editor. PLoS ONE. 2012 Nov 7;7(11):e48613.
52. Wang D, Xu Q, Yuan Q, Jia M, Niu H, Liu X, et al. Proteasome inhibition boosts autophagic degradation of ubiquitinated-AGR2 and enhances the antitumor efficiency of bevacizumab. Oncogene. 2019 May;38(18):3458–74.
53. Cheng A, Genever PG. SOX9 determines RUNX2 transactivity by directing intracellular degradation. Journal of Bone and Mineral Research. 2010 Dec 1;25(12):2680–9.
54. Mauvezin C, Neufeld TP. Bafilomycin A1 disrupts autophagic flux by inhibiting both V-ATPase-dependent acidification and Ca-P60A/SERCA-dependent autophagosome-lysosome fusion. Autophagy. 2015 Aug 3;11(8):1437–8.
55. Moriyasu Y, Inoue Y. Chapter Thirty-Two Use of Protease Inhibitors for Detecting Autophagy in Plants. In: Methods in Enzymology [Internet]. Elsevier; 2008 [cited 2024 Mar 27]. p. 557–80. Available from: https://linkinghub.elsevier.com/retrieve/pii/S0076687908032321
56. Chen W, Smeekens JM, Wu R. Systematic study of the dynamics and half-lives of newly synthesized proteins in human cells. Chem Sci. 2016;7(2):1393–400.
57. Dai CL, Shi J, Chen Y, Iqbal K, Liu F, Gong CX. Inhibition of Protein Synthesis Alters Protein Degradation through Activation of Protein Kinase B (AKT). Journal of Biological Chemistry. 2013 Aug;288(33):23875–83.
58. Matthiesen R, editor. Proteostasis: Methods and Protocols [Internet]. New York, NY: Springer New York; 2016 [cited 2024 Mar 27]. (Methods in Molecular Biology; vol. 1449). Available from: http://link.springer.com/10.1007/978-1-4939-3756-1
59. Morey TM, Esmaeili MA, Duennwald ML, Rylett RJ. SPAAC Pulse-Chase: A Novel Click Chemistry-Based Method to Determine the Half-Life of Cellular Proteins. Front Cell Dev Biol. 2021 Sep 7;9:722560.
60. Zhang XH, Tee LY, Wang XG, Huang QS, Yang SH. Off-target Effects in CRISPR/Cas9-mediated Genome Engineering. Molecular Therapy - Nucleic Acids. 2015;4:e264.
61. Alvarez-Castelao B, Ruiz-Rivas C, Castaño JG. A Critical Appraisal of Quantitative Studies of Protein Degradation in the Framework of Cellular Proteostasis. Biochemistry Research International. 2012;2012:1–11.
62. Moritz B, Becker PB, Göpfert U. CMV promoter mutants with a reduced propensity to productivity loss in CHO cells. Sci Rep. 2015 Dec;5(1):16952.
63. Teschendorf C, Warrington KHJ, Siemann DW, Muzyczka N. Comparison of the EF-1 alpha and the CMV promoter for engineering stable tumor cell lines using recombinant adeno-associated virus. Anticancer research. 2002;22(6A):3325–30.
64. He L, Winterrowd C, Kadura I, Frye C. Transgene copy number distribution profiles in recombinant CHO cell lines revealed by single cell analyses. Biotechnology and Bioengineering. 2012;109(7):1713–22.

65. Wang X, Xu Z, Tian Z, Zhang X, Xu D, Li Q, et al. The EF-1α promoter maintains high-level transgene expression from episomal vectors in transfected CHO-K1 cells. Journal of Cellular and Molecular Medicine. 2017;21(11):3044–54.
66. Warren AJ. Structural basis for the heterodimeric interaction between the acute leukaemia-associated transcription factors AML1 and CBFbeta. The EMBO Journal. 2000 Jun 15;19(12):3004–15.
67. Shin MH, He Y, Marrogi E, Piperdi S, Ren L, Khanna C, et al. A RUNX2-Mediated Epigenetic Regulation of the Survival of p53 Defective Cancer Cells. PLoS Genet. 2016 Feb 29;12(2):e1005884.

Chapter 3

Mutations in the RUNX2 binding pocket of CBFβ alter its cellular activity in osteosarcoma cells

Abstract

Osteosarcoma (OS) is a highly aggressive form of bone cancer that most commonly presents early in age, and treatment options have remained unchanged in the last 30 years. OS tumors are highly hetereogeneic and lack bona-fide driver mutations, hampering therapeutic development and necessitating study of methods to overcome this. Previous data in our hands and another lab have suggested that core binding factor subunit beta (CBFβ), a transcriptional co-activator to the RUNX family of transcription factors, may perform a noncanonical role as a regulator of protein translation. This is of particular interest in OS, as targeting protein translation could provide a mechanism to prevail over the heterogeneity in OS tumor samples. Elucidating the relevance of this translational role of CBFβ to the malignant phenotype of OS is challenging, as CBFβ is shuttled away from the cytoplasm and into the nucleus by RUNX proteins, yet this non-canonical role of CBFβ is suggested to occur in the cytoplasm. These two roles of CBFβ may be antagonistic to each other, so we endeavored to decouple them in order to better study this putative non-canonical role of CBFβ. To this end, we produced CBFβ and RUNX2 in a recombinant system and used synthetic peptides to validate residues key in their interaction. We then generated stable cell lines expressing CBFβ with point mutations at these residues, and assessed the influence of these mutations on CBFβ-RUNX2 interaction and subsequent nuclear shuttling. In our recombinant system and in accordance with previous research, G61 and N63 of CBFβ appear important to CBFβ-RUNX2 interaction. Mutation of these residues and N104 of CBFβ to alanine yielded a mutant form of CBFβ which exhibited drastically reduced RUNX2 binding and nuclear shuttling.

Introduction

Osteosarcoma is the most common form of primary bone cancer in humans and canines, with ~1,000 new cases diagnosed per year in the United States (1). Age of diagnosis of OS has a bimodal distribution, with the first, and largest, peak in the 10-14-year-old age group, with the second for patients aged 65+ (2). The standard of care for OS is so-called MAP therapy (methotrexate, adriamycin, and cisplatin) (3), a regimen which hasn't changed in more than 30 years (4). Much of the difficulty in developing new therapies in OS has been due to the lack of identified driver mutations in this disease. In lieu of being caused by specific mutations which could be leveraged therapeutically, OS instead presents as a collection of widespread chromosomal abnormalities (5), with chromosome counts ranging from haploid up to hexaploid (6,7).

RUNX2 is a member of the RUNX family of DNA-binding transcription factors and is known as the master regulator of bone growth. RUNX2 plays a critical role in chondrocyte maturation and osteoblast differentiation (8), and high levels of RUNX2 (9,10) and many of its gene targets (11–14) have been implicated in poor therapeutic outcome in OS (15,16). CBFβ acts as a transcriptional co-activator to the RUNX proteins, binding to them to form a CBFβ-RUNX heterodimer. CBFβ is crucial for skeletal development (17–19), and although the RUNX proteins can bind DNA on their own (20), their affinity for DNA is greatly enhanced by interaction with CBFβ (21,22). In addition to RUNX2, high expression of CBFβ itself is also correlated with poor prognosis in OS (23). These data have led to the aforementioned proteins being proposed as a novel therapeutic target in OS (24).

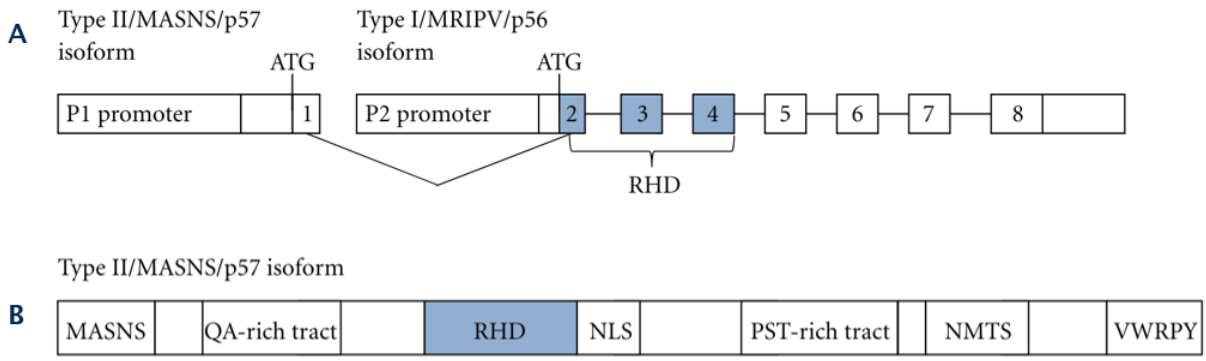

Figure 3.1 A) Gene structure of RUNX2. Isoform MASNS is encoded from all eight exons, with transcription start at promoter P1, while isoform MRIPV is encoded from exons two through eight with transcription initiation at promoter P2. B) Protein structure of RUNX2 Type II isoform. Diagram sourced from (25).

Structure of RUNX2. RUNX proteins are identified by the Runt homology domain (RHD) (25), which is required for their interaction with DNA (26). This domain is located close to the N terminus and is ~90% conserved between each member of the RUNX family, with the PyGPyGGTPy consensus sequence being essential for interaction with DNA as well as CBFβ (27) **(Figure 3.1)**. Upstream of the RHD is the glutamine-alanine (QA) repeat region, which plays a role in transactivation (28). Adjacent to the RHD lies the nuclear localization signal (NLS), a sequence of nine amino acids which allows translocation of RUNX proteins from the cytoplasm to the nucleus (29). The C-terminus is essential for RUNX2 function (30,31), and contains the proline-serine-threonine-rich (PST) region which has both transactivatory and transinhibitory functions (29,31). The nuclear matrix targeting signal (NMTS) is located within the PST region, and in concert with the NLS helps localize RUNX2 to the nucleus (32). Finally, the ending five residues in the PST region, referred to as VWRPY, act as a transcriptional repression domain

(33,34). RUNX2 is expressed as two isoforms, Type II/MASNS/p57 and Type I/MRIPV/p56, which are each produced via initiation of transcription at P1 or P1 promoters, respectively (35).

Mutations in RUNX2 or CBFβ can have significant consequences to health. Mutations in RUNX2 are strongly implicated in cleidocranial dysplasia (CCD) (36), a disease characterized by complications with tooth and bone development. Mutations in patients with CCD are commonly found in the RHD (37), and interfere with DNA binding (38) or heterodimerization with CBFβ (36). Mutations in CBFβ, in the form of translocations, are found in a large percentage of human leukemias (39). These translocations are most commonly in the form of CBFβ-SMMHC, a fusion protein with altered affinity to RUNX1 (40) consisting of the heterodimerization domain of CBFβ fused to the coiled-coil domain of smooth muscle myosin heavy chain (40,41).

CBFβ lacks an NLS (42) and relies on the RUNX proteins to be shuttled into the nucleus. While the traditional role of CBFβ as a transcriptional co-activator in the nucleus is well-described, recent research has proposed that it performs a non-canonical role in the cytoplasm as a regulator of protein translation (43). This is especially interesting in the context of OS, as protein translation is a convergence point of multiple signaling pathways (44), and targeting this process therapeutically could provide a route to overcome the high degree of heterogeneity amongst OS patient tumors (45). According to observations thus far only documented in breast cancer cell lines, CBFβ binds to RNAs through hnRNPK, and thereby regulates the translation of proteins via eIF4B (43).

In our hands as well as published research, knockout of CBFβ leads to a reduction in RUNX protein expression (43), and knockout of one of the RUNX proteins leads to a compensatory up-regulation in other RUNX proteins (46,47). Additionally, shuttling of CBFβ into the nucleus by RUNX proteins may decrease the cytoplasmic pool of CBFβ available to modulate translation.

Given the apparent mutual exclusivity of CBFβ binding to RUNX proteins or hnRNPK (43), and the roles accomplished through binding to each occurring in separate cellular compartments, it's possible these roles are antagonistic in some manner.

The strongly intertwined nature of RUNX proteins and CBFβ makes individual study of CBFβ challenging, so we endeavored to inhibit the transcriptional role of CBFβ in order to isolate and study the role CBFβ may play in protein translation. Inhibition of the transcriptional role of CBFβ via small molecule was first attempted (24,48), however the compound we tested did not significantly interrupt CBFβ interaction with RUNX2. Instead, we opted to inhibit the transcriptional role of CBFβ by introducing point mutations into the RUNX2 binding face of CBFβ, with the goal of interrupting CBFβ-RUNX2 interaction and subsequent nuclear shuttling of CBFβ. Cell lines expressing this mutant form could then allow further study of the role of CBFβ in protein translation, as well as add clarity into potential competition between RUNX proteins and hnRNPK for the same binding site on CBFβ.

Materials and Methods

Cell Lines and Culture Conditions

Parental U2OS and U2OS-derived cell lines were maintained in McCoy's 5A (Iwakata & Grace Modification) media supplemented with 10% FBS and 1% P/S as previously described in Chapter 2.

Recombinant RUNX2 and CBFβ Production

Vector Design: RUNX2 was cloned out of Genscript pcDNA3.1 OHu22872 containing NM_001024630.4 using primers outlined in **Table 1**. RUNX2 was then inserted into pGEX 6.1 expression vector using PasI and XhoI restriction enzymes from New England Biolabs (NEB). Restriction digestion was accomplished sequentially in recommended buffers with 1% agarose gel purification cleanup between digestions. Following gel purification, DNA was extracted from gels using Thermo Fisher GeneJET gel extraction kit according to manufacturer's recommendations, with elution accomplished by 30 µL nuclease-free water. Following this, insert and vector were mixed together in 3:1 stoichiometric ratio of insert:vector and ligated using T4 Ligase from Thermo Fisher according to manufacturer's recommendations. The ligated vector was then transformed into NEB5α *E. coli* according to manufacturer's recommendations, then plated on LB Agar plates containing 100 µg/mL carbenicillin and grown at 37°C overnight. Single colonies growing in the presence of 100 µg/mL carbenicillin were selected and used to inoculate 5 mL of LB broth supplemented with 100 µg/mL carbenicillin and grown overnight at 37°C with 180 rpm shaking. Following overnight outgrowth, plasmid was extracted using Thermo Fisher GeneJET Plasmid Miniprep system according to manufacturer's recommendations, with elution

accomplished by addition of 30 µL nuclease-free water. Eight hundred (800) ng of purified plasmid was sent to Sanger sequencing at Azenta Labs for verification of successful cloning. pGEX vector incorporating RUNX2 was then transformed into NEB T7 Express *E. coli* according to manufacturer's recommendations, then plated on LB Agar plates containing 100 µg/mL carbenicillin and grown at 37°C overnight. Following transformation, a single colony was selected and used to inoculate five mL of LB + 100 µg/mL carbenicillin, which was grown overnight at 37°C with 180 rpm shaking. Following overnight growth, 500 µL of bacterial culture was mixed with 500 µL of 1:1 Glycerol:LB media (v/v) and frozen in cryovials at -80°C until recombinant protein production steps below.

CBFβ was cloned out of Genscript pcDNA3.1 OHu25418 incorporating NM_022845.3 using primers outlined in **Table 1**. Insert was cloned into the pTXB1 expression vector, which imparted an Mxe intein/chitin binding domain (CBD) at the C-terminus. Insertion was accomplished via simultaneous digestion by XhoI and SapI (NEB) restriction enzymes in NEB Cutsmart 3.1 buffer according to manufacturer's recommendations, followed by ligation as described above. Finally, sequence verification, transformation into NEB T7 Express, outgrowth and creation of frozen glycerol stocks was accomplished as described previously.

Table 1: Primers for Recombinant Protein Production

Usage	Primer Sequence
Add TspMI restriction site to RUNX2 N term for cloning into pGEX-6P-1 F	5'-GGTGGTCCCTGGGCATG GCATCAAACAGCCTCTT-3'
Add XhoI restriction site to RUNX2 C-term for cloning into pGEX-6P-1 R	5'-GGTGGTC'TCGAGTCAATA TGGTCGCCAAACAG-3'
Add NdeI restriction site to CBFb N-term for cloning into pTXB1 F	5'-GGTGGTC'ATATGATGCCG CGCGTCGTGCCCGA-3'
Add SapI restriction site to CBFb C- term for cloning into pTXB1 R	5'-GGTGGTTGCTCTTCC'GCAAC GAAGTTTGAGGTCATCAC-3'
Remove extra N-term Met from CBFβ-pTXB1 F	5'-CCGCGCGTCGTGCCCGAC-3'
Remove extra N-term Met from CBFβ-pTXB1 R	5'-CATATGTATATCTCCTTCTTAAAGTT AAACAAAATTATT TCTAGAGGGGAATTGTTATCCGCTC-3'

Recombinant Protein Expression: A glycerol stock containing NEB T7 Express *E. coli* cells harboring either recombinant RUNX2-GST or CBFβ-CBD was thawed at room temp for 1 min, then 10 µL of culture was used to inoculate 50 mL of LB broth supplemented with 100 µg/mL carbenicillin. Inoculated media was grown overnight at 37°C with 180 rpm shaking. The following day, the 50 mL culture was used to inoculate a 1L flask of LB supplemented with 100 µg/mL carbenicillin, which was then grown at 37°C with 180 rpm shaking. Optical density (OD) measurements were taken periodically and culture was induced for protein expression at OD ~0.6 by addition of isopropyl β-D-thiogalactoside (IPTG) (Millipore Sigma) to 0.5 mM final concentration. Following induction, cultures were incubated overnight at 16°C with 150 rpm shaking. The following day cultures were spun down at 3,200g in a tabletop centrifuge set to 4°C until the entire culture was pelleted. The supernatant was discarded and pellets were stored at -80°C overnight. Pellets were then thawed on ice and resuspended using lysis buffer consisting of

20 mL PBS supplemented with 1 cOmplete protease inhibitor cocktail tablet and 0.5mM PMSF final concentration. Bacteria slurry was placed on ice and sonicated for 19 min consisting of 10 seconds on and 10 seconds off, using a Fisherbrand Sonic Dismembrator sonicator with amplitude set to 43. Lysate was then spun down at 17,000 g for 20 min. at 4°C to yield clarified lysate, and pellet was discarded.

Recombinant CBFβ Purification: CBFβ was purified from clarified lysate by 2h rotation at 4°C with 2.5mL bed volume pre-washed NEB chitin resin. Lysate and bead mixture was then poured into a 10 mL Pierce Disposable Column (Thermo Fisher), and 200 mL ice cold PBS was poured through column to wash beads. Beads were then incubated at 4°C for 4 days in 10 mL PBS with 50mM DTT to cleave chitin tag. Free CBFβ was eluted from column into a tube and PBS was added to bring volume to 30 mL total. Solution was then concentrated by centrifugation at 4°C and 3,200g with an Amicon 3 kilodalton molecular weight cutoff spin concentrator tube (Millipore Sigma). Following concentration down to 2 mL total volume, purified protein was desalted by passing through Thermo Fisher Zeba spin desalting columns twice, according to manufacturer's recommendations.

Recombinant RUNX2 Purification: RUNX2 was purified from clarified lysate by 1.5h rotation at 4°C with 1.25mL bed volume pre-washed Pierce Glutathione Agarose GSH beads (Thermo Fisher). Beads were then spun down at 700g at 4°C, then washed 3x with PBS supplemented with 0.1% Triton x-100. Beads were suspended in sufficient PBS + 0.1% Tritox-100 to achieve a 50% slurry, and kept at 4°C until time of assay start.

Recombinant Protein Expression Verification: Recombinant expression of RUNX2 and CBFβ was verified by running on SDS-PAGE as described previously in Chapter 2. Gel was then

stained using GelCode™ Blue Safe Protein Stain according to manufacturer's recommendations. Gel was then imaged using ProteinSimple imaging platform set to epi white imaging settings.

RUNX2-CBFβ Binding Assay

Pulldown Assay Performance: 47 femtomoles of recombinant CBFβ and 378 femtomoles of recombinant RUNX2-GST bound to GSH agarose beads were spiked into 1,920 uL of PBS supplemented with 0.1% Triton x-100 and placed on a rotator overnight at 4°C. Beads were then washed 3x with 1 mL PBS + 0.1% Triton x-100, and bound proteins were eluted by addition of 42 uL SDS-PAGE sample buffer (5:1:14 ratios of 4x Laemmle Buffer:1M DTT in water:1x PBS) and heated at 70°C for 10 min. with occasional vortex mixing. Beads were spun down for 10 seconds at 1,000g and supernatant was diluted 81x with SDS-PAGE sample buffer, then subjected to western blotting analysis as previously described. PVDF membranes were probed with CST α-CBFβ antibody #D4N2N diluted 1:10,000 and CST α-RUNX2 antibody #D1L7F diluted 1:50,000, all in 5% NFDM in TBST.

Peptide Production and Dilution: RUNX2-derived peptide (GNDENYSAEL) and CBFβ-derived peptide (ATGTNLSLQFF) were synthesized by Genscript and solvated in DMSO to 30 mg/mL and stored at 4°C. As RUNX2 and CBFβ-derived peptides have different properties, a separate control peptide for each was chosen. Sequence SSLTNGLFR was selected as a control peptide for CBFβ-derived sequence, and sequence IATEAIENIR was selected as a control peptide for RUNX2-derived sequence. Control peptides were synthesized by Celtek Peptides (Franklin, TN) and also solvated to 30 mg/mL in DMSO and stored at 4°C.

Pulldown with CBFβ-derived Peptide: 378 femtomoles of recombinant RUNX2 was pre-incubated with 3.78 or 37.8 picomoles CBFβ-derived peptide or control peptide for 1h at 4°C on a rotator. Following pre-incubation, 47 femtomoles of recombinant CBFβ was spiked into tube and pulldown was accomplished as described above.

Pulldown with RUNX2-derived Peptide: 47 femtomoles of recombinant CBFβ was pre-incubated with 470 or 4,700 picomoles RUNX2-derived peptide or control peptide for 1h at 4°C on a rotator. Following pre-incubation, 378 femtomoles of recombinant RUNX2 was spiked into tube and pulldown was accomplished as described above.

Structural Modeling

3D structure of CBFβ bound to RUNX2 (PDB #6VGE) (49) was rendered using the PyMOL Molecular Graphics System, Version 2.4.1, Schrödinger, Incorporated. ERG and 16mer DNA strand in original structure were hidden from view and sidechains of CBFβ residues G61, N63, and N104 were made visible along with their respective Hydrogen bonds.

Lentiviral Transduction

Plasmid Design: CBFβ 3x Mut (G61A, N63A, N104A) was generated through site directed mutagenesis of pHIV-EGFP incorporating wild-type (wt) CBFβ_FLAG, generated previously. Mutagenesis was accomplished using NEB Q5 Mutagenesis Kit according to manufacturer's instructions, with primers used listed in **Table 2**. Mutagenesis was accomplished in two separate

reactions, with vector transformed into NEB Stable cells in between reactions as previously described, and plasmids were sent for Sanger sequence verification by Azenta Labs.

Table 2: Primer sequences for Lentiviral Vector Generation

Usage	**Primer Sequence**
Mutate CBFβ N104A F	5'-CATGATTCTGGCCGGAGTCTGTGTTATC-3'
Mutate CBFβ N104A R	5'-GGAGCCTTCAAATATACC -3'
Mutate CBFβ G61A and N63A F	5' CGCACTGTCTCTCCAGTTTTTTCC 3'
Mutate CBFβ G61A and N63A R	5' GTCGCTGTGGCCACAAAAGCGAT 3'
Sequence T7	5'- TCAAGCCTCAGACAGTGGTTC-3'
Begin Sanger sequencing at EF-1α promoter	5'- TCAAGCCTCAGACAGTGGTTC-3'

U2OS CBFβ KO cells were subjected to lentiviral transduction using same protocol as outlined previously, this time using transfer plasmid pHIV-EGFP CBFβ_FLAG (3xMut) generated as described below. Cells infected by 1953x dilution of lentiviral particles were chosen for outgrowth in a T75 flask based on <5% EGFP+ cells. As previously mentioned, this dilution was chosen to minimize risk of double integration from lentivirus. Sorting of individual cells and outgrowth to generate monoclonal cell lines was conducted as previously outlined.

Cellular Electrothermal Shift Assay (CETSA)

U2OS-derived cell lines were grown on 10 cm plates to 70% confluence then harvested via Trypsin. Cells were then washed with PBS twice, diluted 10x with 0.2% Trypan Blue in PBS (MP Biomedicals, LLC, Irvine, CA) and counted with a hemocytometer (Thermo Fisher). A cell suspension of 5.6 million cells/mL was prepared in PBS supplemented with 1x cOmplete protease inhibitor tablet (Thermo Fisher) and 1mM PMSF (Sigma-Aldrich). 100 µL of cell suspension was

placed into each of two PCR tubes, with one tube placed into a SimpliAmp Thermocycler (Life Technologies, Carlsbad, CA) and incubated at 40°C - 68°C (during RUNX2 melting temp assessment) or 49.5°C (during CETSA cell line panel) for 3 min while the other was incubated at room temperature for the same duration. Following incubation, cell suspensions were flash frozen by immersion in liquid nitrogen for 1 min, then thawed at 25°C for 5 min. Cell suspensions were flash frozen and thawed again, then spun down at 20,000g for 20 min. at 4°C. Supernatant was transferred to a fresh tube and mixed with Laemmle buffer and DTT to 1x and 50 mM final concentrations, respectively, and heated at 70°C with occasional vortex mixing for 10 minutes. Sample was then analyzed via western blotting as previously described.

Nuclear and Cytoplasmic Fractionation

Nuclear and cytoplasmic fractionations were performed with Thermo Fisher NE-PER Kit, #78833 with slight modifications to manufacturer's recommendations. In short, the nuclear pellet was subjected to an additional wash with 200:11 (v/v) Cytoplasmic Extraction Reagent (CER) I :CER II, and pellet was vortex mixed with wash for 5 minutes. Wash was then removed with gel-loading pipette tip. Nuclear Extraction Reagent (NER) was added in manufacturer's recommended proportions, and nuclear pellet was broken up by 8 cycles of sonicating for 30s, vortexing for 15s, and placing on ice for 5 min. Samples were then centrifuged at 16,000g for 10 min. at 4°C, and placed on ice. Extracts were then mixed with NuPage Laemmle Buffer and DTT to 1x and 50mM final concentrations, respectively, and analyzed via western blotting as described previously.

Statistical Analyses

Figure 3.7C,D: Error bars are SD, n=5 (biological); * = $p<0.05$, **** = $p<0.001$, one-way ANOVA with Tukey's post hoc test. ***Figure 3.8D:*** Error bars are SD, n=3 (biological); *** = $p<0.001$, **** = $p<0.0001$, one-way ANOVA with Tukey's post hoc test.

Results

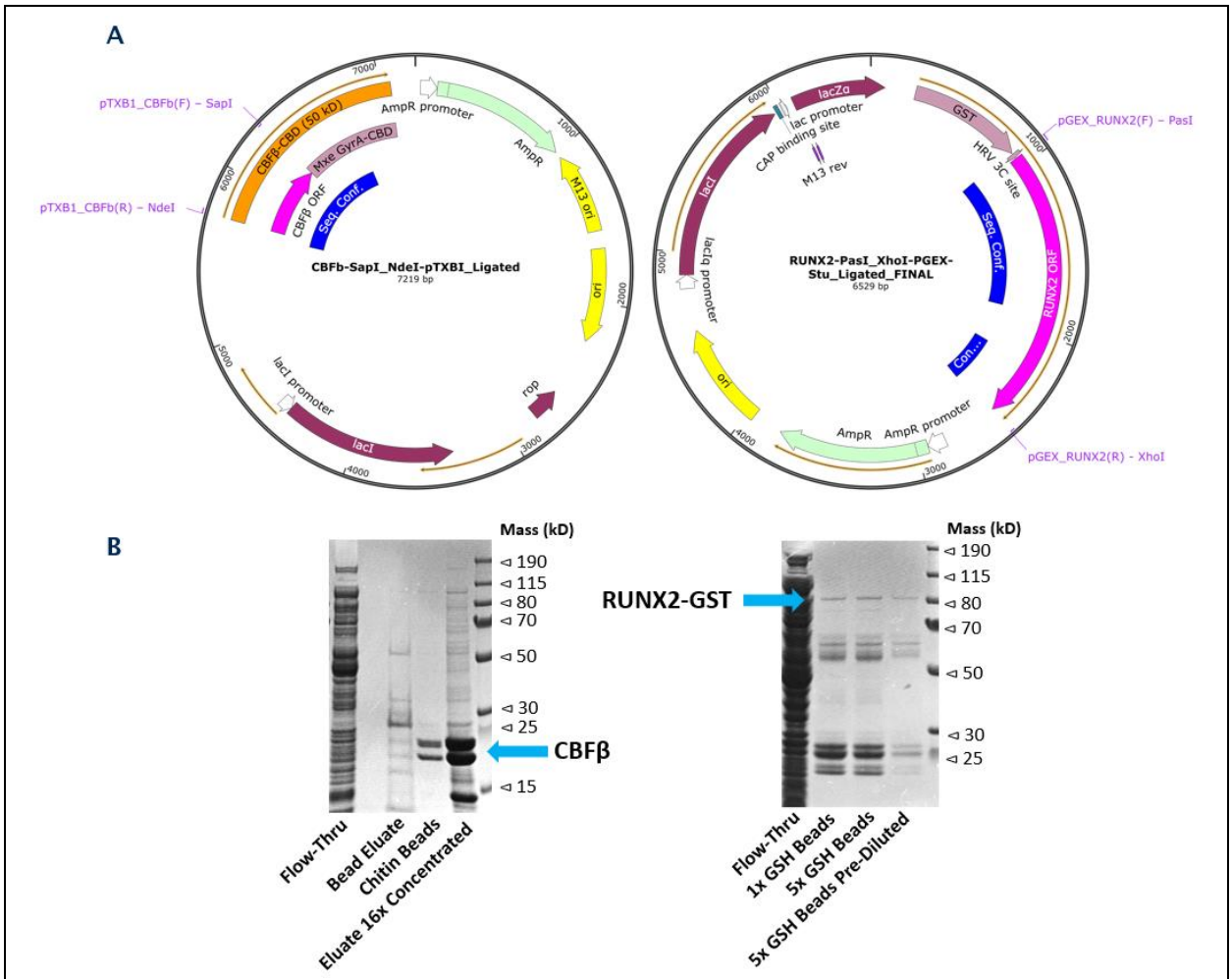

Figure 3.2 A) Plasmid maps of CBFβ cloned into pTXB1 expression vector at left, and RUNX2 cloned into pGEX expression vector at right. Cloning was verified by Sanger sequencing, with sequencing confirmed regions highlighted in blue. Primers for cloning in with restriction enzymes were highlighted in purple text. B) Coomassie blue stained SDS-PAGE gels of fractions generated during purification process, with purified protein loaded in 2nd lane from right on each gel.

CBFβ and RUNX2 were successfully cloned into pTXB1 and pGEX vectors, expressed, and purified recombinantly. Cloning of CBFβ and RUNX2 into their respective expression vectors was successful as verified by Sanger sequencing. Purification endeavors of both proteins were also

successful, with the above gels representing eluates from a 1L culture of NEB5α cells. Purified CBFβ produced much darker bands on the gel than did RUNX2-GST. Faint bands additional to proteins of interest were present in both purified CBFβ and RUNX2.

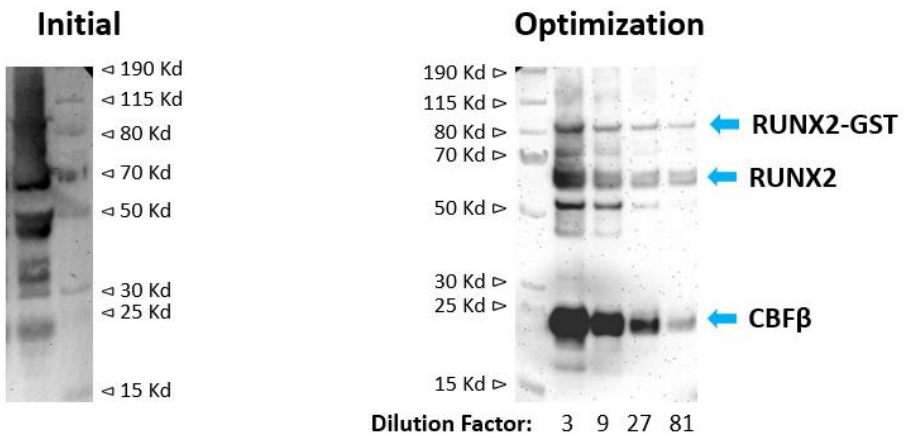

Figure 3.3 Western blot readout of recombinant CBFβ-RUNX2 pulldown assay pre- and post-optimization.

Optimization of CBFβ-RUNX2 recombinant pulldown assay. A pulldown assay was conducted to verify interaction of recombinant CBFβ and RUNX2. Initial western blot was unreadable and successful interaction of recombinant CBFβ and RUNX2 could not be concluded. Pulldown conditions and antibody concentrations were optimized to yield a cleaner blot, and verify conclusively that recombinant CBFβ and RUNX2 do indeed interact. Optimized conditions were then used for further pulldown assays.

Figure 3.4 Diagram of reference sequences for RUNX2 and CBFβ with residues involved in their interaction highlighted in red. Sections highlighted in grey represent sequences chosen for candidate peptide inhibitors.

RUNX2 region G108-L117 and CBFβ region G61-G69 were selected for targeting via a synthetic peptide. We delved into the literature and compiled a list of all residues which appear to contribute to CBFβ-RUNX2 interaction, generating the above figure as guidance. Based on these data, we elected to use peptides mirroring the sequence of RUNX2 in region G108-L117 and the sequence of CBFβ in region G61-G69.

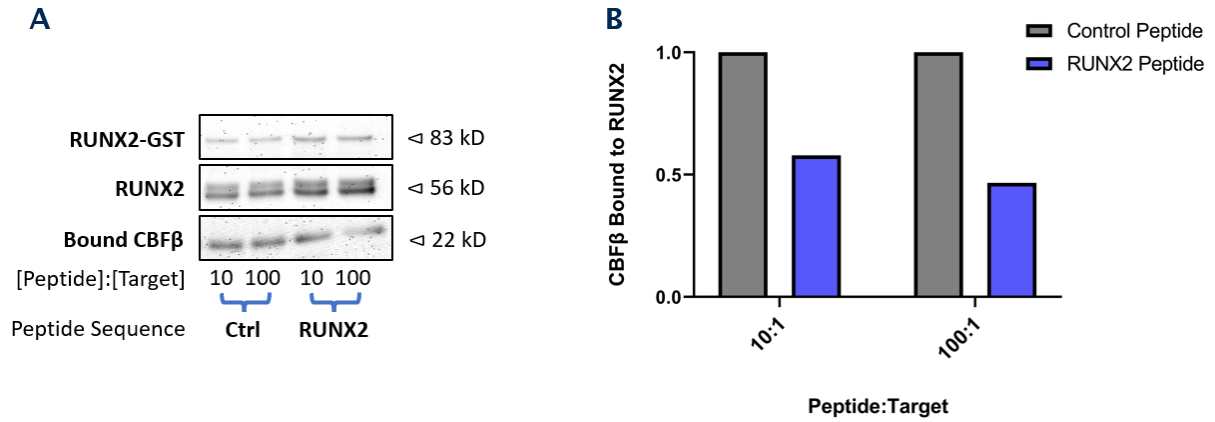

Figure 3.5 A) Western blotting data of recombinant binding assay conducted in the presence of 10 or 100x molar excess of a peptide mirroring the G108-L117 region of RUNX2. B) Densitometry of the blot in A, evaluating the quantity of CBFβ remaining bound to RUNX2-GST, normalized to RUNX2-GST.

Recombinant RUNX2 and CBFβ interaction is inhibited by a peptide mirroring the sequence of RUNX2. When pulldown of recombinant CBFβ by recombinant RUNX2-GST was attempted in the presence of a peptide crafted after the sequence of RUNX2 (GNDENYSAEL), we saw a dose-dependent inhibition of CBFβ-RUNX2 interaction. This was evaluated by normalizing CBFβ to RUNX2-GST, then normalizing that to equal quantity of control peptide. We did not see inhibition of CBFβ-RUNX2 interaction when attempting pulldown in the presence of a peptide mirroring the sequence of CBFβ (ATGTNLSLQFF) (data not shown).

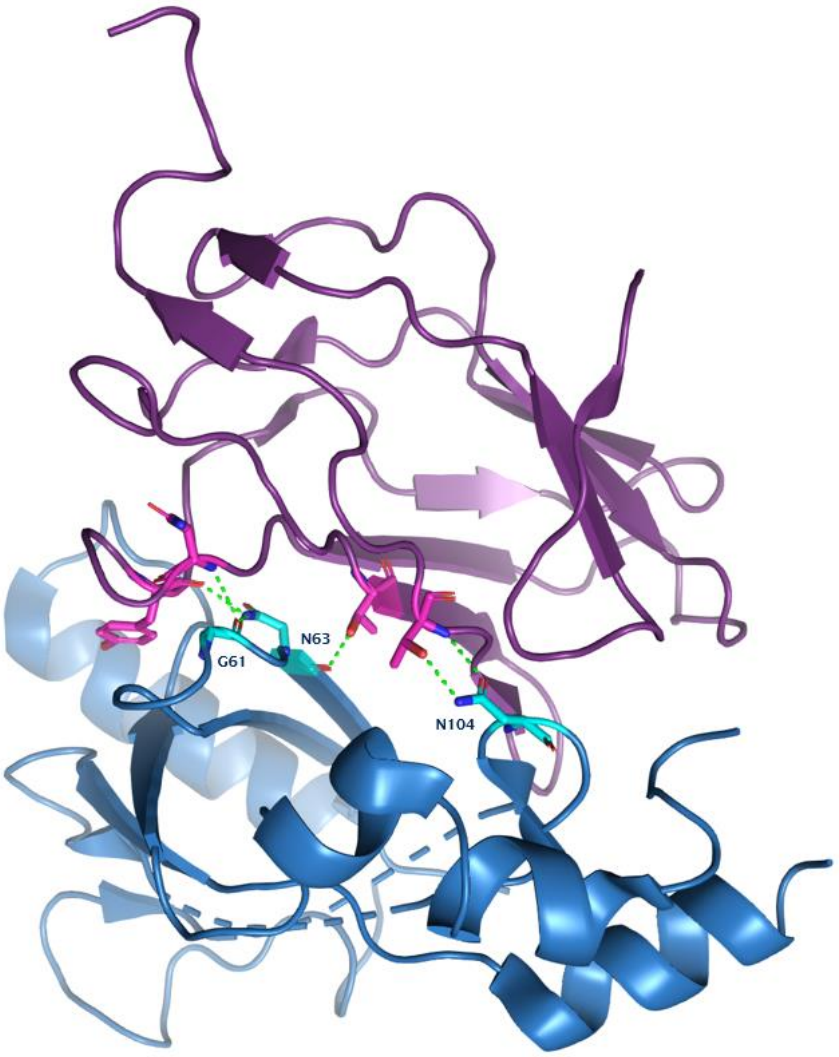

Figure 3.6 Rendering of PDB #6VGE showing RUNX2 (purple) interacting with CBFβ (blue). Residues of CBFβ targeted for mutation are visualized in teal, with residues on RUNX2 they interact with visualized in magenta. Hydrogen bonds between key residues of CBFβ and RUNX2 are highlighted in neon green.

Structure of CBFβ bound to RUNX2 provides visual clues of key amino acids. RUNX2 bound to CBFβ was rendered in Pymol referencing structure #6VGE, with color coding done to accentuate the two proteins as well as clearly display the key residues selected for mutation into alanine.

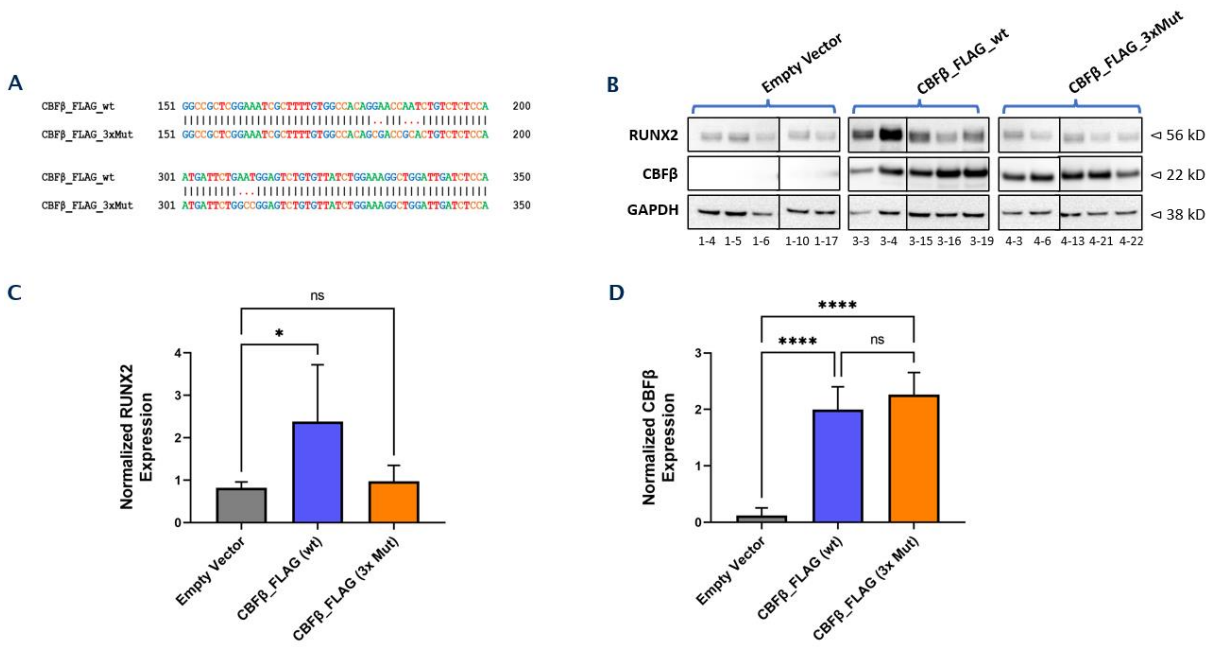

Figure 3.7 A) Color coded sequence diagram illustrating base pair changes made to CBFβ_FLAG_WT in order to produce CBFβ _FLAG_3xMut. B) Representative western blot images showing RUNX2, CBFβ, and GAPDH expression in U2OS CBFβ KO cells transduced with lentiviral transfer plasmids containing either Empty Vector, CBFβ _FLAG_wt, or CBFβ _FLAG_3xMut. Numerical designations below each lane denote clone number used, five clones total. C) Densitometry of RUNX2 expression from previous blot, normalized to GAPDH. D) Densitometry of CBFβ expression from previous blot, normalized to GAPDH.

Stable expression of a mutant form of CBFβ is unable to rescue low RUNX2 protein expression. To investigate the significance of CBFβ-RUNX2 binding in the regulation of RUNX2 protein expression by CBFβ, we mutated previously validated residues glycine 61, asparagine 63, and an additional residue, asparagine 104, of CBFβ to alanine using site-directed mutagenesis (SDM) to generate CBFβ_FLAG_3xMut. Stable expression of CBFβ_FLAG_3xMut did not rescue low RUNX2 expression in the same manner as CBFβ_FLAG_wt. The expression level of CBFβ_FLAG_3xMut transgene did not differ significantly from that of CBFβ_FLAG_wt.

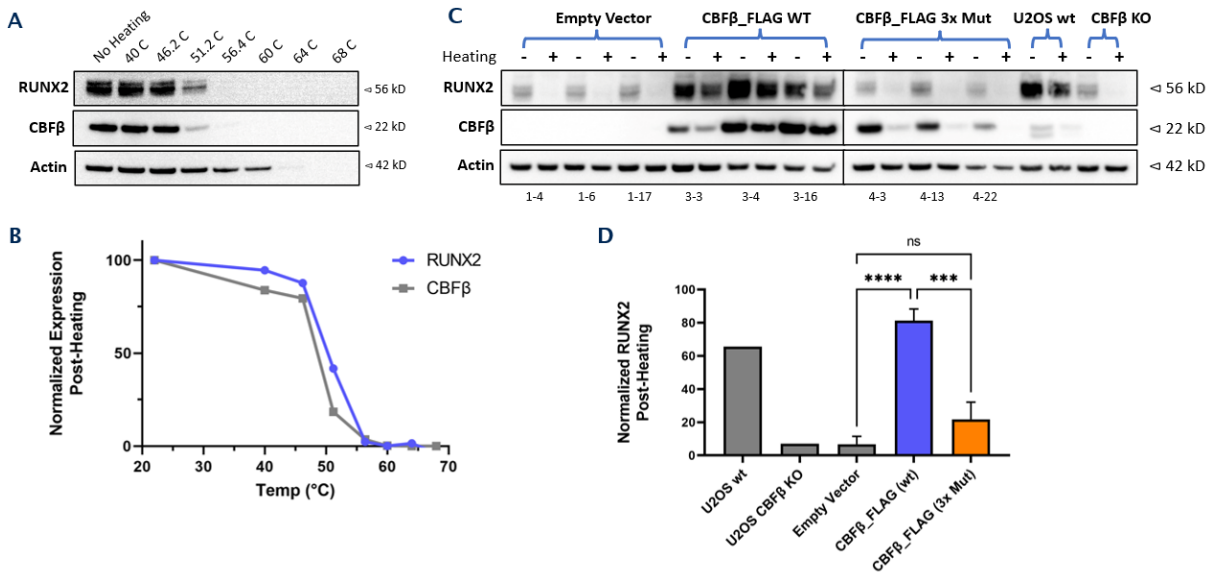

Figure 3.8 A) Representative western blot images of RUNX2, CBFβ and actin levels in U2OS WT cells from CETSA pilot study. B) Melt curve of RUNX2 and CBFβ from CETSA pilot study, with RUNX2 in each sample normalized to actin, then normalized to unheated sample. C) Representative western blot images of RUNX2, CBFβ, and actin from CETSA panel. Numbers below blot denote which monoclonal cell line was used. D) Densitometry of RUNX2 present after heating, normalized to actin, then normalized to unheated sample.

Mutations in CBFβ shift the melting temperature of RUNX2. In order to investigate whether key mutations in CBFβ had affected CBFβ-RUNX2 interaction, we conducted a cellular electrothermal shift assay (CETSA) on our transduced cells. A melt curve was first conducted to determine the melting temperature (Tm) of RUNX2 in CBFβ_FLAG_WT cells, and cell suspensions were subjected to a range of temperatures from 22°C to 68°C. Following normalization to actin and then unheated sample, the melting temperature of RUNX2 was found to be ~50°C. 49.5°C was selected for future heat treatments, and CETSA was conducted on five clones each of Empty Vector, CBFβ_FLAG_WT, and CBFβ_FLAG_3xMut cells as well as U2OS WT and U2OS CBFβ KO cells. The Tm of RUNX2 in U2OS WT cells was similar to that of CBFβ_FLAG_WT cells, while the Tm of RUNX2 in CBFβ KO cells was similar to that of Empty Vector and CBFβ_3xMut_FLAG cells. Most importantly, expression of CBFβ_3xMut_FLAG

caused a statistically significant downward shift in RUNX2 Tm relative to cells expressing CBFβ_FLAG_WT.

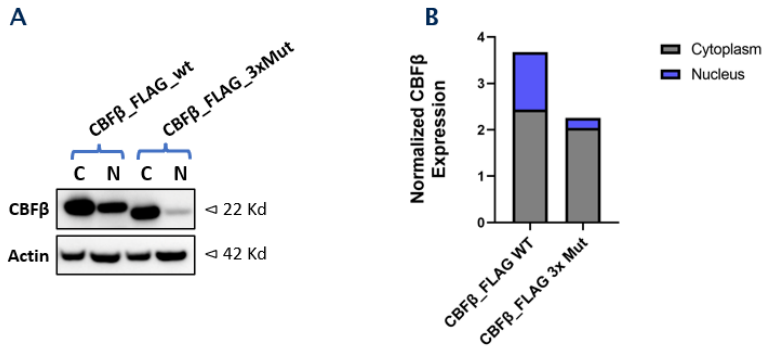

Figure 3.9 A) Representative western blot images of CBFβ and actin expression in cytoplasmic (C) and nuclear (N) fractions of cells expressing CBFβ_FLAG_wt and CBFβ_FLAG_3xMut. B) Densitometry of aforementioned western blot evaluating CBFβ expression in both cellular compartments, normalized to actin.

Mutations in CBFβ inhibit nuclear shuttling of CBFβ. In order to investigate the functional significance of point mutations in CBFβ, we next subjected CBFβ_FLAG_WT and CBFβ_3xMut_FLAG-expressing cells to nuclear/cytoplasmic fractionation followed by western blotting for CBFβ and actin. CBFβ_FLAG_WT was present in both the cytoplasm and the nucleus, as expected, while CBFβ_FLAG_3xMut was localized predominantly to the cytoplasm. Actin was present in both compartments and functioned as our housekeeping gene for this experiment.

Discussion

CBFβ and RUNX2 were successfully cloned, expressed, and purified, verified via SDS-PAGE with Coomassie blue staining. Although recombinant CBFβ produced a more intense band than RUNX2, this was likely due to the 8x concentration step imparted to CBFβ during purification while RUNX2 remained stuck to affinity beads and was not concentrated. We did see a few additional bands in our purified CBFβ, however further purification of recombinant CBFβ was not possible due to aggregation issues when run on a Fast Protein Liquid Chromatography (FPLC) system. Additional bands were also present in recombinant RUNX2-GST, which likely correspond to free GST tag (26 kD) and *apo* RUNX2 (56 kD) produced by cleavage at HRV-3C protease site by endogenous proteases. Altogether, these impurities were faint in comparison to our protein of interest and therefore low in abundance (**Figure 3.2)**.

We next performed and optimized a pulldown assay using our recombinantly expressed proteins, and confirmed that recombinant CBFβ and RUNX2 do interact (**Figure 3.3)**. Using this recombinant pulldown assay, we evaluated if targeting certain key residues of CBFβ and RUNX2 would interrupt their interaction. The G61-G69 region of CBFβ and corresponding G108-L117 face on RUNX2 were selected based on previous work highlighting these regions as important in CBFβ-RUNX2 interaction (50,51) (**Figure 3.4)**. We chose to synthesize a relatively short peptide targeting this region, as this would afford greater permeability into living cells when mixed with a cell penetrating peptide carrier (52–54). Repeat of pulldown assay in the presence of peptide GNDENYSAEL, crafted from RUNX2 region G108-L117, led to a dose-dependent inhibition of CBFβ-RUNX2 interaction when normalized to RUNX2-GST (**Figure 3.5**). Conducting the pulldown assay in the presence of peptide GTNLSLQFF, crafted from CBFβ region G61-G69, did not inhibit CBFβ-RUNX2 interaction (data not shown). Nevertheless, as inhibition of CBFβ-

RUNX2 interaction with peptide GNDENYSAEL was successful, and exhibited a dose-dependent effect, we felt confident in moving forward with further studies targeting residues G61 and N63 of CBFβ.

With the likelihood of dual roles for CBFβ occurring simultaneously, in distinct subcellular regions, and the protein interactions essential to each seemingly exclusionary of each other (43), studying each role individually proved difficult. In order to isolate and investigate the translational role of CBFβ, we attempted to halt its transcriptional capabilities by generating cell lines expressing a mutant form of CBFβ designed to be unable to bind with the RUNX proteins. With the residues key in CBFβ-RUNX2 interaction now validated in our previous recombinant protein assay, we utilized SDM followed by lentiviral transduction to generate viral particles carrying CBFβ_FLAG_3xMut and used these to infect U2OS CBFβ KO cells. To be specific, CBFβ_FLAG_3xMut was generated by mutating our previously validated residues, G61 and N63, to alanine. Additionally, we elected to also mutate N104 to alanine because of data suggesting it plays an important role in CBFβ-RUNX2 interaction as well (50).

The side-chains of these three key residues, G61, N63, and N104, along with the hydrogen bonds they form with corresponding residues on RUNX2 are highlighted in **Figure 3.6**. Visualization with Pymol was helpful to make sure these residues do indeed lie on the RUNX2 interacting face of CBFβ. We then evaluated RUNX2 expression in our cell lines expressing our triple mutant of CBFβ, and found that CBFβ_FLAG_3xMut transgene was unable to rescue low RUNX2 expression in CBFβ KO cells (**Figure 3.7**). This observation was not due to hampered transgene expression, as CBFβ levels were consistent between CBFβ_FLAG_WT and CBFβ_FLAG_3xMut.

We were somewhat surprised that CBFβ_FLAG_3xMut was unable to rescue low RUNX2 expression in U2OS CBFβ KO cells, as our previous data indicated that stabilization of RUNX2 via binding to CBFβ and subsequent protection from degradation made a relatively minor contribution to overall RUNX2 levels. Previous research also suggested that CBFβ binding and stabilization of RUNX proteins is not the dominant factor dictating RUNX protein levels (43), so this result was initially puzzling indeed. Previous research suggested that CBFβ interaction with hnRNPK or RUNX proteins is mutually exclusive (43), so it's possible that these two binding partners of CBFβ compete for the same residues, and our mutations had inadvertently altered the interaction of CBFβ with both. Inhibiting the interaction of CBFβ and hnRNPK would, in theory, lead to reduced expression of proteins under the purview of CBFβ, as interaction with hnRNPK is the mechanism by which this translational role of CBFβ is reported to occur (43). In order to fully unravel this, it is necessary to validate that 1) mutations in CBFβ did inhibit binding with RUNX2 in living cells, 2) RUNX2 protein expression levels are strongly regulated by CBFβ, and 3) mutations in CBFβ alter its ability to facilitate translation of RUNX2 and other proteins. The first point will be addressed below while points two and three will be covered in a latter chapter through use of ribosome footprinting (55–57) and direct detection of biotinylated tags (DiDBiT) (58). Data generated for another project in our lab (not shown) seems to support the third point here, as CBFβ_FLAG_3xMut cells appear to double at a slower rate than CBFβ_FLAG_WT cells, which could be due to decreased overall protein synthesis resulting from the inability of CBFβ to participate in protein translation.

While we had validated these residues as crucial to CBFβ-RUNX2 interaction in our cell-free system, and used this data to generate CBFβ_FLAG_3xMut, it was necessary to validate that we had indeed interrupted their binding in living cells. The simplest method to measure alterations

to a protein-protein interaction would have been to conduct a co-IP, which was our initial strategy. Unfortunately, RUNX2 proved incredibly challenging to co-IP, as its mass of 56 kD causes it to run parallel to the IgG heavy chain of any pulldown antibody used. Due to this, we were not able to get a clean blot for co-IP of RUNX2 as it was always obscured by background signal from the heavy chain of the pulldown antibody. Numerous workarounds to this were attempted, including usage of Protein A-HRP secondary antibodies, IgG light-chain specific HRP secondary antibodies, four different elution buffers, three different pulldown antibodies, and running SDS-PAGE in non-reducing conditions. To our chagrin, none of these were able to produce a clean blot, and stumped us as well as the technical support staff at four different reagent companies.

Due to these setbacks, we switched to CETSA, and used this assay to assess if CBFβ_FLAG_3xMut had inhibited RUNX2 binding compared to CBFβ_FLAG_WT. CETSA was first developed as a label-free method to evaluate target engagement in drug development, and is based on the principle that changes in the interactions of a particular protein will increase or decrease its melting temperature (Tm), thus shifting it from a soluble to an insoluble state (59). While this remains its most common usage (60), we hypothesized CETSA could also prove useful for our application. As cellular proteins have a wide range of melting temperatures (61) and their individual interactomes differ greatly between cell lines (62), it was necessary to first determine the Tm of RUNX2 in cells expressing CBFβ_FLAG_WT. We conducted a melt curve using temperatures spanning 40°C to 68°C, and after normalizing to actin, we measured the Tm of RUNX2 to be approximately 49.5°C (**Figure 3.8A,B**). We then used this same temperature for future studies, and a decrease in RUNX2 protein remaining after heating, when compared to CBFβ_FLAG_WT, was interpreted as a decrease in Tm and therefore a decrease in RUNX2 interaction with other proteins.

While RUNX2 protein is expressed at different levels in our cell lines, as shown previously, this did not confound our results as each cell line is normalized to its individual RUNX2 expression level. RUNX2 displayed a similar Tm between U2OS WT cells and CBFβ_FLAG_WT cells, indicating that our stably expressed CBFβ_FLAG_WT interacted with endogenous RUNX2 to the same extent as in U2OS WT cells (**Figure 3.8C,D**) and suggesting that our rescue experiment had successfully recapitulated normal CBFβ-RUNX2 interaction. RUNX2 experienced a downward shift in Tm in both U2OS CBFβ KO and Empty Vector cells, which was expected as RUNX2 in both lines had lost its interacting partner CBFβ. Most prominently, RUNX2 experienced a statistically significant downward shift in Tm in CBFβ_FLAG_3xMut cells, indicating that we had been successful in generating a CBFβ mutant with inhibited RUNX2 binding.

CBFβ lacks a nuclear localization signal (NLS) (42,63) and must be shuttled into the nucleus onboard the RUNX proteins (43,64); therefore inhibition of CBFβ-RUNX protein binding should result in decreased nuclear accumulation of CBFβ. We evaluated this by performing nuclear/cytoplasmic fractionation followed by western blotting, and were able to confirm these mutations interrupted nuclear shuttling of CBFβ (**Figure 3.9**). Cells expressing CBFβ_FLAG_WT demonstrated CBFβ within both cytoplasmic and nuclear compartments, in line with previous studies in our hands and others (43), and confirming our affinity tag had not interrupted shuttling. In contrast to this, CBFβ_FLAG_3xMut was predominantly localized to the cytoplasm, suggesting that our mutations had interrupted nuclear shuttling of CBFβ. The nuclear fraction did still exhibit a faint band corresponding to CBFβ, which may be explained by the actions of Crlz-1 (also known as SAS10 or UTP3) which interacts with CBFβ (65) and has been postulated to play a role in CBFβ nuclear shuttling (66,67) and OS development (68). While Crlz-1 may influence the cellular

distribution of CBFβ, from our data it does not appear to be the predominant factor governing nuclear shuttling of CBFβ.

Our choice of actin as a housekeeping gene for both nuclear and cytoplasmic fractions has been met with much skepticism by colleagues, as actin was long been thought to be exclusive to the cytoplasm. This was primarily due to a lack of reliable data detecting actin in the nucleus by immunofluorescence microscopy (69), however convincing evidence has since been put forth demonstrating actin in the nucleus of mammalian cells as well as numerous others (70–82). In previous experiments (not shown) we evaluated the purity of nuclear and cytoplasmic fractions generated with this method by blotting for nuclear-specific and cytoplasmic-specific markers Histone H3 and GAPDH, respectively, and validated that cross-contamination between fractions did not occur.

Our goal in generating CBFβ_FLAG_3xMut was to inhibit the transcriptional activity of CBFβ, and thereby de-couple the transcriptional and translational roles of CBFβ. These data thus far suggest we have accomplished the former, as a mutant form of CBFβ with reduced RUNX2 binding and subsequent nuclear shuttling is likely to be less effective as a transcriptional co-activator to the RUNX proteins. This assertion could be validated in future endeavors via qPCR of RUNX2 target genes implicated in the malignant phenotype of OS (15,16) such as vascular endothelial growth factor (VEGF) (11,12), alkaline phosphatase (ALP) (13), or matrix metalloproteinase 9 (MMP-9) (14). As mentioned previously, it is possible that these mutations have also affected the translational role of CBFβ, and additional data generated by this project in a latter chapter will provide more detail into the influence of these specific residues as well as that of CBFβ overall on the malignant phenotype of OS.

Acknowledgements

We would like to thank Dr. Chris Lucchesi and the Dr. Xinbin Chen Lab at UC Davis for providing reagents, lab space, and mentoring which made production of recombinant RUNX2 and CBFβ possible. pTXB1 and pGEX 6.1 expression vectors were gifts from Dr. Xinbin Chen's Lab at UC Davis.

We would also like to thank Dr. Andrew Cruz for suggesting CETSA as an alternative method to measure binding interaction of our proteins.

pMDLg/pRRE, pRSV-Rev, and pMD2.G were gifts from Didier Trono (Addgene plasmid # 12251 ; http://n2t.net/addgene:12251; RRID:Addgene_12251), (Addgene plasmid # 12253 ; http://n2t.net/addgene:12253; RRID:Addgene_12253), (Addgene plasmid # 12259 ; http://n2t.net/addgene:12259; RRID:Addgene_12259). pHIV-EGFP was a gift from Bryan Welm & Zena Werb (Addgene plasmid # 21373; http://n2t.net/addgene:21373; RRID:Addgene_21373).

This project was supported in part by NIH K01OD026526, NIH R03OD031958, and startup funds provided to Dr. Wittenburg through the UC Davis Comprehensive Cancer Center.

References

1. Hagleitner MM, De Bont ESJM, Te Loo DMWM. Survival Trends and Long-Term Toxicity in Pediatric Patients with Osteosarcoma. Sarcoma. 2012;2012:1–5.
2. Ottaviani G, Jaffe N. The Epidemiology of Osteosarcoma. In: Jaffe N, Bruland OS, Bielack S, editors. Pediatric and Adolescent Osteosarcoma [Internet]. Boston, MA: Springer US; 2010. p. 3–13. Available from: https://doi.org/10.1007/978-1-4419-0284-9_1
3. Eilber F, Giuliano A, Eckardt J, Patterson K, Moseley S, Goodnight J. Adjuvant chemotherapy for osteosarcoma: a randomized prospective trial. J Clin Oncol. 1987 Jan;5(1):21–6.
4. Yu D, Zhang S, Feng A, Xu D, Zhu Q, Mao Y, et al. Methotrexate, doxorubicin, and cisplatinum regimen is still the preferred option for osteosarcoma chemotherapy: A meta-analysis and clinical observation. Medicine. 2019 May;98(19):e15582.
5. Morrow JJ, Khanna C. Osteosarcoma Genetics and Epigenetics: Emerging Biology and Candidate Therapies. Crit Rev Oncog. 2015;20(3–4):173–97.
6. Sandberg AA, Bridge JA. Updates on the cytogenetics and molecular genetics of bone and soft tissue tumors: osteosarcoma and related tumors. Cancer Genet Cytogenet. 2003 Aug;145(1):1–30.
7. Helman LJ, Meltzer P. Mechanisms of sarcoma development. Nat Rev Cancer. 2003 Sep;3(9):685–94.
8. Wysokinski D, Pawlowska E, Blasiak J. RUNX2: A Master Bone Growth Regulator That May Be Involved in the DNA Damage Response. DNA and Cell Biology. 2015 May;34(5):305–15.
9. Nathan SS, Pereira BP, Zhou Y fang, Gupta A, Dombrowski C, Soong R, et al. Elevated expression of Runx2 as a key parameter in the etiology of osteosarcoma. Mol Biol Rep. 2009 Jan;36(1):153–8.
10. Sadikovic B, Thorner P, Chilton-MacNeill S, Martin JW, Cervigne NK, Squire J, et al. Expression analysis of genes associated with human osteosarcoma tumors shows correlation of RUNX2 overexpression with poor response to chemotherapy. BMC Cancer. 2010 Dec;10(1):202.
11. Zelzer E, Glotzer DJ, Hartmann C, Thomas D, Fukai N, Soker S, et al. Tissue specific regulation of VEGF expression during bone development requires Cbfa1/Runx2. Mechanisms of Development. 2001;
12. Kwon TG, Zhao X, Yang Q, Li Y, Ge C, Zhao G, et al. Physical and functional interactions between Runx2 and HIF-1α induce vascular endothelial growth factor gene expression. J Cell Biochem. 2011 Dec;112(12):3582–93.
13. Weng J jie, Su Y. Nuclear matrix-targeting of the osteogenic factor Runx2 is essential for its recognition and activation of the alkaline phosphatase gene. Biochimica et Biophysica Acta (BBA) - General Subjects. 2013 Mar;1830(3):2839–52.
14. Pratap J, Javed A, Languino LR, Van Wijnen AJ, Stein JL, Stein GS, et al. The Runx2 Osteogenic Transcription Factor Regulates Matrix Metalloproteinase 9 in Bone Metastatic Cancer Cells and Controls Cell Invasion. Molecular and Cellular Biology. 2005 Oct 1;25(19):8581–91.
15. Bajpai J, Sharma M, Sreenivas V, Kumar R, Gamnagatti S, Khan SA, et al. VEGF expression as a prognostic marker in osteosarcoma. Pediatric Blood & Cancer. 2009 Dec;53(6):1035–9.

16. Han J, Yong B, Luo C, Tan P, Peng T, Shen J. High serum alkaline phosphatase cooperating with MMP-9 predicts metastasis and poor prognosis in patients with primary osteosarcoma in Southern China. World J Surg Onc. 2012 Dec;10(1):37.
17. Warren AJ, Williams RL, Rabbitts TH. Structural basis for the heterodimeric interaction between the acute leukaemia-associated transcription factors AML1 and CBFb.
18. Yoshida CA, Furuichi T, Fujita T, Fukuyama R, Kanatani N, Kobayashi S, et al. Core-binding factor β interacts with Runx2 and is required for skeletal development. Nat Genet. 2002 Dec;32(4):633–8.
19. Kundu M, Javed A, Jeon JP, Horner A, Shum L, Eckhaus M, et al. Cbfβ interacts with Runx2 and has a critical role in bone development. Nat Genet. 2002 Dec;32(4):639–44.
20. Ogawa E, Inuzuka M, Maruyama M, Satake M, Naito-Fujimoto M, Ito Y, et al. Molecular cloning and characterization of PEBP2 beta, the heterodimeric partner of a novel Drosophila runt-related DNA binding protein PEBP2 alpha. Virology. 1993 May;194(1):314–31.
21. Adya N, Castilla LH, Liu PP. Function of CBFβ/Bro proteins. Seminars in Cell & Developmental Biology. 2000 Oct;11(5):361–8.
22. Kagoshima H, Shigesada K, Satake M, Ito Y, Miyoshi H, Ohki M, et al. The Runt domain identifies a new family of heteromeric transcriptional regulators. Trends Genet. 1993 Oct;9(10):338–41.
23. Feng Y, Liao Y, Zhang J, Shen J, Shao Z, Hornicek F, et al. Transcriptional activation of CBFβ by CDK11p110 is necessary to promote osteosarcoma cell proliferation. Cell Commun Signal. 2019 Dec;17(1):125.
24. Alegre F, Ormonde AR, Godinez DR, Illendula A, Bushweller JH, Wittenburg LA. The interaction between RUNX2 and core binding factor beta as a potential therapeutic target in canine osteosarcoma. Vet Comparative Oncology. 2020 Mar;18(1):52–63.
25. Braun T, Woollard A. RUNX factors in development: Lessons from invertebrate model systems. Blood Cells, Molecules, and Diseases. 2009 Jul;43(1):43–8.
26. Gergen JP, Butler BA. Isolation of the Drosophila segmentation gene runt and analysis of its expression during embryogenesis. Genes Dev. 1988 Sep;2(9):1179–93.
27. Chuang LSH, Ito K, Ito Y. RUNX family: Regulation and diversification of roles through interacting proteins. Intl Journal of Cancer. 2013 Mar 15;132(6):1260–71.
28. Zeng L, Wei J, Zhao N, Sun S, Wang Y, Feng H. A novel 18-bp in-frame deletion mutation in RUNX2 causes cleidocranial dysplasia. Arch Oral Biol. 2018 Dec;96:243–8.
29. Cohen Jr. MM. Perspectives on RUNX genes: An update. American J of Med Genetics Pt A. 2009 Dec;149A(12):2629–46.
30. Komori T. Roles of Runx2 in Skeletal Development. Adv Exp Med Biol. 2017;962:83–93.
31. Liu TM, Lee EH. Transcriptional regulatory cascades in Runx2-dependent bone development. Tissue Eng Part B Rev. 2013 Jun;19(3):254–63.
32. Young DW, Zaidi SK, Furcinitti PS, Javed A, Van Wijnen AJ, Stein JL, et al. Quantitative signature for architectural organization of regulatory factors using intranuclear informatics. Journal of Cell Science. 2004 Oct 1;117(21):4889–96.
33. Aronson BD, Fisher AL, Blechman K, Caudy M, Gergen JP. Groucho-Dependent and -Independent Repression Activities of Runt Domain Proteins. Molecular and Cellular Biology. 1997 Sep 1;17(9):5581–7.
34. Imai Y, Kurokawa M, Tanaka K, Friedman AD, Ogawa S, Mitani K, et al. TLE, the Human Homolog of Groucho, Interacts with AML1 and Acts as a Repressor of AML1-Induced

Transactivation. Biochemical and Biophysical Research Communications. 1998 Nov;252(3):582–9.
35. Elango N, Li Y, Shivshankar P, Katz MS. Expression of RUNX2 isoforms: Involvement of cap-dependent and cap-independent mechanisms of translation. Journal of Cellular Biochemistry. 2006;99(4):1108–21.
36. Matheny CJ, Speck ME, Cushing PR, Zhou Y, Corpora T, Regan M, et al. Disease mutations in RUNX1 and RUNX2 create nonfunctional, dominant-negative, or hypomorphic alleles. EMBO J. 2007 Feb 21;26(4):1163–75.
37. Berkay EG, Elkanova L, Kalaycı T, Uludağ Alkaya D, Altunoğlu U, Cefle K, et al. Skeletal and molecular findings in 51 Cleidocranial dysplasia patients from Turkey. Am J Med Genet A. 2021 Aug;185(8):2488–95.
38. Han M, Kim H, Wee H, Lim K, Park N, Bae S, et al. The cleidocranial dysplasia-related R131G mutation in the Runt-related transcription factor RUNX2 disrupts binding to DNA but not CBF-β. J of Cellular Biochemistry. 2010 May;110(1):97–103.
39. Look A. Oncogenic transcription factors in the human acute leukemias. Science (New York, NY). 1997 Nov;278(5340):1059—1064.
40. Lukasik SM, Zhang L, Corpora T, Tomanicek S, Li Y, Kundu M, et al. Altered affinity of CBFβ-SMMHC for Runx1 explains its role in leukemogenesis. Nat Struct Biol. 2002 Sep;9(9):674–9.
41. Liu P, Tarlé SA, Hajra A, Claxton DF, Marlton P, Freedman M, et al. Fusion between transcription factor CBF beta/PEBP2 beta and a myosin heavy chain in acute myeloid leukemia. Science. 1993 Aug 20;261(5124):1041–4.
42. Wang Q, Stacy T, Miller JD, Lewis AF, Gu TL, Huang X, et al. The CBFᴺ Subunit Is Essential for CBF ⎵ 2 (AML1) Function In Vivo.
43. Malik N, Yan H, Moshkovich N, Palangat M, Yang H, Sanchez V, et al. The transcription factor CBFB suppresses breast cancer through orchestrating translation and transcription. Nat Commun. 2019 May 6;10(1):2071.
44. Polunovsky VA, Bitterman PB. The Cap-Dependent Translation Apparatus Integrates and Amplifies Cancer Pathways. RNA Biology. 2006 Jan;3(1):10–7.
45. Schiavone K, Garnier D, Heymann MF, Heymann D. The Heterogeneity of Osteosarcoma: The Role Played by Cancer Stem Cells. In: Birbrair A, editor. Stem Cells Heterogeneity in Cancer [Internet]. Cham: Springer International Publishing; 2019 [cited 2022 Nov 9]. p. 187–200. (Advances in Experimental Medicine and Biology; vol. 1139). Available from: https://link.springer.com/10.1007/978-3-030-14366-4_11
46. Kamikubo Y. Genetic compensation of RUNX family transcription factors in leukemia. Cancer Science. 2018 Aug;109(8):2358–63.
47. Morita K, Suzuki K, Maeda S, Matsuo A, Mitsuda Y, Tokushige C, et al. Genetic regulation of the RUNX transcription factor family has antitumor effects. Journal of Clinical Investigation. 2017 May 22;127(7):2815–28.
48. Illendula A, Gilmour J, Grembecka J, Tirumala VSS, Boulton A, Kuntimaddi A, et al. Small Molecule Inhibitor of CBFβ-RUNX Binding for RUNX Transcription Factor Driven Cancers. EBioMedicine. 2016 Jun;8:117–31.
49. Hou C, Mandal A, Rohr J, Tsodikov OV. Allosteric interference in oncogenic FLI1 and ERG transactions by mithramycins. Structure. 2021 May;29(5):404-412.e4.

50. Tang YY, Shi J, Zhang L, Davis A, Bravo J, Warren AJ, et al. Energetic and Functional Contribution of Residues in the Core Binding Factor β (CBFβ) Subunit to Heterodimerization with CBFα. Journal of Biological Chemistry. 2000 Dec;275(50):39579–88.
51. Nagata T, Gupta V, Sorce D, Kim Y, Ito Y, Werner MH. Immunoglobulin motif DNA recognition and heterodimerization of the PEBP2/CBF Runt domain. nature structural biology. 1999;6(7):6.
52. Luo XG, Ma DY, Wang Y, Li W, Wang CX, He YY, et al. Fusion with pep-1, a cell-penetrating peptide, enhances the transmembrane ability of human epidermal growth factor. Bioscience, Biotechnology, and Biochemistry. 2016 Mar 3;80(3):584–90.
53. Almarwani B, Phambu EN, Alexander C, Nguyen HAT, Phambu N, Sunda-Meya A. Vesicles mimicking normal and cancer cell membranes exhibit differential responses to the cell-penetrating peptide Pep-1. Biochimica et Biophysica Acta (BBA) - Biomembranes. 2018 Jun;1860(6):1394–402.
54. Wang L, Wang N, Zhang W, Cheng X, Yan Z, Shao G, et al. Therapeutic peptides: current applications and future directions. Sig Transduct Target Ther. 2022 Feb 14;7(1):48.
55. Douka K, Agapiou M, Birds I, Aspden JL. Optimization of Ribosome Footprinting Conditions for Ribo-Seq in Human and Drosophila melanogaster Tissue Culture Cells. Front Mol Biosci. 2022 Jan 25;8:791455.
56. Ingolia NT, Brar GA, Rouskin S, McGeachy AM, Weissman JS. The ribosome profiling strategy for monitoring translation in vivo by deep sequencing of ribosome-protected mRNA fragments. Nat Protoc. 2012 Aug;7(8):1534–50.
57. Jang C, Lahens NF, Hogenesch JB, Sehgal A. Ribosome profiling reveals an important role for translational control in circadian gene expression. Genome Res. 2015 Dec;25(12):1836–47.
58. Schiapparelli LM, McClatchy DB, Liu HH, Sharma P, Yates JR, Cline HT. Direct Detection of Biotinylated Proteins by Mass Spectrometry. J Proteome Res. 2014 Sep 5;13(9):3966–78.
59. Molina DM, Jafari R, Ignatushchenko M, Seki T, Larsson EA, Dan C, et al. Monitoring Drug Target Engagement in Cells and Tissues Using the Cellular Thermal Shift Assay. Science. 2013 Jul 5;341(6141):84–7.
60. Lundgren S. Focusing on Relevance: CETSA-Guided Medicinal Chemistry and Lead Generation. ACS Med Chem Lett. 2019 May 9;10(5):690–3.
61. Ghosh K, Dill K. Cellular Proteomes Have Broad Distributions of Protein Stability. Biophysical Journal. 2010 Dec;99(12):3996–4002.
62. Sharifi Tabar M, Parsania C, Chen H, Su XD, Bailey CG, Rasko JEJ. Illuminating the dark protein-protein interactome. Cell Reports Methods. 2022 Aug;2(8):100275.
63. Tahirov TH, Inoue-Bungo T, Morii H, Fujikawa A, Sasaki M, Kimura K, et al. Structural Analyses of DNA Recognition by the AML1/Runx-1 Runt Domain and Its Allosteric Control by CBFᴺ. :13.
64. Khan A, Campbell K, Cameron E, Blyth K. The RUNX/CBFβ Complex in Breast Cancer: A Conundrum of Context. Cells. 2023 Feb 16;12(4):641.
65. Sakuma T, Li QL, Jin Y, Choi LW, Kim EG, Ito K, et al. Cloning and expression pattern of a novel PEBP2b-binding protein (charged amino acid rich leucine zipper-1 [Crl-1]) in the mouse. Mechanisms of Development. 2001;
66. Park SK, Lim JH, Kang CJ. Crlz1 activates transcription by mobilizing cytoplasmic CBFβ into the nucleus. Biochimica et Biophysica Acta (BBA) - Gene Regulatory Mechanisms. 2009 Nov;1789(11–12):702–8.

67. Choi SY, Pi JH, Park SK, Kang CJ. Crlz-1 Controls Germinal Center Reaction by Relaying a Wnt Signal to the Bcl-6 Expression in Centroblasts during Humoral Immune Responses. JI. 2019 Nov 15;203(10):2630–43.
68. Liu B, Zhang Z, Dai EN, Tian JX, Xin JZ, Xu L. Modeling osteosarcoma progression by measuring the connectivity dynamics using an inference of multiple differential modules algorithm. Molecular Medicine Reports. 2017 Feb;16(2):1047–54.
69. Hofmann WA. Chapter 6 Cell and Molecular Biology of Nuclear Actin. In: International Review of Cell and Molecular Biology [Internet]. Elsevier; 2009 [cited 2024 Mar 27]. p. 219–63. Available from: https://linkinghub.elsevier.com/retrieve/pii/S1937644808018066
70. Brunel C, Lelay MN. Two-dimensional analysis of proteins associated with heterogenous nuclear RNA in various animal cell lines. Eur J Biochem. 1979 Sep;99(2):273–83.
71. Crowley KS, Brasch K. Does the interchromatin compartment contain actin? Cell Biol Int Rep. 1987 Jul;11(7):537–46.
72. Cruz JR, De La Torre C, De La Espina SMD. Nuclear actin in plants. Cell Biology International. 2008 May;32(5):584–7.
73. Jockusch BM, Brown DF, Rusch HP. Synthesis and Some Properties of an Actin-Like Nuclear Protein in the Slime Mold *Physarum polycephalum*. J Bacteriol. 1971 Nov;108(2):705–14.
74. Katsumaru H, Fukui Y. In vivo identification of Tetrahymena actin probed by DMSO induction nuclear bundles. Exp Cell Res. 1982 Feb;137(2):353–63.
75. Maundrell K, Scherrer K. Characterization of pre-messenger-RNA-containing nuclear ribonucleoprotein particles from avian erythroblasts. Eur J Biochem. 1979 Sep;99(2):225–38.
76. Merriam RW, Hill RJ. The germinal vesicle nucleus of Xenopus laevis oocytes as a selective storage receptacle for proteins. J Cell Biol. 1976 Jun;69(3):659–68.
77. Ohnishi T, Kawamura H, Yamamoto T. Extraction of a protein resembling actin from the cell nucleus of the calf thymus. J Biochem. 1963 Sep;54:298–300.
78. Parfenov VN, Davis DS, Pochukalina GN, Sample CE, Bugaeva EA, Murti KG. Nuclear actin filaments and their topological changes in frog oocytes. Exp Cell Res. 1995 Apr;217(2):385–94.
79. Paulin D, Nicolas JF, Jacquet M, Jakob H, Gros F, Jacob F. Comparative protein patterns in chromatins from mouse teratocarcinoma cells. Exp Cell Res. 1976 Oct 1;102(1):169–78.
80. Sahlas DJ, Milankov K, Park PC, De Boni U. Distribution of snRNPs, splicing factor SC-35 and actin in interphase nuclei: immunocytochemical evidence for differential distribution during changes in functional states. J Cell Sci. 1993 Jun;105 (Pt 2):347–57.
81. Sauman I, Berry SJ. An actin infrastructure is associated with eukaryotic chromosomes: structural and functional significance. Eur J Cell Biol. 1994 Aug;64(2):348–56.
82. Skubatz H, Orellana MV, Yablonka-Reuveni Z. Cytochemical evidence for the presence of actin in the nucleus of the voodoo lily appendix. Histochem J. 2000 Aug;32(8):467–74.

Chapter 4

Profiling the interactome and translatome of CBFβ in osteosarcoma cells

Abstract

Previous chapters had generated a large assortment of data focusing on the potential for CBFβ to regulate levels of RUNX2 in a post-transcriptional manner. In building on these previous data, we expanded our approach from investigating the influence of CBFβ on solely RUNX2, to investigating the influence of CBFβ on global phenomena in the cell. The assays performed in this chapter serve to answer two questions: 1) which proteins interact with CBFβ? And 2) which genes/proteins have expression regulated, at least in part, by CBFβ? Firstly, we performed affinity purification immunoprecipitation mass spectrometry (IP-MS) of CBFβ_WT_FLAG cells, and generated a list of medium- and high-confidence binding partners of CBFβ. We then performed gene ontology on these partners, and found multiple terms associated with protein translation to be highly enriched. Importantly, both members of the nascent polypeptide associated complex (NAC), a heterodimer crucial in protein expression, were identified as high confidence interactors. Additionally, we revealed proteins which specifically rely on residues G61, N63, and/or N104 of CBFβ for their interaction. Secondly, we performed two somewhat orthogonal assays; Ribo-Seq (with parallel RNAseq) and Direct Detection of Biotinylated proteins (DiDBiT), to reveal a list of genes/proteins which may have their expression regulated by CBFβ at transcription and/or translational level. We performed gene ontology on these targets, and observed enrichment of numerous pathways implicated in OS, and cancer at large, such as PD-L1, MAPK, and VEGF, among genes translationally regulated by CBFβ. Notably, both Ribo-Seq and DiDBiT analyses yielded strong enrichment of genes associated with Rho GTPases, which are known to play key roles in tumor initiation and progression as well as proliferation and apoptosis.

Introduction

Osteosarcoma (OS) is the most common form of primary bone cancer in humans and canines, and most often presents early in life (1). The treatment outlook in OS hasn't changed in the last 30 years, in part due to the lack of identified driver mutations as well as OS being relatively uncommon when compared to other cancer types (2,3). In terms of location, OS lesions most frequently occur at the metaphysis, the portion of bone which contains the growth plate (4). The lack of identifiable driver mutations combined with the high degree of heterogeneity amongst OS patient tumors (5) has made development of targeted therapies challenging. Development of medicines which are able to overcome this heterogeneity could lead to dramatic successes in OS patients, but more study is needed to identify convergence points which could be targeted across large groups of patients. Protein translation has been proposed as such a convergence point (6), and this study will delve into this process. Core binding factor beta (CBFβ) is a binding partner to the RUNX family of DNA-binding transcription factors, and formation of the CBFβ-RUNX protein heterodimer allows RUNX proteins to better bind to DNA and facilitate transcription (7,8). RUNX2 is the master regulator of bone growth and differentiation (9), and high expression of it (10,11) as well as CBFβ (12) are implicated in poor disease prognosis in OS. These factors led to the interaction of these proteins, and the roles of CBFβ specifically, to be studied in detail in our lab (13).

CBFβ has been proposed to participate in regulation of cap-dependent protein translation in breast cancer cells (14), although thus far this is the only cancer type where this noncanonical role of CBFβ has been identified. Our study aims to interrogate whether this role also occurs in OS, and to what extent CBFβ may impact OS malignancy. Previous chapters described efforts to explain the reduction in RUNX2 protein expression upon loss of CBFβ, which may be due to a

post-transcriptional mechanism as loss of CBFβ did not decrease RUNX2 mRNA expression. Although CBFβ has been proposed to stabilize RUNX2, protecting it from proteasomal degradation (15,16), previous data in this dissertation suggest that stabilization of RUNX2 by CBFβ may not fully explain this decrease in RUNX2 protein.

Building on our previous data, the current experiments aimed to delve deeper into the impact of CBFβ on protein translation, and gene expression overall, in OS. The overall process of gene expression is very complex, with regulation at many steps, and assays such as western blotting or qPCR are limited in their ability to interrogate this process fully. While an increase in expression at the mRNA level is often referenced as impactful to a cell, there are numerous cases in which transcriptional and translational data diverge (17–20). In order to study the impact of CBFβ on protein translation, and gene expression overall, we performed two somewhat orthogonal assays; Ribo-Seq (21–23) and DiDBiT (24). The quantity of a given protein is a convergence of two antagonistic processes: protein synthesis, and protein degradation. In this study, we are focused on the former, with Ribo-Seq revealing the translation efficiency of a given gene, and DiDBiT revealing the overall synthesis rate of a given protein.

Materials and Methods

Cell Lines and Culture Conditions

U2OS-derived cell lines were generated as previously described, and maintained in McCoy's 5A media supplemented with 10% FBS and 1% P/S.

FLAG Immunoprecipitation Mass Spectrometry

Sample Collection: Empty Vector, CBFβ_WT_FLAG, and CBFbebta_3xMut_FLAG cells were grown onto 15 cm plates until reaching 70% confluence. Media was then removed, cells were washed with 15 mL PBS, which was then removed. 3 mL of Trypsin was then added and cells were incubated at 37°C until fully dissociated from plate. 7 mL of media was added to plate and suspended cells were transferred to a 15 mL conical tube. An additional 5 mL media wash was added to the plate to capture remaining cells, which were then put into the same 15 mL conical tube. Conical tubes were centrifuged 500g 5 min. and media was removed. Cell pellet was resuspended in 4 mL PBS and transferred to a 5 mL conical tube, and was then spun down 500g for 5 min. Following this, PBS wash was removed and cells were resuspended into 1 mL PBS, then transferred to a 1.5 mL conical tube. Cells were again spun down 500g for 5 min, PBS was removed, and 350 μL of NET Lysis Buffer (50 mM Tris, 250 mM NaCl, 5mM EDTA, and 1% NP-40, in water, supplemented with 1x cOmplete protease inhibitor tablet and 1mM PMSF) was added per sample. Cells were lysed according to standard cell lysate collection procedure outlined in western blotting protocol in Chapter 2 and kept on ice moving forward. Protein concentration of each sample was then quantified via BCA, and samples were normalized to each other by addition of NET lysis buffer to yield samples all containing 350 μg of protein. Isotype control

sample was created by combining equal protein amounts of CBFβ_WT_FLAG and CBFβ_3xMut_FLAG lysate together. All told, 20 samples were created, each containing 350 µg of protein at 1.2 mg/mL.

Immunoprecipitation: Pulldown antibody (Sigma Aldrich M2 FLAG or SCBT α-GAPDH SC-47724) was added at 1:100 antibody µg:lysate µg and tubes were placed on a rotator overnight at 4°C. The next day, a 1,700 µL slurry of magnetic protein G MagBeads (Genscript, Piscataway, NJ) was pipetted into a 1.5 mL conical tube, placed on a magnetic tube rack, and shipping diluent was removed. Beads were then resuspended in 1 mL NET lysis buffer, as prepared previously, followed by placement on magnetic rack and removal of supernatant. This wash was repeated 3 more times. Following this, the beads were resuspended in 1.5 mL of NET lysis buffer, and 65 µL of washed bead slurry was added to each tube of lysate. The lysate + antibody + magnetic bead mixture was incubated on a rotator at room temperature for 1h. Following this, the tubes were placed on a magnetic separation rack and supernatant was removed, and beads were washed 3x as described previously. Supernatant was removed, and immunoprecipitated proteins were eluted by addition of 300 µL of 500 µg/mL FLAG peptide (MedChem Express, Monmouth Junction, NJ) in NET lysis buffer, and vortex mixed at 2,000 rpm for 10 min. Supernatant was removed and placed in a clean tube, and an additional elution was done with another 300 µL of FLAG peptide in lysis buffer. Supernatant from second elution was combined with the elution from the first elution.

Protein Clean-Up: Samples were transferred to a clean 2 mL conical tube, and 600 µL of MeOH (Thermo Fisher), 200 µL of chloroform (Thermo Fisher), and 600 µL MilliQ H2O were added. Samples were vortexed for 5 minutes, then spun down 15,000g for 5 min. Aqueous and organic layers were removed with a gel loading pipette tip, leaving the interface in-between corresponding to protein. 1,200 µL of MeOH was added to each tube, and vortex mixing and

centrifugation was repeated. Following this, supernatant was removed and pellet was allowed to air dry for 10 min.

Reduction, Alkylation, Digestion: Pellets were then resuspended in 200 µL of 4M Urea and 50mM Ammonium Bicarbonate (Sigma Aldrich). 2.02 µL of 500 mM TCEP (Sigma Aldrich) was added to each sample and samples were incubated at 55C with 2,000 rpm shaking for 30 min. 2.02 µL of 1mM Iodoacetamide was added to each tube, and samples were vortex mixed 1,000 rpm for 20 min, at room temperature and sheltered from light. Following this, 275 µL of 50mM Ambic, 1.25 µL of ProteaseMAX, and 16 µL of Trypsin (Promega Corporation Madison, WI) (200 µg/mL in H2O) were added to each tube. Tubes were incubated at 37°C with 1,600 rpm shaking for 4h. Following incubation, reaction was quenched by addition of 0.1% trifluoroacetic acid (TFA) (Sigma Aldrich) final concentration, and tubes were stored -80C until clean-up.

LC-MS/MS Sample Clean-Up: Peptides were incubated at room temperature until thawed. Samples were cleaned up using Sep-Pak C18 cartridges (Waters), which were primed in a series of wash steps. Using a vacuum manifold running at approx. 3 psi vacuum, cartridges were washed with 3 mL acetonitrile (Thermo Fisher), 3 mL of 0.5% acetic acid in water, 3 mL of 50% acetonitrile in water, and 3 mL of 0.1% TFA in water. Thawed peptide mixtures were vortex mixed for 2 minutes, then loaded into cartridges and pulled through sorbent at ~2 psi vacuum. Cartridges were then washed with 3 mL 0.1% TFA in water then 250 µL of 0.5% acetic acid in water. Peptides were then eluted into a clean tube using 1 mL of 0.5% acetic acid, 80% acetonitrile in water, and evaporated to dryness in a Speed Vac.

LC-MS Parameters: For each sample, half of the total volume was loaded onto a disposable Evotip C18 trap column (Evosep Biosytems, Denmark) as per the manufacturer's instructions. Briefly, Evotips were wetted with 2-propanol, equilibrated with 0.1% formic acid,

and then loaded using centrifugal force at 1200g. Evotips were subsequently washed with 0.1% formic acid, and then 200 µL of 0.1% formic acid was added to each tip to prevent drying. The tipped samples were subjected to nanoLC on a Evosep One instrument (Evosep Biosystems). Tips were eluted directly onto a PepSep analytical column, dimensions: 150umx25cm C18 column (PepSep, Denmark) with 1.5 µm particle size (100 Å pores) (Bruker Daltronics), and a ZDV spray emmiter (Bruker Daltronics). Mobile phases A and B were water with 0.1% formic acid (v/v) and 80/20/0.1% ACN/water/formic acid (v/v/vol), respectively. The standard pre-set method of 60 samples-per-day was used, which is a 21 minute run.

Mass Spectrometry: Performed on a hybrid trapped ion mobility spectrometry-quadrupole time of flight mass spectrometer (timsTOF HT, (Bruker Daltonics, Bremen, Germany) with a modified nano-electrospray ion source (CaptiveSpray, Bruker Daltonics). In the experiments described here, the mass spectrometer was operated in Parallel Accumulation–Serial Fragmentation (PASEF) mode. Desolvated ions entered the vacuum region through the glass capillary and deflected into the TIMS tunnel which is electrically separated into two parts (dual TIMS). Here, the first region is operated as an ion accumulation trap that primarily stores all ions entering the mass spectrometer, while the second part performs trapped ion mobility analysis. The dual TIMS analyzer was operated at a fixed duty cycle close to 100% using equal accumulation and ramp times of 85 ms each.

Data-independent analysis (DIA) scheme consisted of one MS scan followed by MSMS scans taken with 36 precursor windows at width of 25Th per 1.09 sec cycle, over the mass range 300-1200 Dalton. The TIMS scans layer the doubly and triply charged peptides over a ion mobility -1/k0- range of 0.7-1.3 V*sec/cm2. The collision energy was ramped linearly as a function of the mobility from 59 eV at 1/K0=1.4 to 20 eV at 1/K0=0.6.

Data Processing: Data was processed with Spectronaut 18.6 (Biognosys, Schlieren, Switzerland) using the directDIA workflow with the default settings. Briefly, trypsin/P Specific was set for the enzyme allowing two missed cleavages. Fixed modifications were set for Carbamidomethyl, and variable modification were set to Acetyl (Protein N-term) and Oxidation. For DIA search identification, PSM and Protein Group FDR was set at 0.01%. A minimum of 1 peptides per protein group were required for quantification. Proteins with an average log2ratio >0.58 and in CBFβ WT cells compared to EV, or CBFβ WT cells compared to isotype control, with p and q values <0.05, were binned as medium confidence interactors of CBFβ_WT_FLAG. Proteins possessing average log2ratio >0.58 CBFβ WT cells compared to both EV and isotype control, with p and q values <0.05, were binned as high confidence interactors of CBFβ_WT_FLAG. High confidence interactors of CBFβ_WT_FLAG possessing an average log2ratio >0.58 in CBFβ WT cells compared to CBFβ_3xMut_FLAG cells were binned as high confidence interactors of CBFβ reliant upon G61, N63, and/or N104 residues of CBFβ for interaction. CBFβ_FLAG_3xMut pulldown replicate 4 was eliminated from analysis as some sample was lost in processing.

Direct Detection of Biotinylated Tags (DiDBiT)

Sample Collection: DiDBiT was performed as previously described (24). Briefly, U2OS-derived cell lines were plated onto 15 cm dishes and grown to reach 70% confluence. Following this, media was removed, and cells were washed 2x with PBS. Cells were then starved of Methionine by 45 minute incubation in DMEM, high glucose, no glutamine, no methionine, no cystine (Gibco, Thermo Fisher). DMEM was then supplemented with 10% dialyzed FBS, 1% P/S, 1mM Sodium Pyruvate, 4mM L-Glutamine, and 200 uM L-Cystine HCl (Thermo Fisher).

Following starvation, media was removed and cells were then incubated for 4h with aforementioned media supplemented with 1mM L-azidohomoalanine (Click Chemistry Tools, Vector Laboratories, Newark, CA). Click conjugation and sample clean-up were accomplished as previously described by Schiapparelli et al (24).

LC-MS/MS Analysis: Sample reconstitution, injection, and LC-MS method was the same as mentioned previously.

Data Processing: Surrogate peptide areas for peptides possessing the L-azidohomoalanine (AHA) (+523.2749) modification were summed from each protein and then summed together from two separate runs. The area for each peptide in CBFβ_WT_FLAG cells was then divided by the areas in EV cells, and any protein with >20% higher signal between WT/EV was linked as a possible protein under the purview of CBFβ. Proteins identified by at least 1 peptide possessing AHA modification, and quantifiable in both biological replicates, were included in analysis. Proteins which exhibited a 20% or greater increase in abundance of AHA modified peptides in CBFβ_WT_FLAG cells compared to EV cells were binned as potential translational targets of CBFβ. From this pool, proteins which also exhibited a 20% or greater decrease in abundance of AHA modified peptides in CBFβ_3xMut_FLAG cells compared to CBFβ_WT_FLAG were binned as potential targets of CBFβ reliant upon residues G61, N63, and/or N104 of CBFβ for their translation.

Ribosome Footprinting (Ribo-Seq)

Sample Collection: Ribosome footprinting was performed by TB-Seq, Inc. (South San Francisco, California) as previously described (21,25,26). Cells were grown on 15 cm plates (Corning) until reaching 70-80% confluence and then collected as follows. Six plates were used per cell line, per biological replicate. Media was removed and cells were washed with 5 mL of ice cold 1x Nuclease-Free PBS (Thermo Fisher) supplemented with 100 μg/mL Cycloheximide (Sigma Aldrich). Dishes were placed on ice in an RNAse-free environment and wash was removed, then 3 more mL of Nuclease-Free PBS was added. Cells were collected via cell scraper and transferred into a 15 mL conical tube. An additional 2 mL of Nuclease Free PBS was added to plate and residual remaining cells were washed down, and added to the same 15 mL Falcon tube. Tubes were then spun down at 300g for 5 min. at 4°C, supernatant was removed, and pellet was flash frozen in liquid nitrogen before transferring to -80C storage prior to analysis. Pellets were stored on dry ice during transit to TB-Seq, who performed the Ribo-Seq analysis.

Ribosome Profiling: Cells were resuspended in ice cold lysis buffer (20 mM Tris HCl, pH 7.4, 100 mM NaCl, 5 mM MgCl2 1% Triton X100, 1 mM DTT, 20U/ml Turbo DNase I, 0.1 % NP40, 100 μg/ml cycloheximide) and the soluble cytoplasmic fraction was isolated by centrifugation at top speed in a microcentrifuge for 20 min at 4°C (21,23). Supernatants were collected and clarified lysates were digested with RNase I for 45 min at room temp. Digestion was stopped with SuperaseIN and monosomes purified by size exclusion chromatography on MicroSpin S-400 HR columns (GE Healthcare) as described (22). Size selection of footprints with length 25-33 nt was performed by electrophoresis on 15% TBE-urea gels. Illumina ready RIBO-seq libraries were prepared using a SMARTer smRNA-seq kit (TakaraBio, Kusatsu, Shiga, Japan). Library concentrations were measured by qubit fluorometer and their quality assessed on an

Agilent 2100 bioanalyzer. RIBO-seq libraries were sequenced on an Illumina Novaseq 6000 sequencer, single read, 1x50 cycles.

RNAseq: To obtain matched RNA-seq libraries total RNA was purified from an aliquot of cell lysate and rRNA was depleted from total RNA using a NEBNext rRNA depletion kit v2 (NEB) following manufacturer instructions. mRNA fragmentation was conducted for 20 min at 94 ℃ to generate RNA fragments of sizes similar to those of the ribosome footprints. SMARTer smRNA-seq kit (TakaraBio) was used to generate Illumina ready RNA-seq libraries. Library concentrations were measured by qubit fluorometer and their quality assessed on an Agilent 2100 bioanalyzer. RNA-seq libraries were sequenced on an Illumina Novaseq 6000 sequencer, single read, 1x50 cycles.

Data Analysis: Gene expression results for 19,811 protein-coding genes annotated in Ensembl 104 for the NCBI human hg38.p13 genome assembly are reported based on RIBO-seq and RNA-seq coverages. Based on the observed distribution of ribosome footprint lengths (see Section 4.3), we selected all RIBO-seq reads of lengths in the range 31-39 nucleotides as representing footprints of actively translating ribosomes. Shorter reads are thought to derive from ribosomes in an inactive state (ribosome in inactive “rotated conformation”, or ribosomes not charged with tRNA at the A_site) (27) whereas longer reads may represent stacked disomes in different states. In the case of RNA-seq reads, the vast majority of which have the maximum possible length 47 nt, reads of all lengths were included. Statistical analyses of differential gene transcription (RNA) and translation (RIBO) were performed with the quasi-likelihood F-test procedure implemented in the EdgeR package (28). EdgeR reports for each gene log2-fold-change in expression between conditions, the p-values obtained testing each gene for differential coverage between conditions, and the False Discovery Rate (FDR) associated with each p-value threshold,

evaluated with the Benjamini Hochberg procedure. Changes in Translation Efficiency, i.e., changes in the ratio of levels of translation over levels of transcription, were evaluated with models and statistical analyses implemented in the DTEG procedure (29) (DTEG-TE) and in the anota2seq procedure (A2S) (30). Genes were selected for differential transcription (RNA-seq), translation (RIBO-seq), Translation Efficiency, or buffering.

Genes were selected by p-value ≤ 0.01 in respective tests, as estimated by EdgeR (RNA and RIBO), DTEG (TE-DTEG) and anota2seq (TE-A2S and Buffering) differential-expression models. RNA is number of differentially transcribed genes based on RNA-seq coverage; RIBO is number of differentially translated genes based on RIBO-seq coverages; TE is number of genes with significant changes in Translation Efficiency. Buffering is number of genes with changes in transcription buffered by translational regulation.

Gene Ontology and Pathway Analysis of Identified Proteins/Genes

Gene ontology, Reactome, and KEGG pathway analysis was performed using DAVID bioinformatics resource (31,32). Venn diagram figures were generated using DeepVenn (33). Gene ontology and pathway analysis figures were generated using SRPlot (34).

Results

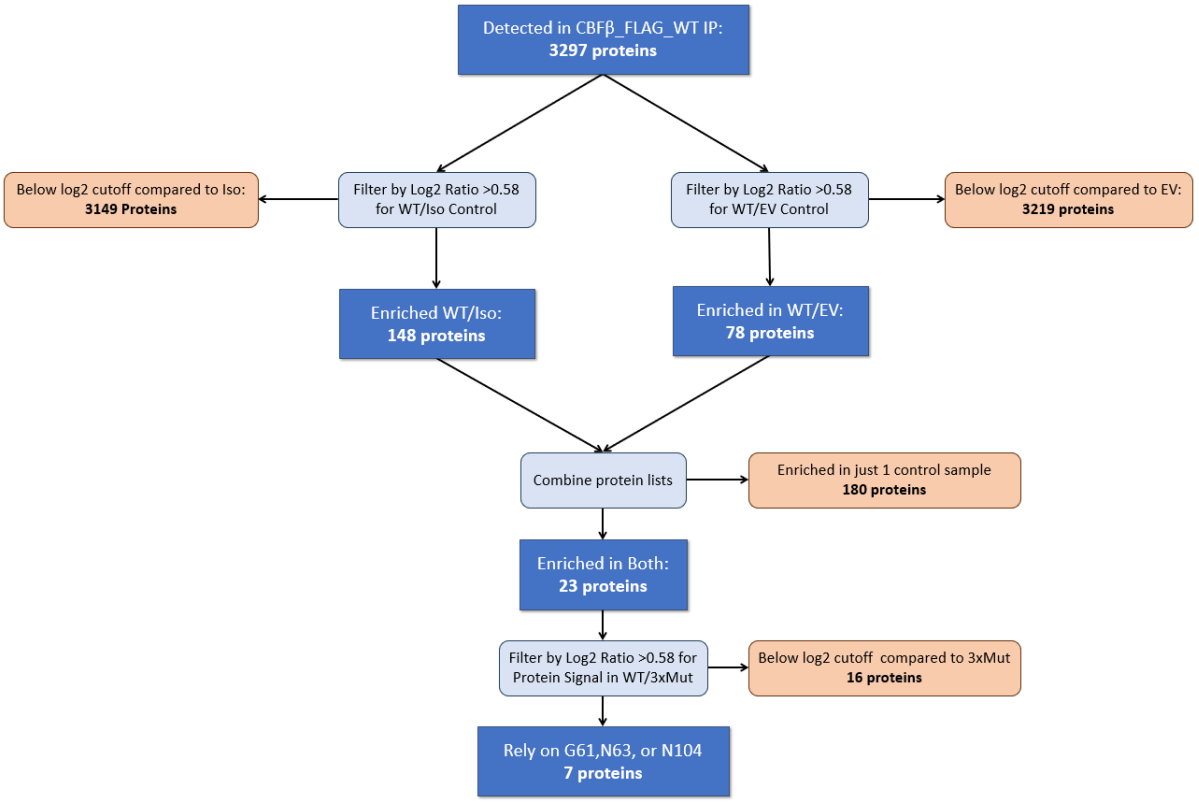

Figure 4.1 Data processing workflow used to identify interactors specific to CBFβ_WT_FLAG, when compared to enrichment in empty vector (EV) cells or isotype control (Iso) pulldown.

Proteins detected in IP-MS pulldowns were selectively filtered to identify specific interactors of CBFβ. Out of a total 3,297 proteins identified in pulldown of CBFβ_WT_FLAG, twenty-three (23) were enriched compared to both isotype and empty vector controls and were classified as high confidence interactors of CBFβ. 180 proteins were enriched compared to just one control, isotype or empty vector, and were binned as medium confidence interactors of CBFβ. Finally, of these twenty-three, seven were found to be significantly enriched in CBFβ_WT_FLAG compared to CBFβ_3xMut_FLAG.

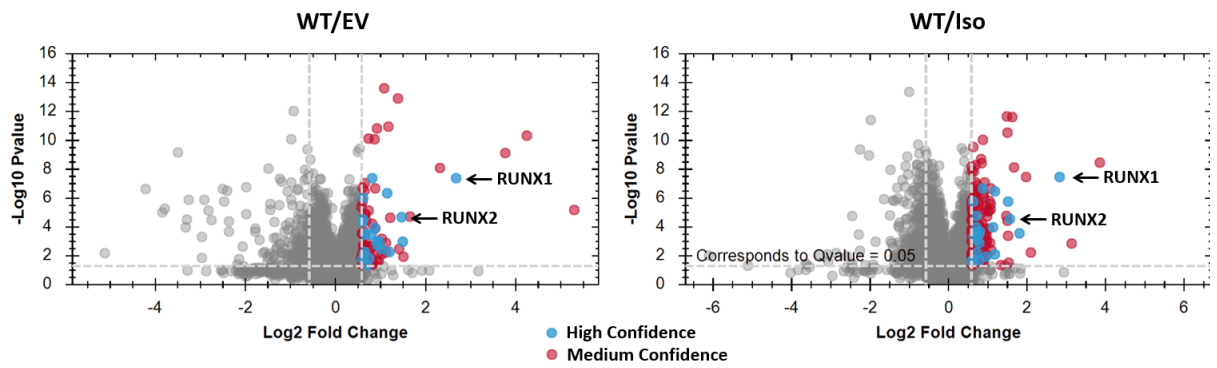

Figure 4.2 Proteins identified as specific interactors of CBFβ_WT_FLAG when compared to isotype (Iso) or empty vector (EV) controls are highlighted in blue or red, depending on confidence. RUNX1 and RUNX2 are highlighted.

Volcano plots of proteins identified as medium or high confidence interactors of CBFβ. Both RUNX1 and RUNX2 showed up as high confidence interactors of CBFβ. Each protein identified as a blue circle above was binned as a high confidence interactor of CBFβ, while red circles were medium confidence interactors.

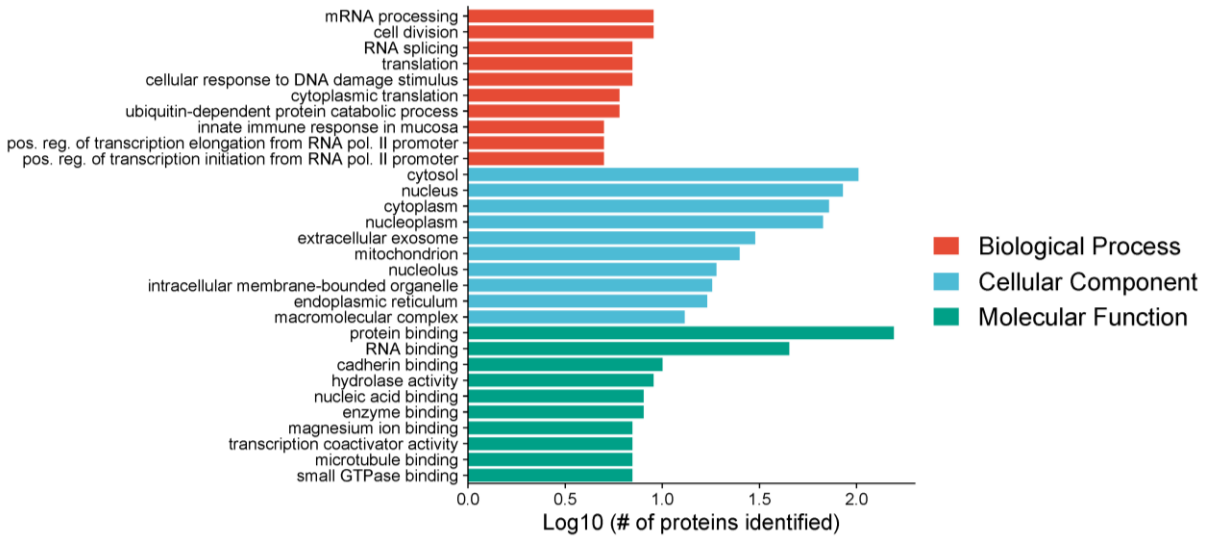

Figure 4.3 Enriched Gene Ontology (GO) terms for biological processes, cellular components, and molecular functions among proteins binned as medium confidence interactors of CBFβ.

Enriched GO terms among medium confidence interactors of CBFβ. The biological process terms translation and cytoplasmic translation came up highly ranked among proteins pulled down. Also highly ranked was mRNA processing and RNA splicing. A variety of cellular components were represented in the pulldown as well as numerous molecular functions.

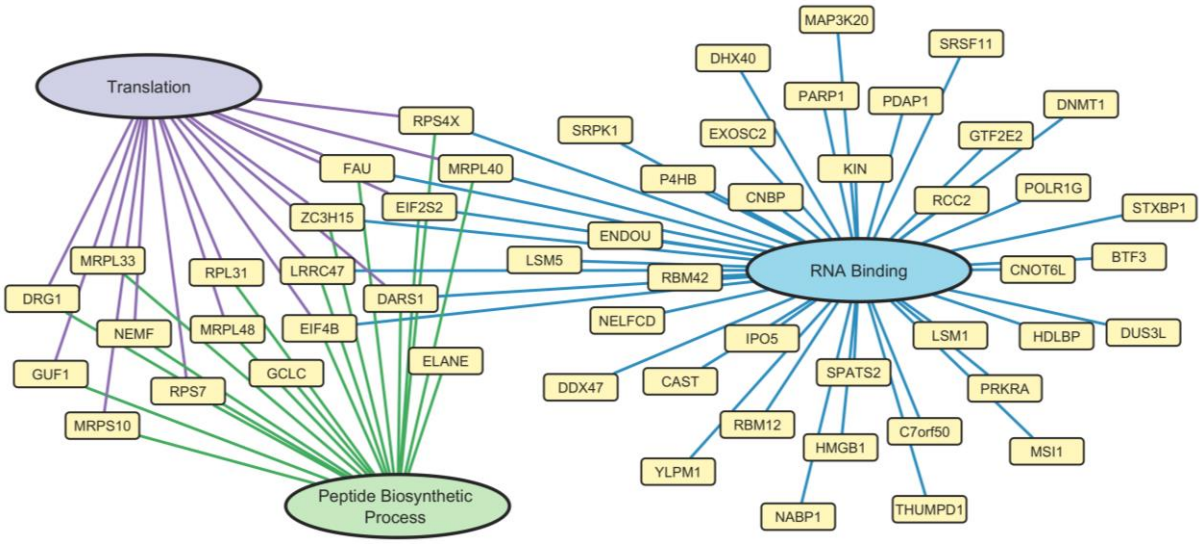

Figure 4.4 Map of a subset of proteins significantly enriched in CBFβ_FLAG_WT pulldown compared to either EV or Isotype control.

Network demonstrating specific proteins linked to GO terms surrounding protein translation. Each protein listed in graphic above was associated with at least one of the following GO terms: translation, peptide biosynthetic process, or RNA binding. Some proteins were associated with multiple terms. Of the total 224 total proteins identified, 54 were shown above.

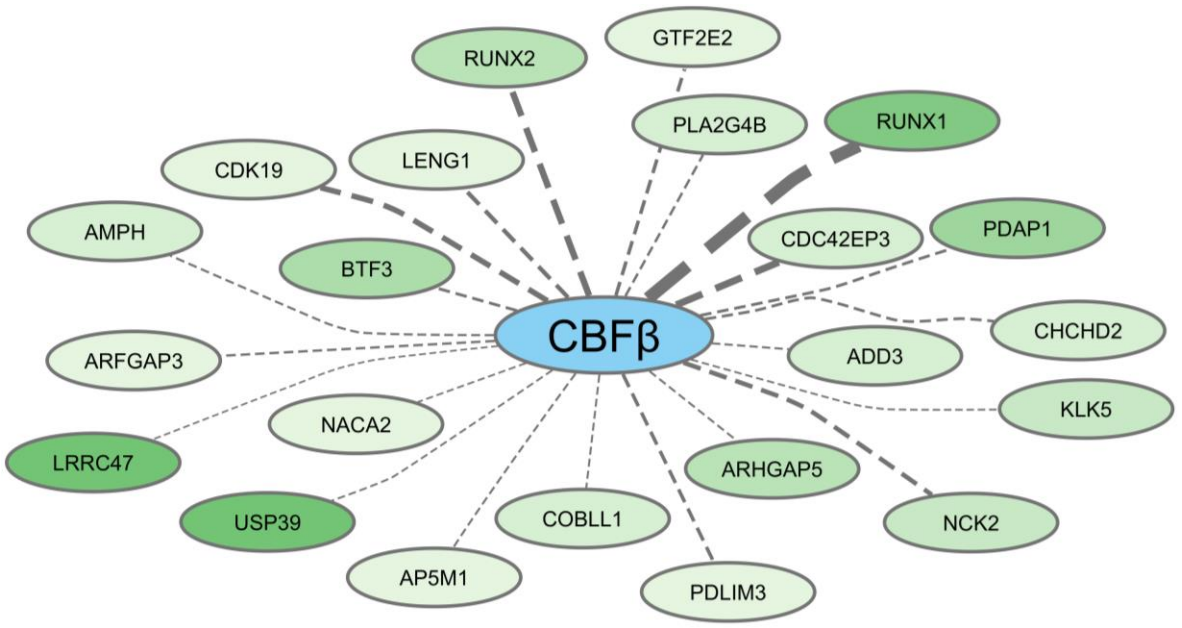

Figure 4.5 High confidence interactors of CBFβ. Intensity of green color denotes quantity of unique peptides used to identify each protein, and thickness of dotted line denotes fold enrichment of protein in pulldown relative to both controls.

Interaction network outlining high confidence interactors of CBFβ. Both RUNX1 and RUNX2 showed up as high confidence interactors of CBFβ, along with numerous others. RUNX1 experienced the highest fold enrichment in pulldown of CBFβ_FLAG_WT compared to control, denoted by the thickest dotted line connecting it to CBFβ.

A

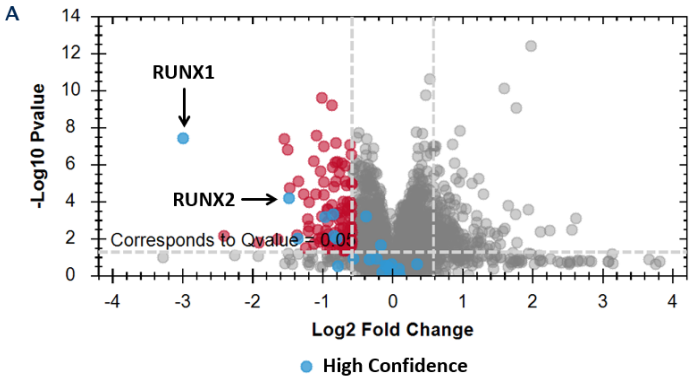

B

Protein	Fold Inhibition
RUNX1	8.0
RUNX2	2.8
CDC42EP3	2.6
CHCHD2	1.9
CDK19	1.8
NCK2	1.8
ARFGAP3	1.7

Figure 4.6 A) Volcano plots of proteins with decreased enrichment when bound to CBFβ_3xMut_FLAG compared to CBFβ_WT_FLAG. B) High confidence interactors of CBFβ which exhibited reduced binding to CBFβ_3xMut_FLAG compared to CBFβ WT FLAG.

High confidence interactors of CBFβ with reduced binding to CBFβ_3xMut_FLAG. In total, seven (7) proteins of the twenty-three (23) high confidence interactors identified displayed reduced enrichment when pulled down by CBFβ_3xMut_FLAG. Of these, RUNX1 had the most drastic reduction in binding, with an eight-fold reduction in enrichment by CBFβ_3xMut_FLAG.

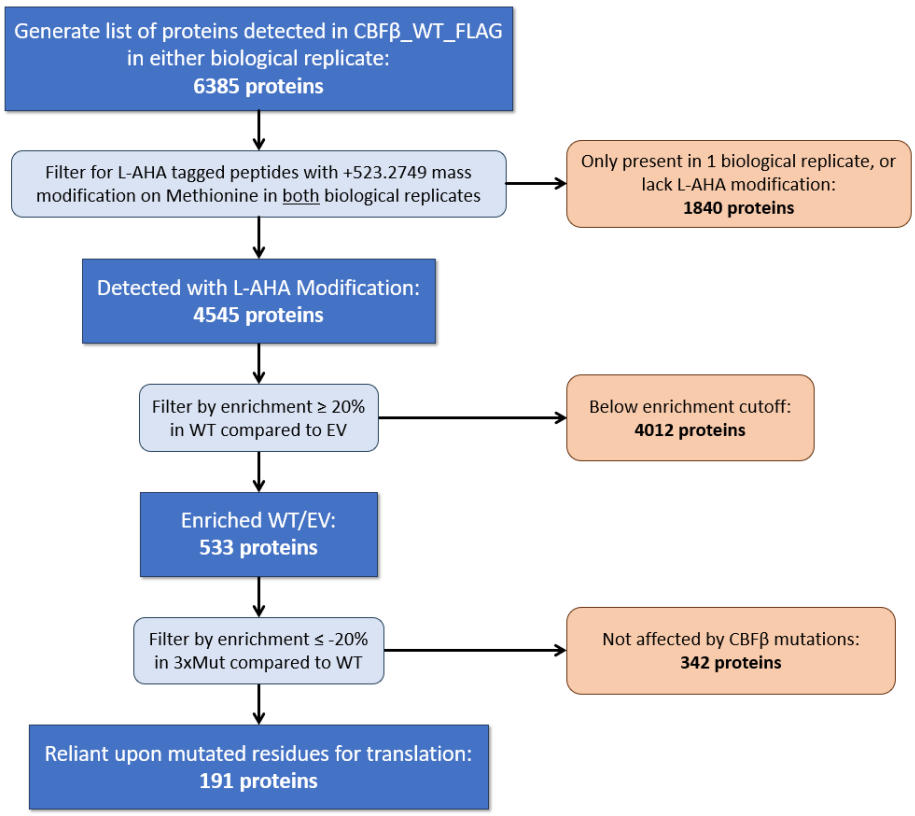

Figure 4.7 Workflow used to identify differentially translated genes in the presence of CBFβ_WT_FLAG or CBFβ_3xMut_FLAG relative to EV.

Proteins detected in DiDBiT pulldowns were selectively filtered to identify differentially translated proteins. Out of a total 6,385 proteins identified, 533 were detected in both biological replicates with enrichment ≥20% of L-AHA modified peptides in CBFβ_WT_FLAG cells compared to EV. Of these, 191 proteins exhibited a ≥ 20% decrease in enrichment when expressed in CBFβ_3xMut_FLAG producing cells.

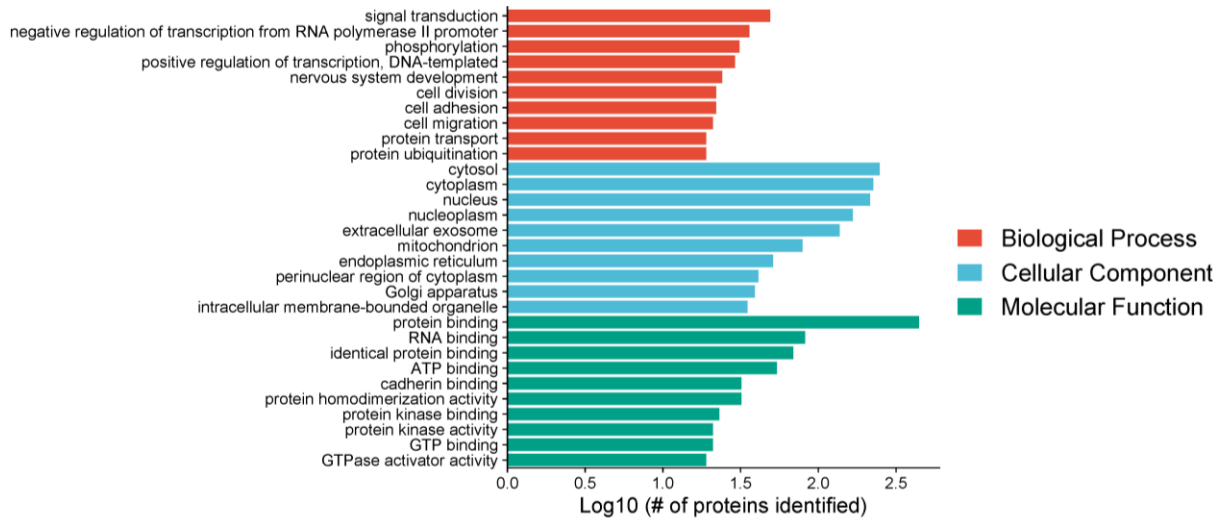

Figure 4.8 Enriched GO terms for biological processes, cellular components, and molecular functions among proteins which exhibited a 20% or greater change in abundance of L-AHA modified peptides in CBFβ_WT_FLAG compared to EV.

Enriched GO terms among proteins enriched in CBFβ_WT_FLAG, as identified by DiDBiT. Biological process terms associated with transcription were highly ranked as well as those associated with cell division, adhesion, and migration. A variety of cellular components were represented as well as numerous molecular functions, including protein, RNA, ATP, and GTP binding.

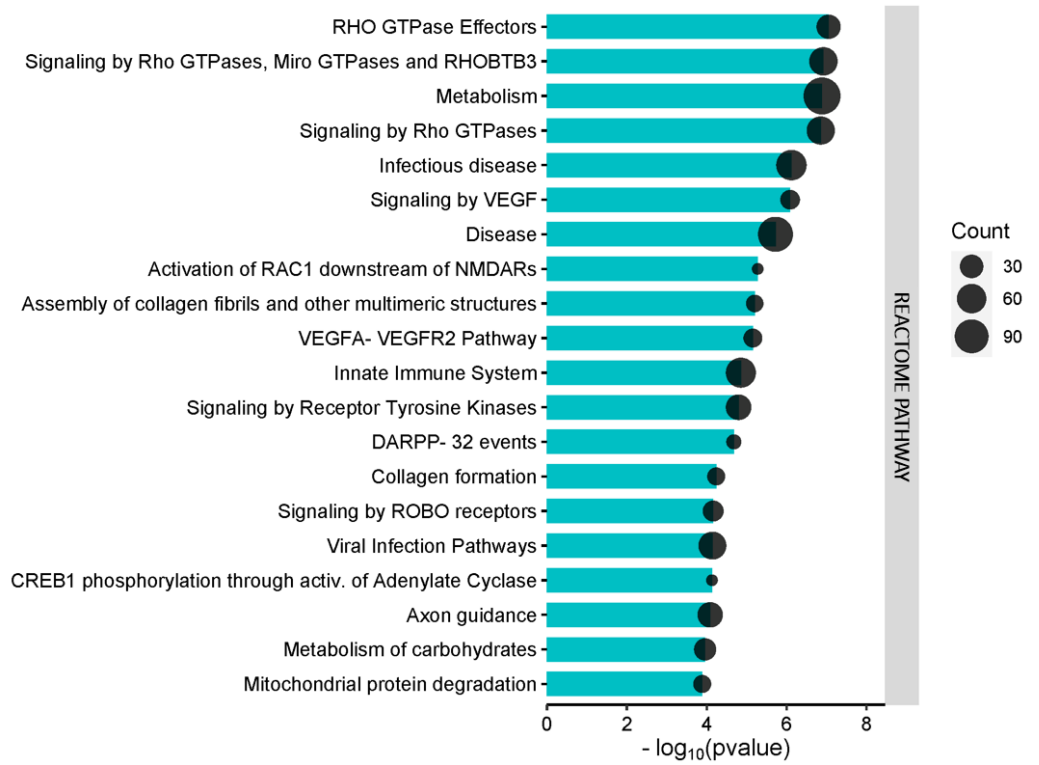

Figure 4.9 Reactome pathway analysis of 533 proteins which exhibited a 20% or greater change in abundance of L-AHA modified peptides in CBFβ_WT_FLAG compared to EV.

Enriched Reactome terms among proteins enriched in CBFβ_WT_FLAG, as identified by DiDBiT. Rho GTPase-associated Reactome terms came up highly ranked among proteins identified in DiDBiT as well as those associated with VEGF.

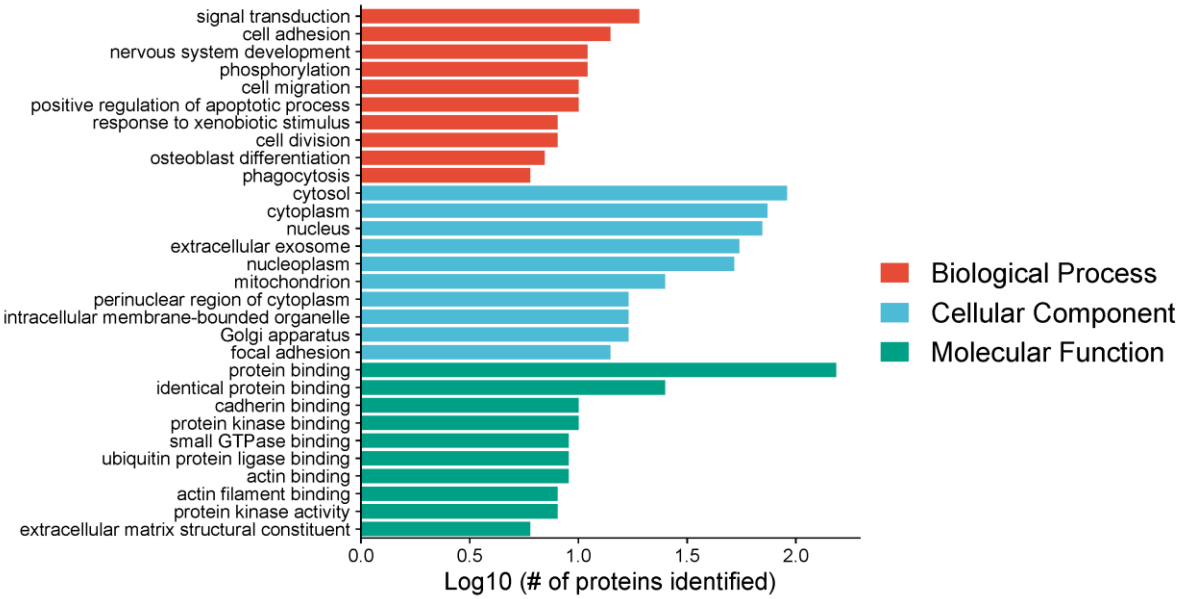

Figure 4.10 GO for DiDBiT proteins which went up in WT and went down in mutant.

Enriched GO terms among proteins enriched in CBFβ_WT_FLAG and decreased in CBFβ_3xMut_FLAG, as identified by DiDBiT. The biological process terms signal transduction, cell adhesion, and cell migration/division were highly ranked, as well as numerous cellular components. Binding to a variety of targets such as cadherin, protein kinases, and small GTPases were highly ranked in molecular function.

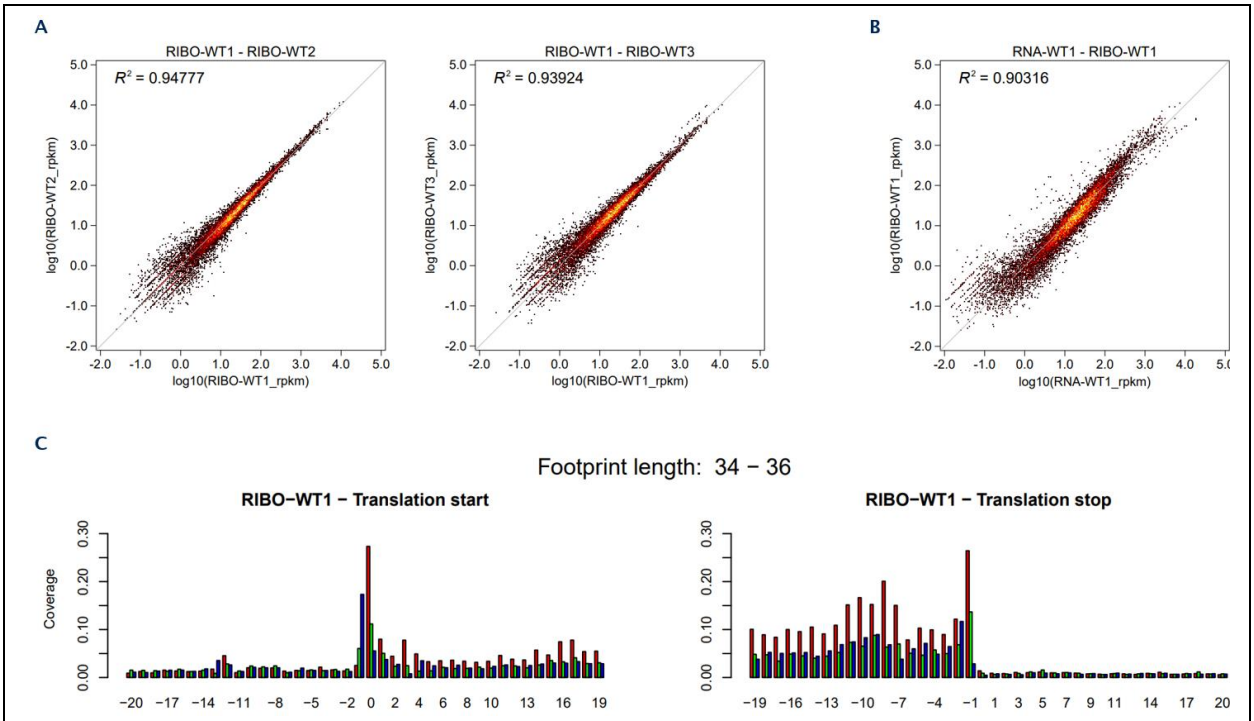

Figure 4.11 A) Consistencies between for CBFβ_WT_FLAG biological replicate 1 and other two biological replicates. B) Congruency of ribosome footprint RPKM vs. RNAseq RPKM. C) Riboseq metagene coverages checking for characteristic 3-periodicity in footprint reads.

Quality control data for Ribo-Seq analysis. Representative images for the first biological replicate for CBFβ_WT_FLAG are displayed above. Other biological replicates as well as those for EV cells were similar, with R squared values > 0.90 in all. Characteristic 3-periodicity of Ribo-Seq reads was present in WT1 as well as all other replicates.

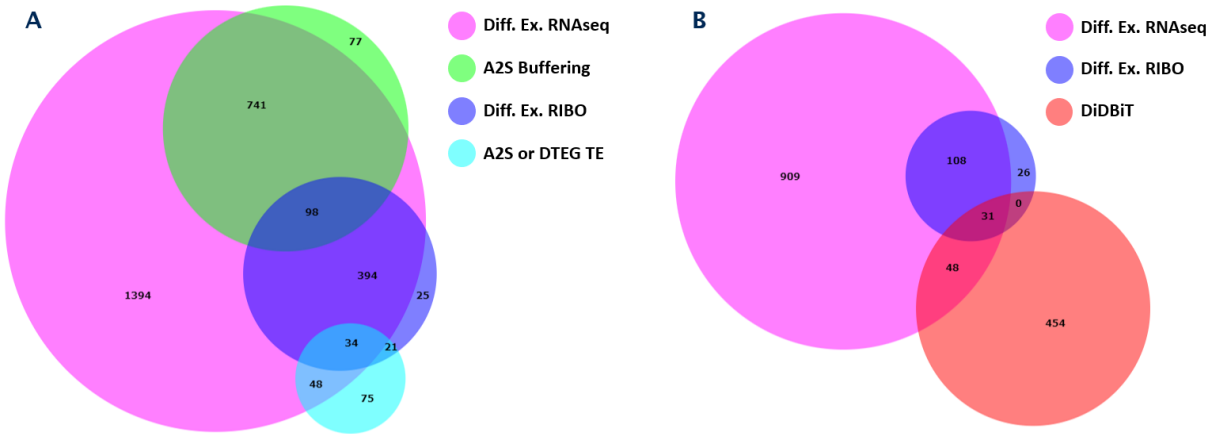

Figure 4.12 A) Venn diagram of genes experiencing significant changes in the above parameters, up or down, in Ribo-Seq analysis of CBFβ_WT_FLAG vs. EV. Genes were binned as differentially expressed (diff. ex) in RNAseq analysis (fuscia), ribosome footprint analysis (purple), possessing altered translation efficiency via Anota2seq (A2S) or DTEG analyses (blue), or translationally buffered in Anota2seq (green). B) Venn diagram of genes experiencing a significant increase in expression in CBFβ_WT_FLAG compared to EV, as measured by RNAseq (fuscia), ribosome footprint analysis (purple), or DiDBiT (red).

Grouping of genes identified in Ribo-Seq and comparison with those identified in DiDBiT.

A total of 2,715 genes were identified as differentially expressed at the RNA level between CBFβ_WT_FLAG and EV cells. Of these, many were binned as buffered via A2S, differentially expressed in ribosome footprinting abundance, and altered in translational efficiency. Overlaps between the aforementioned groups are illustrated above. 79 genes identified as differentially expressed via DiDBiT were corroborated by RNAseq data, with ribosome footprints of 31 of these also significantly enriched in CBFβ_WT_FLAG cells compared to EV.

Table 4.1: Genes up-regulated in CBFβ_WT_FLAG cells vs. EV across DiDBiT, RNAseq, and RIBO-Seq assays

Gene	Name	HGNC ID
AHNAK	AHNAK nucleoprotein	HGNC:347
ALDH2	aldehyde dehydrogenase 2 family member	HGNC:404
ARHGAP28	Rho GTPase activating protein 28	HGNC:25509
CBFB	core-binding factor subunit beta	HGNC:1539
CD70	CD70 molecule	HGNC:11937
CDC42EP3	CDC42 effector protein 3	HGNC:16943
CDKN1A	cysteine rich DPF motif domain containing 1	HGNC:33710
COL6A3	collagen type VI alpha 3 chain	HGNC:2213
CPA4	carboxypeptidase A4	HGNC:15740
ERBIN	erbb2 interacting protein	HGNC:15842
EZR	ezrin	HGNC:12691
FKBP9	FKBP prolyl isomerase 9	HGNC:3725
GPHN	gephyrin	HGNC:15465
HCFC1R1	host cell factor C1 regulator 1	HGNC:21198
KRT86	keratin 86	HGNC:6463
LAMB3	laminin subunit beta 3	HGNC:6490
MIS18A	MIS18 kinetochore protein A	HGNC:1286
NPC2	NPC intracellular cholesterol transporter 2	HGNC:14537
PALLD	palladin, cytoskeletal associated protein	HGNC:17068
PDCD2	programmed cell death 2	HGNC:8762
PLXNB2	plexin B2	HGNC:9104
PPME1	protein phosphatase methylesterase 1	HGNC:30178
RHOBTB3	Rho related BTB domain containing 3	HGNC:18757
SBF1	SET binding factor 1	HGNC:10542
SERPINA1	serpin family A member 1	HGNC:8941
SLC2A3	solute carrier family 2 member 3	HGNC:11007
SYTL3	synaptotagmin like 3	HGNC:15587
TBC1D10A	TBC1 domain family member 10A	HGNC:23609
TBC1D2	TBC1 domain family member 2	HGNC:18026
TBC1D22A	TBC1 domain family member 22A	HGNC:1309

Specific genes upregulated in CBFβ_WT_FLAG cells vs. EV, as measured by DiDBiT, RNAseq, and RIBO-Seq. The above 31 genes were increased in expression across all three assays. Listed are gene ID, name, and HUGO Gene Nomenclature Committee (HGNC) identification.

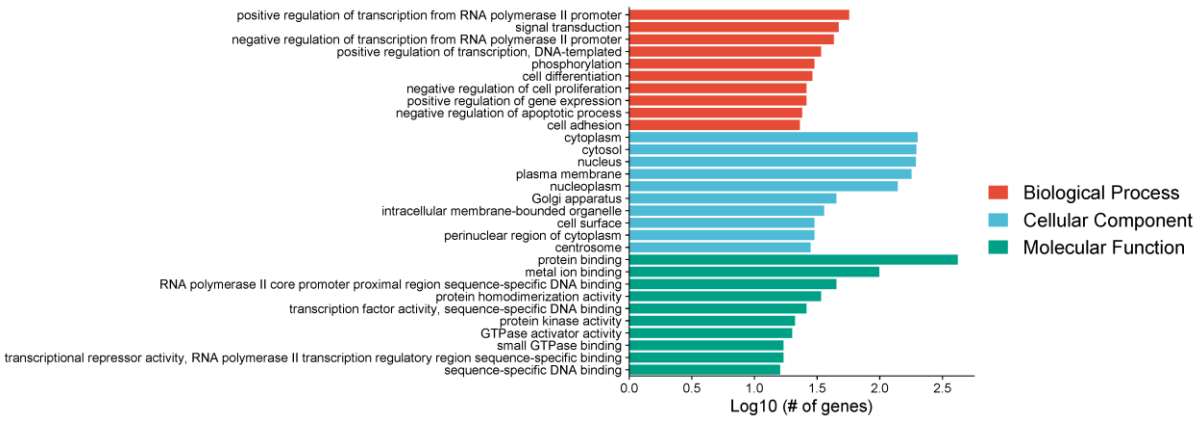

Figure 4.13 GO analysis of genes in Ribo-Seq which either underwent an increase in TE in CBFβ_WT_FLAG compared to EV, or exhibited positive translational buffering in CBFβ_WT_FLAG compared to EV.

GO analysis of genes with increased translation efficiency or positive translational buffering in the presence of CBFβ_WT_FLAG. Among genes identified, GO terms associated with transcription and gene expression overall ranked very highly. Also notable was genes involved in signal transduction as well as proliferation and cell adhesion. As in previous GO analyses, numerous cellular components as well as molecular functions were represented.

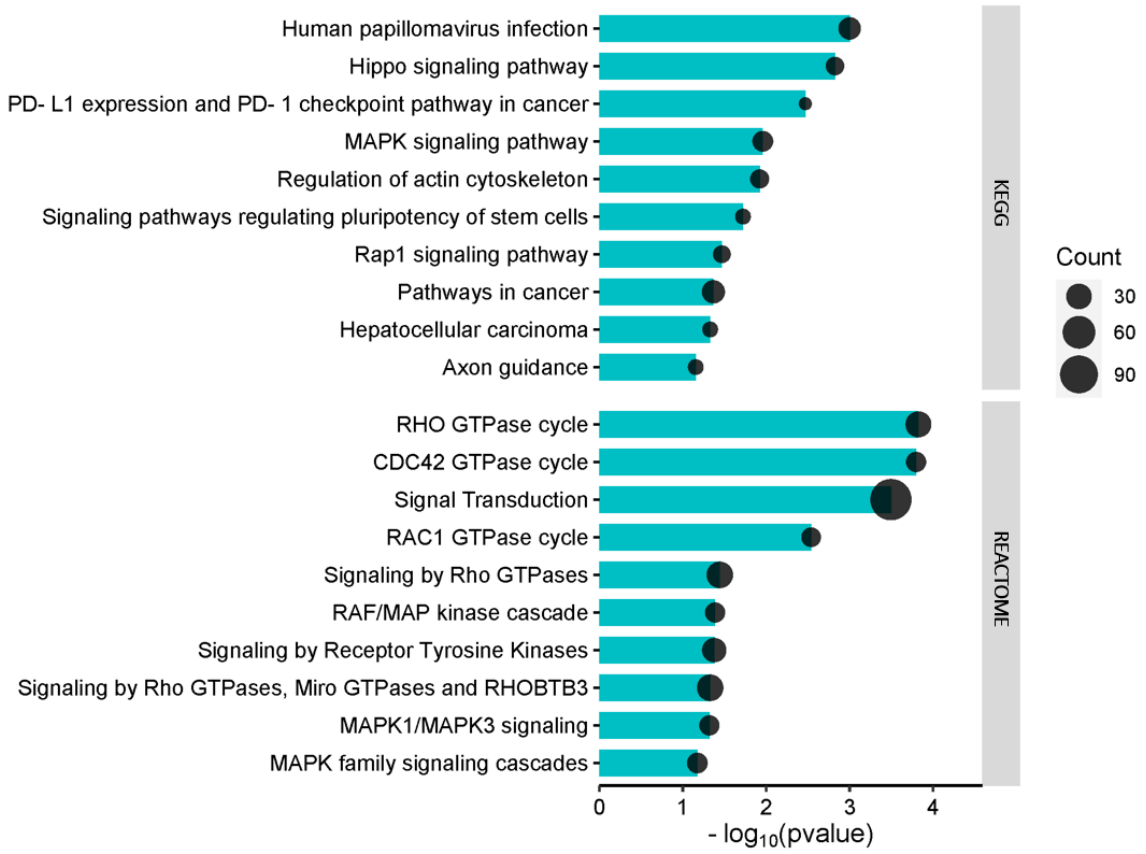

Figure 4.14 KEGG pathway and Reactome analysis of genes in Ribo-Seq which either underwent an increase in TE in CBFβ_WT_FLAG compared to EV, or exhibited negative translational buffering in CBFβ_WT_FLAG compared to EV.

Reactome and KEGG pathway analyses of genes with increased translation efficiency or translational buffering in the presence of CBFβ_WT_FLAG. Multiple signaling pathways, many implicated in cancer, were represented in Reactome pathway analysis of aforementioned genes. Rho GTPase actions as well as MAPK signaling ranked highly in KEGG pathway analysis.

Discussion

IP-MS of CBFβ revealed 3,297 initial proteins detected, which were subjected to successive filtrations to reveal medium and high-confidence CBFβ interactors (**Figure 4.1**). Encouragingly, both RUNX1 and RUNX2, known interactors of CBFβ (15,35–38), were enriched relative to both controls (**Figure 4.2**). This corroborated our previous data on interaction of our transgene with endogenous targets, increasing our confidence in the legitimacy of novel interacting partners observed.

Among proteins identified as medium confidence interactors, a total of 224 proteins, gene ontology revealed high enrichment of biological process terms mRNA processing, translation, and cytoplasmic translation (**Figure 4.3**). This lined up well with our hypothesis, that CBFβ may participate in protein translation. Medium confidence interactors were enriched in the cellular component term "nucleus", which was expected, however GO term "cytoplasm" was also highly enriched. As the translational role of CBFβ is postulated to occur in the cytoplasm, the enrichment of the cytoplasmic term bolsters these claims of a role for CBFβ outside of the nucleus. It was interesting that "mRNA processing" came up highly enriched on the GO biological process terms, as well as "RNA binding" on molecular function terms. CBFβ was suggested to interact with hnRNPK, a multifunctional protein involved in transcription, RNA splicing, and protein translation (39). While hnRNPK was not identified as an interactor in our screen, numerous other proteins implicated in mRNA processing were identified. Among the medium confidence interactors was eIF4B, a member of the eukaryotic translation initiation complex (40) which plays a key role in protein translation, and was previously reported to interact with CBFβ (14). Cul5, an E3 ligase which has previously been reported to interact with CBFβ (41), also showed up as a medium confidence interactor, further increasing our confidence in these data. Many of the

medium confidence interactors were associated with GO terms “translation” and “peptide biosynthetic process”, including eIF4B (**Figure 4.4**).

Further filtration for proteins significantly enriched when compared to both EV and Isotype controls yielded a list of twenty-three (23) proteins, which we binned as high confidence interactors of CBFβ (**Figure 4.5**). As mentioned previously, RUNX1 and RUNX2 were among this group. RUNX1 experienced a higher enrichment in pulldown than RUNX2, as evidenced by the thicker line connecting it to CBFβ. This was also encouraging, as previous studies reported CBFβ-RUNX interaction to alter RUNX1 stability more drastically than RUNX2, possibly due to the CBFβ-RUNX1 interaction being of a higher affinity than CBFβ-RUNX2 (15). In addition to known interacting partners RUNX1 and RUNX2, twenty-one (21) proteins were also identified, none of which are mentioned in The Human Protein Atlas or String-db protein interaction databases. To our knowledge, this represents the first comprehensive study of CBFβ interacting proteins in OS.

While the full relevance of these interactions remains to be understood, many of the proteins identified as high confidence interactors of CBFβ are implicated in important cellular processes and disease. Among the list was ubiquitin specific peptidase 39 (USP39), a member of the deubiquitinase (DUB) family of enzymes. DUB’s play key roles in maintaining protein homeostasis in the cell, and have been implicated in a wide array of diseases (42,43). USP39 is no exception, and has been reported to have an oncogenic role in osteosarcoma (44) as well as numerous other cancers (45–54). In fact, studies of USP39 in osteosarcoma were conducted in U2OS cells, the same parental line as the cells used in this project. This oncogenic function of USP39 is thought to take place through two mechanisms: 1) stabilization of beta-catenin via direct de-ubiquitination and 2) downregulation of TRIM26 by reduction of TRIM26 pre-mRNA

maturation (54). It's also possible that USP39 may keep pro-survival proteins such as Bcl-2, survivin, and Mcl-1 upregulated in these cells, further contributing to its oncogenic behavior. Also identified as a high confidence interactor of CBFβ was NCK2, an adapter protein which associates with tyrosine-phosphorylated growth factor receptors. Elevated levels of NCK2 are implicated in melanoma proliferation, migration, and invasion (55) as well as invasion in breast cancer and prostate cancer cell lines (56). CDK19 was also identified, and upregulation of this protein correlates with unfavorable prognosis in hepatocellular carcinoma (HCC) (57).

Interestingly, NACA2 and BTF3, two members of the same complex, also came up on our screen. Together, NACA and BTF3 comprise the nascent polypeptide-associated complex (NAC), which is located at the ribosome exit tunnel (58). This complex functions as a chaperone, assisting in protein folding, and protects the nascent polypeptide sequences from proteolysis as the new protein is translated (59). Loss of this complex is embryonic lethal, and association with NAC is likely the first interaction undergone by the newly synthesized peptide (59). This complex is also implicated in controlling translation initiation (60) as well as oncogenic activity in colorectal cancer (61) and prostate cancer (62). Further study is required to elucidate how interaction with CBFβ affects the activity of NAC, as this complex plays an indispensable role in nascent protein synthesis.

Analysis of CBFβ_3xMut_FLAG-associated proteins in relation to those identified to interact with CBFβ_WT_FLAG revealed seven (7) proteins which appear to be reliant upon residues G61, N63, or N104, or a combination, for their binding to CBFβ. Among this list was RUNX1 and RUNX2, in agreement with previously shown CETSA data which suggested CBFβ-RUNX2 interaction to be inhibited by these mutations. Also in this list were CDK19 and NCK2, as well as three other proteins: CDC42EP3, CHCHD2, and ARFGAP3.

Following identifying specific interactors of CBFβ, we conducted DiDBiT (24) to elucidate which proteins may be increased in synthesis rate upon re-introduction of CBFβ_WT_FLAG into CBFβ KO cells. A total of 6,385 unique proteins were identified in CBFβ_WT_FLAG cells, which were successively filtered for L-AHA methionine modification, presence in both biological replicates, and enrichment ≥ 20% in CBFβ_WT_FLAG cells relative to EV (**Figure 4.7**). This revealed a list of 533 proteins which are putative translational targets of CBFβ. Further filtration in comparison of this list to proteins identified in CBFβ_3xMut_FLAG cells revealed 191 proteins which may be reliant upon CBFβ residues G61, N63, and N104 for their translation.

Gene ontology was applied to this list of 533 proteins, revealing high enrichment of biological process terms signal transduction, transcription, cell division, adhesion, and migration (**Figure 4.8**). Many of these pathways are de-regulated in cancer, and it's possible CBFβ plays a larger role in them than previously thought. Numerous cellular components were identified, as well as molecular functions involving binding of RNA, ATP, and GTP.

Reactome pathway analysis was next applied to this list of 533 proteins, and revealed high enrichment of pathways involving Rho GTPase signaling as well as VEGF (**Figure 4.9**). Rho GTPase signaling has been implicated in OS (63) and VEGF is a well-known poor prognostic indicator in OS (64). Numerous proteins implicated in cancer were found on this list, notable inclusions being SYDE1 (65), BRD2 (66), NRP1(67), HMOX1 (68), and CD70 (69).

GO was next applied to the 191 proteins enriched in CBFβ_WT_FLAG cells relative to EV as well as CBFβ_3xMut_FLAG cells, which we are classifying as potentially dependent upon CBFβ residues G61, N63, and/or N104 for their translation (**Figure 4.10**). Enriched biological process terms in this list included signal transduction and cell adhesion, as well as cell division

and osteoblast differentiation, all of potential interest in OS. A variety of molecular functions were represented, in particular numerous binding capabilities in the molecular function GO class.

It's important to note that DiDBiT is a measure of overall nascent protein synthesis rate, and looks purely at the rate of production of each protein. As such, a protein could theoretically be up-regulated at the mRNA level, experience no change in regulation at the translation level, and still show up as enriched in DiDBiT. This protein would therefore show up as up-regulated by CBFβ_WT_FLAG on DiDBiT, although in terms of CBFβ influencing protein translation, nothing significant may have occurred. Additionally, proteins which have longer half-lives would experience slower rates of translation (70) and may not be identified via DiDBiT, as insufficient quantities of these proteins may be produced in order to be detected via LC-MS/MS. In order to evaluate the role of CBFβ in translational regulation more specifically, and generate a more comprehensive list of proteins without the inherent bias of DiDBiT, we performed Ribo-Seq, or Ribosome Footprinting analysis, on CBFβ_WT_FLAG as well as EV cells.

Ribo-Seq consists of bulk RNA sequencing of a sample coupled with parallel processing and deep sequencing of individual portions of each mRNA strand protected by the presence of a ribosome (21). Comparing the quantity of ribosome reads ascribed to a gene to the quantity of mRNA present for that gene allows measurement of ribosomal quantity per mRNA strand, which allows us to infer the rate at which a particular mRNA is being translated.

Quality control checks of Ribo-Seq analysis (**Figure 4.11**) demonstrated that analysis was performed properly. This experiment was performed in three biological replicates per cell line, and demonstrated good consistency between replicates. Congruency, a measure of correlation between quantity of RNA produced and quantity of ribosome footprints detected, was high for replicates as well. In **Figure 4.11 B**, the genes which fall outside of the linear correlation for congruency are

those which are subject to alterations in translational efficiency (TE) or ribosomal buffering based on the presence of CBFβ. Ribosome footprint reads passed QC check as well, with characteristic 3 periodicity displayed in all replicates shown in **Figure 4.11 C**. Although QC data for just the first biological replicate of CBFβ_WT_FLAG cells was shown, QC graphs for all other samples were extremely similar.

Many genes were found to be altered in transcription quantity, translation quantity, translational efficiency, or ribosomal buffering in CBFβ_WT_FLAG cells compared to EV (**Figure 4.12A**). There was considerable overlap between these categories, but inclusion in one category doesn't necessitate inclusion in another.

Transcription quantity (via RNAseq) measures the quantity of mRNA strands transcribed for a given gene. Translation quantity (via deep sequencing of ribosomal footprints) is a measure of quantity of a given protein being produced. The "bread and butter" of Ribo-Seq lies in comparing these two measurements, and generating two new metrics: translation efficiency (TE) and ribosomal buffering. TE is a measure of ribosome occupancy on a given gene, and is calculated by relating the quantity of ribosome footprint reads for that gene compared to the overall quantity of mRNA of that gene as measured by RNAseq. This is a measure of how efficiently the cell produces that protein from a given mRNA input. Higher efficiency means that mRNA is more actively translated. Ribosomal buffering occurs when a gene experiences a change in transcription, but the effect of this on protein quantity produced is blunted, or buffered, by a compensatory change in translation in the opposite direction. For example, if a gene is down-regulated at the mRNA level by a certain fold, the translation efficiency of this gene may also be increased, meaning the level of protein produced would not be reduced by the same fold. It's possible the overall quantity of protein produced remains the same, but without measuring buffering one may

presume there were no alterations in gene expression, when in fact radical changes in regulation had occurred.

As we are investigating the role of CBFβ in translation, we are interested in the genes which experienced a change in ribosome footprints (Diff. Ex. RIBO), those altered in TE as measured via Anota2Seq (A2S) or DTEG algorithms (denoted A2S or DTEG TE), and those which experienced ribosomal buffering as defined by A2S (A2S buffering), as well as any overlaps between these groups. A gene may be included in just one of these categories, or multiple, and be of interest.

We next analyzed similarities between DiDBiT data and Ribo-Seq (**Figure 4.12B**). As mentioned previously, DiDBiT does not take rate of transcription into account, and focuses solely on the rate of nascent protein synthesis between CBFβ_WT_FLAG and EV cells. For this reason, we avoided the A2S buffering category as well as A2S or DTEG TE and instead looked at overlap between overall production of mRNA (as measured by RNAseq), overall rate of protein synthesis (Diff. Ex. RIBO), and nascent proteins elevated in synthesis in CBFβ_WT_FLAG cells via DiDBiT. Of the proteins identified as having differential synthesis quantity via Ribo-Seq or DiDBiT, 31 were found to be up-regulated in both experiments. These 31 proteins (**Table 1**) are certainly of high interest, and further study is needed to investigate the relative importance of a gene being identified only in DiDBiT, or Ribo-Seq, or across both.

RUNX2 was present in the list of differentially translated proteins as identified by DiDBiT, although it did not reach this cutoff in Ribo-Seq analysis. The RNAseq portion of Ribo-Seq analysis measured RUNX2 mRNA levels to be nearly identical between EV and CBFβ_WT_FLAG cells, corroborating earlier data that this discrepancy in RUNX2 protein production must be via a post-transcriptional mechanism. In terms of ribosomal footprint reads,

RUNX2 RIBO reads per kilobase per million mapped reads (RPKM) was ~7.12 in EV and ~7.78 in CBFβ_WT_FLAG cells, indicating elevated RUNX2 protein production in CBFβ_WT_FLAG cells. Although this did not make it to the enrichment cutoff to be binned as differentially expressed in terms of ribosome footprint reads, it was encouraging to see a difference between the two cell lines in RUNX2 protein production which was not mirrored in transcription. Stabilization of RUNX2 via binding to CBFβ may still play a role in the discrepancy of RUNX2 protein, but RUNX2 being identified as differentially synthesized via DiDBiT still suggests CBFβ to influence overall production of RUNX2.

We next applied gene ontology to genes identified as positively influenced in translation in the presence of CBFβ_WT_FLAG via Ribo-Seq (**Figure 4.13**). Included in this list were genes which underwent an increase in TE in CBFβ_WT_FLAG cells compared to EV cells. Also included were genes that exhibited positive translation buffering in CBFβ_WT_FLAG cells compared to EV. Positive buffering refers to genes which were down-regulated in transcription in CBFβ_WT_FLAG cells relative to EV, but simultaneously exhibited a compensatory increase in translation efficiency. This does not necessarily lead to an increase in the overall quantity of protein produced, but does speak to up-regulation of expression of these genes at the translational level resulting from the presence of CBFβ_WT_FLAG. Altogether, this list totaled 586 genes.

Enriched GO terms among these genes included biological process terms specific to transcription and gene expression. Interestingly, cell differentiation and cell adhesion were also mentioned, processes known to be implicated in cancer. As in previous GO studies, multiple cellular components were represented. Interestingly, the term “small GTPase binding”, enriched among DiDBiT candidates (**Figure 4.10**) was also enriched in Ribo-Seq analysis. Small GTPases as well as their downstream effectors have been implicated in a variety of cancers including OS

(71–74). Notably, multiple members and regulators of the RAS family, a group of proteins infamous in their association with cancer (75–77) were identified in this gene list.

Following this, these same genes were subjected to Reactome and KEGG pathway analysis (**Figure 4.14**). KEGG pathway analysis revealed enrichment of multiple pathways extensively implicated in cancer, such as PD-L1 (78), MAPK (79), and RAP1 (80), as well as enrichment of the "pathways in cancer" term itself. Furthermore, the KEGG term "hepatocellular carcinoma" (HCC) was also strongly enriched, which was interesting as proteins implicated in HCC were also among the list of high confidence interactors of CBFβ identified via IP-MS (**Figure 4.5**). Reactome pathway analysis also demonstrated MAPK signaling cascade enrichment as well as multiple terms associated with GTPase cycles such as RHO, CDC42 and RAC1. Importantly, Rho GTPase activity was also highly ranked among genes identified via DiDBiT (**Figure 4.9**).

In conclusion, we have generated a comprehensive list of medium- and high-confidence interacting partners of CBFβ in OS cells. This represents the first of its kind in OS. mRNA processing and translation terms were highly enriched in GO analysis of CBFβ interactors, and the medium-confidence interacting partners list included proteins previously reported to interact with CBFβ. Bonafide binding partners of CBFβ, RUNX1 and RUNX2, appeared in our screen, giving us confidence in the validity of our assay. Numerous proteins identified in our assay as high-confidence interactors of CBFβ have implications in cancer and OS specifically, and both members of the NAC complex, a heterodimer strongly implicated in protein translation, were among this list. Additionally, we identified seven proteins which may depend upon CBFβ residues G61, N63, and/or N104 for their interaction. We also conducted DiDBiT as well as Ribo-Seq to identify genes which CBFβ may translationally regulate, and pathway analyses of these genes revealed many enriched terms which are of interest in OS and cancer biology at large. Notably, DiDBiT and Ribo-

Seq both revealed Rho GTPase activity to be strongly enriched among their respective gene lists, suggesting CBFβ may play a significant role in regulation of this pathway. As these experiments represent an enormous quantity of data with a wide array of future directions, more study is needed to understand the full significance of CBFβ in OS, and the outcome of CBFβ-mediated regulation of the most salient targets identified. Encouragingly, GO analysis of putative interacting partners, and regulatory targets, of CBFβ revealed a multitude of terms strongly implicated in cancer. Based on these data, it appears highly likely that CBFβ plays a role in protein translation in OS, and that proteins implicated in OS and cancer at large fall under its regulatory purview.

Acknowledgements

We would like to thank Michelle Salemi and Dr. Brett Phinney of the UC Davis proteomics core for their assistance in performing proteomic LC-MS/MS analysis for this project for the IP-MS and DiDBiT assays.

We would also like to acknowledge Dr. Silvia Tornaletti and Dr. Luciano Brocchieri of TB-Seq, Inc. for performing Ribo-Seq and providing extensive data packages to us.

This project was supported in part by NIH K01OD026526, NIH R03OD031958, and startup funds provided to Dr. Wittenburg through the UC Davis Comprehensive Cancer Center.

References

1. Fletcher CDM, World Health Organization, International Agency for Research on Cancer, editors. WHO classification of tumours of soft tissue and bone. 4th ed. Lyon: IARC Press; 2013. 468 p. (World Health Organization classification of tumours).
2. Mirabello L, Troisi RJ, Savage SA. Osteosarcoma incidence and survival rates from 1973 to 2004: Data from the Surveillance, Epidemiology, and End Results Program. Cancer. 2009 Apr;115(7):1531–43.
3. Duggan MA, Anderson WF, Altekruse S, Penberthy L, Sherman ME. The Surveillance, Epidemiology, and End Results (SEER) Program and Pathology: Toward Strengthening the Critical Relationship. American Journal of Surgical Pathology. 2016 Dec;40(12):e94–102.
4. Ottaviani G, Jaffe N. The Epidemiology of Osteosarcoma. In: Jaffe N, Bruland OS, Bielack S, editors. Pediatric and Adolescent Osteosarcoma [Internet]. Boston, MA: Springer US; 2010. p. 3–13. Available from: https://doi.org/10.1007/978-1-4419-0284-9_1
5. Schiavone K, Garnier D, Heymann MF, Heymann D. The Heterogeneity of Osteosarcoma: The Role Played by Cancer Stem Cells. In: Birbrair A, editor. Stem Cells Heterogeneity in Cancer [Internet]. Cham: Springer International Publishing; 2019 [cited 2022 Nov 9]. p. 187–200. (Advances in Experimental Medicine and Biology; vol. 1139). Available from: https://link.springer.com/10.1007/978-3-030-14366-4_11
6. Polunovsky VA, Bitterman PB. The Cap-Dependent Translation Apparatus Integrates and Amplifies Cancer Pathways. RNA Biology. 2006 Jan;3(1):10–7.
7. Adya N, Castilla LH, Liu PP. Function of CBFβ/Bro proteins. Seminars in Cell & Developmental Biology. 2000 Oct;11(5):361–8.
8. Kagoshima H, Shigesada K, Satake M, Ito Y, Miyoshi H, Ohki M, et al. The Runt domain identifies a new family of heteromeric transcriptional regulators. Trends Genet. 1993 Oct;9(10):338–41.
9. Wysokinski D, Pawlowska E, Blasiak J. RUNX2: A Master Bone Growth Regulator That May Be Involved in the DNA Damage Response. DNA and Cell Biology. 2015 May;34(5):305–15.
10. Nathan SS, Pereira BP, Zhou Y fang, Gupta A, Dombrowski C, Soong R, et al. Elevated expression of Runx2 as a key parameter in the etiology of osteosarcoma. Mol Biol Rep. 2009 Jan;36(1):153–8.
11. Sadikovic B, Thorner P, Chilton-MacNeill S, Martin JW, Cervigne NK, Squire J, et al. Expression analysis of genes associated with human osteosarcoma tumors shows correlation of RUNX2 overexpression with poor response to chemotherapy. BMC Cancer. 2010 Dec;10(1):202.
12. Feng Y, Liao Y, Zhang J, Shen J, Shao Z, Hornicek F, et al. Transcriptional activation of CBFβ by CDK11p110 is necessary to promote osteosarcoma cell proliferation. Cell Commun Signal. 2019 Dec;17(1):125.
13. Alegre F, Ormonde AR, Godinez DR, Illendula A, Bushweller JH, Wittenburg LA. The interaction between RUNX2 and core binding factor beta as a potential therapeutic target in canine osteosarcoma. Vet Comparative Oncology. 2020 Mar;18(1):52–63.
14. Malik N, Yan H, Moshkovich N, Palangat M, Yang H, Sanchez V, et al. The transcription factor CBFB suppresses breast cancer through orchestrating translation and transcription. Nat Commun. 2019 May 6;10(1):2071.

15. Qin X, Jiang Q, Matsuo Y, Kawane T, Komori H, Moriishi T, et al. Cbfb Regulates Bone Development by Stabilizing Runx Family Proteins. Journal of Bone and Mineral Research. 2015 Apr 1;30(4):706–14.
16. Lim KE, Park NR, Che X, Han MS, Jeong JH, Kim SY, et al. Core Binding Factor β of Osteoblasts Maintains Cortical Bone Mass via Stabilization of Runx2 in Mice. Journal of Bone and Mineral Research. 2015 Apr 1;30(4):715–22.
17. Cenik C, Cenik ES, Byeon GW, Grubert F, Candille SI, Spacek D, et al. Integrative analysis of RNA, translation, and protein levels reveals distinct regulatory variation across humans. Genome Res. 2015 Nov;25(11):1610–21.
18. Gry M, Rimini R, Strömberg S, Asplund A, Pontén F, Uhlén M, et al. Correlations between RNA and protein expression profiles in 23 human cell lines. BMC Genomics. 2009 Dec;10(1):365.
19. Perl K, Ushakov K, Pozniak Y, Yizhar-Barnea O, Bhonker Y, Shivatzki S, et al. Reduced changes in protein compared to mRNA levels across non-proliferating tissues. BMC Genomics. 2017 Dec;18(1):305.
20. Prabahar A, Zamora R, Barclay D, Yin J, Ramamoorthy M, Bagheri A, et al. Unraveling the complex relationship between mRNA and protein abundances: a machine learning-based approach for imputing protein levels from RNA-seq data. NAR Genomics and Bioinformatics. 2024 Jan 5;6(1):lqae019.
21. Ingolia NT, Brar GA, Rouskin S, McGeachy AM, Weissman JS. The ribosome profiling strategy for monitoring translation in vivo by deep sequencing of ribosome-protected mRNA fragments. Nat Protoc. 2012 Aug;7(8):1534–50.
22. Aeschimann F, Xiong J, Arnold A, Dieterich C, Großhans H. Transcriptome-wide measurement of ribosomal occupancy by ribosome profiling. Methods. 2015 Sep;85:75–89.
23. McGlincy NJ, Ingolia NT. Transcriptome-wide measurement of translation by ribosome profiling. Methods. 2017 Aug;126:112–29.
24. Schiapparelli LM, McClatchy DB, Liu HH, Sharma P, Yates JR, Cline HT. Direct Detection of Biotinylated Proteins by Mass Spectrometry. J Proteome Res. 2014 Sep 5;13(9):3966–78.
25. Douka K, Agapiou M, Birds I, Aspden JL. Optimization of Ribosome Footprinting Conditions for Ribo-Seq in Human and Drosophila melanogaster Tissue Culture Cells. Front Mol Biosci. 2022 Jan 25;8:791455.
26. Jang C, Lahens NF, Hogenesch JB, Sehgal A. Ribosome profiling reveals an important role for translational control in circadian gene expression. Genome Res. 2015 Dec;25(12):1836–47.
27. Wu CCC, Zinshteyn B, Wehner KA, Green R. High-Resolution Ribosome Profiling Defines Discrete Ribosome Elongation States and Translational Regulation during Cellular Stress. Molecular Cell. 2019 Mar;73(5):959-970.e5.
28. Chen Y, Lun ATL, Smyth GK. From reads to genes to pathways: differential expression analysis of RNA-Seq experiments using Rsubread and the edgeR quasi-likelihood pipeline. F1000Res. 2016;5:1438.
29. Chothani S, Adami E, Ouyang JF, Viswanathan S, Hubner N, Cook SA, et al. deltaTE: Detection of Translationally Regulated Genes by Integrative Analysis of Ribo-seq and RNA-seq Data. CP Molecular Biology. 2019 Dec;129(1):e108.
30. Oertlin C, Watt K, Ristau J, Larsson O. Anota2seq Analysis for Transcriptome-Wide Studies of mRNA Translation. Methods Mol Biol. 2022;2418:243–68.

31. Huang DW, Sherman BT, Lempicki RA. Systematic and integrative analysis of large gene lists using DAVID bioinformatics resources. Nat Protoc. 2009 Jan;4(1):44–57.
32. Sherman BT, Hao M, Qiu J, Jiao X, Baseler MW, Lane HC, et al. DAVID: a web server for functional enrichment analysis and functional annotation of gene lists (2021 update). Nucleic Acids Research. 2022 Jul 5;50(W1):W216–21.
33. Hulsen T. DeepVenn – a web application for the creation of area-proportional Venn diagrams using the deep learning framework Tensorflow.js.
34. Tang D, Chen M, Huang X, Zhang G, Zeng L, Zhang G, et al. SRplot: A free online platform for data visualization and graphing. Yin Y, editor. PLoS ONE. 2023 Nov 9;18(11):e0294236.
35. Hou C, Mandal A, Rohr J, Tsodikov OV. Allosteric interference in oncogenic FLI1 and ERG transactions by mithramycins. Structure. 2021 May;29(5):404-412.e4.
36. Akamatsu Y, Shigesada K. A simple screening for mutant DNA binding proteins: application to murine transcription factor PEBP2a subunit, a founding member of the Runt domain protein family. 1997;7.
37. Kundu M, Javed A, Jeon JP, Horner A, Shum L, Eckhaus M, et al. Cbfβ interacts with Runx2 and has a critical role in bone development. Nat Genet. 2002 Dec;32(4):639–44.
38. Dimerization with PEBP2β protects RUNX1/AML1 from ubiquitin–proteasome-mediated degradation [Internet]. [cited 2024 Mar 31]. Available from: https://www.embopress.org/doi/epdf/10.1093/emboj/20.4.723
39. Xu Y, Li R, Zhang K, Wu W, Wang S, Zhang P, et al. The multifunctional RNA-binding protein hnRNPK is critical for the proliferation and differentiation of myoblasts. BMB Rep. 2018 Jul 31;51(7):350–5.
40. Shahbazian D, Parsyan A, Petroulakis E, Hershey JWB, Sonenberg N. eIF4B controls survival and proliferation and is regulated by proto-oncogenic signaling pathways. Cell Cycle. 2010 Oct 15;9(20):4106–9.
41. Guo Y, Dong L, Qiu X, Wang Y, Zhang B, Liu H, et al. Structural basis for hijacking CBF-β and CUL5 E3 ligase complex by HIV-1 Vif. Nature. 2014 Jan;505(7482):229–33.
42. Wang Y, Shi Y, Niu K, Yang R, Lv Q, Zhang W, et al. Ubiquitin specific peptidase 3: an emerging deubiquitinase that regulates physiology and diseases. Cell Death Discov. 2024 May 21;10(1):243.
43. Liao Y, Zhou D, Wang P, Yang M, Jiang N. Ubiquitin specific peptidase 11 as a novel therapeutic target for cancer management. Cell Death Discov. 2022 Jun 17;8(1):292.
44. Gan Z, Han K, Lin S, Hu H, Shen Z, Min D. Knockdown of ubiquitin-specific peptidase 39 inhibited the growth of osteosarcoma cells and induced apoptosis in vitro. Biol Res. 2017 Dec;50(1):15.
45. Wang H, Ji X, Liu X, Yao R, Chi J, Liu S, et al. Lentivirus-mediated inhibition of USP39 suppresses the growth of breast cancer cells in vitro. Oncology Reports. 2013 Dec;30(6):2871–7.
46. An Y, Yang S, Guo K, Ma B, Wang Y. Reduced USP39 expression inhibits malignant proliferation of medullary thyroid carcinoma in vitro. World J Surg Onc. 2015 Dec;13(1):255.
47. Yuan X, Sun X, Shi X, Jiang C, Yu D, Zhang W, et al. USP39 promotes the growth of human hepatocellular carcinoma in vitro and in vivo. Oncology Reports. 2015 Aug;34(2):823–32.

48. Lin Z, Xiong L, Lin Q. Ubiquitin-specific protease 39 is overexpressed in human lung cancer and promotes tumor cell proliferation in vitro. Mol Cell Biochem. 2016 Nov;422(1–2):97–107.
49. Zhao Y, Zhang B, Lei Y, Sun J, Zhang Y, Yang S, et al. Knockdown of USP39 induces cell cycle arrest and apoptosis in melanoma. Tumor Biol. 2016 Oct;37(10):13167–76.
50. Cai J, Liu T, Huang P, Yan W, Guo C, Xiong L, et al. USP39, a direct target of microRNA-133a, promotes progression of pancreatic cancer via the AKT pathway. Biochemical and Biophysical Research Communications. 2017 Apr;486(1):184–90.
51. Xing Z, Sun F, He W, Wang Z, Song X, Zhang F. Downregulation of ubiquitin-specific peptidase 39 suppresses the proliferation and induces the apoptosis of human colorectal cancer cells. Oncol Lett [Internet]. 2018 Feb 15 [cited 2024 Jun 24]; Available from: http://www.spandidos-publications.com/10.3892/ol.2018.8061
52. Liu C, Yao X, Li M, Xi Y, Zhao L. USP39 regulates the cell cycle, survival, and growth of human leukemia cells. Bioscience Reports. 2019 Apr 30;39(4):BSR20190040.
53. Dong X, Liu Z, Zhang E, Zhang P, Wang Y, Hang J, et al. USP39 promotes tumorigenesis by stabilizing and deubiquitinating SP1 protein in hepatocellular carcinoma. Cellular Signalling. 2021 Sep;85:110068.
54. Wang W, Lei Y, Zhang G, Li X, Yuan J, Li T, et al. USP39 stabilizes β-catenin by deubiquitination and suppressing E3 ligase TRIM26 pre-mRNA maturation to promote HCC progression. Cell Death Dis. 2023 Jan 27;14(1):63.
55. Labelle-Côté M, Dusseault J, Ismaïl S, Picard-Cloutier A, Siegel PM, Larose L. Nck2 promotes human melanoma cell proliferation, migration and invasion in vitro and primary melanoma-derived tumor growth in vivo. BMC Cancer. 2011 Dec;11(1):443.
56. Chaki SP, Barhoumi R, Rivera GM. Nck adapter proteins promote podosome biogenesis facilitating extracellular matrix degradation and cancer invasion. Cancer Medicine. 2019 Dec;8(17):7385–98.
57. Cai X, Deng J, Zhou J, Cai H, Chen Z. Cyclin-dependent kinase 19 upregulation correlates with an unfavorable prognosis in hepatocellular carcinoma. BMC Gastroenterol. 2021 Oct 14;21(1):377.
58. Liu Y, Hu Y, Li X, Niu L, Teng M. The Crystal Structure of the Human Nascent Polypeptide-Associated Complex Domain Reveals a Nucleic Acid-Binding Region on the NACA Subunit,. Biochemistry. 2010 Apr 6;49(13):2890–6.
59. Beatrix B, Sakai H, Wiedmann M. The α and β Subunit of the Nascent Polypeptide-associated Complex Have Distinct Functions. Journal of Biological Chemistry. 2000 Dec;275(48):37838–45.
60. Zheng AJL, Thermou A, Daskalogianni C, Malbert-Colas L, Karakostis K, Le Sénéchal R, et al. The nascent polypeptide-associated complex (NAC) controls translation initiation *in cis* by recruiting nucleolin to the encoding mRNA. Nucleic Acids Research. 2022 Sep 23;50(17):10110–22.
61. Wang H, Xing J, Wang W, Lv G, He H, Lu Y, et al. Molecular Characterization of the Oncogene BTF3 and Its Targets in Colorectal Cancer. Front Cell Dev Biol. 2021 Feb 11;8:601502.
62. Zhang Y, Gao X, Yi J, Sang X, Dai Z, Tao Z, et al. BTF3 confers oncogenic activity in prostate cancer through transcriptional upregulation of Replication Factor C. Cell Death Dis. 2021 Jan 5;12(1):12.

63. Wang J, Yuan L, Xu X, Zhang Z, Ma Y, Hong L, et al. Rho-GEF Trio regulates osteosarcoma progression and osteogenic differentiation through Rac1 and RhoA. Cell Death Dis. 2021 Dec 11;12(12):1148.
64. Bajpai J, Sharma M, Sreenivas V, Kumar R, Gamnagatti S, Khan SA, et al. VEGF expression as a prognostic marker in osteosarcoma. Pediatric Blood & Cancer. 2009 Dec;53(6):1035–9.
65. Han Z, Zhuang X, Yang B, Jin L, Hong P, Xue J, et al. SYDE1 Acts as an Oncogene in Glioma and has Diagnostic and Prognostic Values. Front Mol Biosci. 2021 Oct 14;8:714203.
66. Shi C, Zhang H, Wang P, Wang K, Xu D, Wang H, et al. PROTAC induced-BET protein degradation exhibits potent anti-osteosarcoma activity by triggering apoptosis. Cell Death Dis. 2019 Oct 25;10(11):815.
67. Zhu H, Cai H, Tang M, Tang J. Neuropilin-1 is overexpressed in osteosarcoma and contributes to tumor progression and poor prognosis. Clin Transl Oncol. 2014 Aug;16(8):732–8.
68. Singhabahu R, Kodagoda Gamage SM, Gopalan V. Pathological significance of heme oxygenase-1 as a potential tumor promoter in heme-induced colorectal carcinogenesis. Cancer Pathogenesis and Therapy. 2024 Apr;2(2):65–73.
69. Flieswasser T, Van Den Eynde A, Van Audenaerde J, De Waele J, Lardon F, Riether C, et al. The CD70-CD27 axis in oncology: the new kids on the block. J Exp Clin Cancer Res. 2022 Dec;41(1):12.
70. Alvarez-Castelao B, Ruiz-Rivas C, Castaño JG. A Critical Appraisal of Quantitative Studies of Protein Degradation in the Framework of Cellular Proteostasis. Biochemistry Research International. 2012;2012:1–11.
71. Deng B, Deng J, Yi X, Zou Y, Li C. ROCK2 Promotes Osteosarcoma Growth and Glycolysis by Up-Regulating HKII via Phospho-PI3K/AKT Signalling. CMAR. 2021 Jan;Volume 13:449–62.
72. Haga RB, Ridley AJ. Rho GTPases: Regulation and roles in cancer cell biology. Small GTPases. 2016 Oct 1;7(4):207–21.
73. Matos P. Small GTPases in Cancer: Still Signaling the Way. Cancers. 2021 Mar 25;13(7):1500.
74. Yin G, Huang J, Petela J, Jiang H, Zhang Y, Gong S, et al. Targeting small GTPases: emerging grasps on previously untamable targets, pioneered by KRAS. Sig Transduct Target Ther. 2023 May 23;8(1):212.
75. Murugan AK, Grieco M, Tsuchida N. RAS mutations in human cancers: Roles in precision medicine. Seminars in Cancer Biology. 2019 Dec;59:23–35.
76. Prior IA, Hood FE, Hartley JL. The Frequency of Ras Mutations in Cancer. Cancer Research. 2020 Jul 15;80(14):2969–74.
77. Li S, Balmain A, Counter CM. A model for RAS mutation patterns in cancers: finding the sweet spot. Nat Rev Cancer. 2018 Dec;18(12):767–77.
78. Jiang Y, Chen M, Nie H, Yuan Y. PD-1 and PD-L1 in cancer immunotherapy: clinical implications and future considerations. Human Vaccines & Immunotherapeutics. 2019 May 4;15(5):1111–22.
79. Braicu C, Buse M, Busuioc C, Drula R, Gulei D, Raduly L, et al. A Comprehensive Review on MAPK: A Promising Therapeutic Target in Cancer. Cancers. 2019 Oct 22;11(10):1618.

80. Looi CK, Hii LW, Ngai SC, Leong CO, Mai CW. The Role of Ras-Associated Protein 1 (Rap1) in Cancer: Bad Actor or Good Player? Biomedicines. 2020 Sep 7;8(9):334.

Chapter 5

Conclusions and Future Directions

General Conclusions of the Dissertation Work

The studies within this dissertation entail efforts to describe a noncanonical role of CBFβ in osteosarcoma (OS), and enhance our understanding of whether CBFβ could present a novel therapeutic target in OS. While there has been considerable effort in researching new therapeutic approaches in OS, one aspect of OS which makes development of therapies difficult is the high degree of heterogeneity among patient tumors. This, coupled with OS having a very low prevalence, has caused OS therapeutic development to stagnate in comparison to other cancers. In fact, OS therapies have not appreciably changed in the last 30 years. Protein translation acts as a convergence point of multiple signaling pathways, and could provide a mechanism to overcome the heterogeneity of the OS patient population. This project focuses on studying the role of CBFβ in protein translation in OS, and investigates it as a potential therapeutic target.

The data gathered in this project began with study of the interaction of RUNX2, a DNA binding transcription factor, and CBFβ, a co-activator to RUNX2. RUNX2 expression, as well as that of its gene targets, is elevated in OS and correlated with poor prognosis, which brought this protein and its binding partner into our focus. Development of a CBFβ knockout (KO) cell line and profiling via western blotting revealed a decrease in RUNX2 protein expression upon loss of CBFβ, which was interesting and unexpected. The foundation of this research was built on another project studying a small molecule allosteric inhibitor of the CBFβ-RUNX2 interaction, which was the reason for development of the CBFβ KO cell line. With further profiling of this cell line, the mechanism of this reduction in RUNX2 expression became the focus of this work.

In chapter 2 we demonstrate that CBFβ regulates RUNX2 expression via a post-transcriptional mechanism. Using western blotting, we confirmed the reduction in RUNX2 protein expression upon loss of CBFβ, and via qPCR and RNA-seq we established that this discrepancy

did not occur at the mRNA level. This implied a post-transcriptional mechanism at play, and as RUNX2 is already being explored as a therapeutic target in OS, this new mechanism of CBFβ regulation of RUNX2 expression could provide a novel therapeutic target in OS. Following this, using proteasome and translation inhibitors, we demonstrate that a reduction in RUNX2 stability due to loss of its binding partner CBFβ does not fully explain this reduction in RUNX2 expression at the protein level. Around the same time, another study in breast cancer noted a similar reduction in RUNX1 expression upon loss of CBFβ, and postulated this to result from CBFβ playing a role in protein translation. To investigate whether this may also be occurring in OS, we used a Click-iT Alexa488 protein translation assay to measure global protein translation, and observed a reduction in global protein translation in U2OS cells upon loss of CBFβ. This role was reported in breast cancer to occur via CBFβ interaction with hnRNPK, and we used reciprocal co-immunoprecipitation (co-IP) to validate that this interaction occurs in OS cells as well. Finally, we used lentiviral transduction to re-introduce wild-type (WT) CBFβ back into our CBFβ KO cells, and verified that RUNX2 protein expression increased in the presence of CBFβ. This confirmed that we were observing a CBFβ-dependent effect, and not being misled by nonspecific CRISPR activity.

These results were very encouraging, but the dual roles of CBFβ presented a complex mechanism to study. CBFβ exerts a transcriptional role when present in the nucleus and bound to the RUNX proteins, yet this translational role reportedly occurs in the cytoplasm. Furthermore, CBFβ cannot move freely from the cytoplasm to the nucleus by itself, and is instead shuttled into the nucleus onboard the RUNX proteins. In this manner, it is possible that interaction with RUNX proteins would reduce the cytoplasmic pool of CBFβ, and negatively affect the performance of its

translational role. Additionally, knockout of one RUNX protein leads to compensatory increases in other RUNX proteins, making individual study of the translational role of CBFβ difficult.

In chapter 3, we describe efforts made to design and validate a mutant form of CBFβ, designed to display decreased affinity toward the RUNX proteins and instead remain in the cytoplasm. Using recombinant protein production combined with peptide inhibitors, we validated residues G61 and N63 of CBFβ to be important in CBFβ-RUNX2 interaction. We then generated a mutant of CBFβ with alanines at these residues as well as N104, and re-introduced this mutant form into our CBFβ KO cells to generate CBFβ _FLAG_3xMut. We conducted cellular electrothermal shift assay (CETSA) and validated that our mutations had significantly interrupted CBFβ-RUNX2 interaction, resulting in inhibited binding between RUNX2 and our mutant form of CBFβ as compared to WT CBFβ. Next, we conducted nuclear/cytoplasmic fractionation to investigate the functional consequence of our mutant form of CBFβ on RUNX protein mediated nuclear shuttling. We observed a strong inhibition of shuttling of CBFβ _FLAG_3xMut into the nucleus onboard RUNX proteins, validating that we had accomplished our goal of retaining CBFβ in the cytoplasm in order to study its translational role.

At this point we had generated compelling data suggesting that CBFβ may play a novel role in protein translation in OS, however our studies thus far had focused purely on the relationship between CBFβ and RUNX2. In chapter 4 we extend our data collection beyond RUNX2 and performed three assays which look at all proteins within the cell. The assays in chapter 4 served to answer two questions: 1) what is the full list of proteins that CBFβ interacts with in OS cells? And 2) what is the full list of proteins which may have their translation affected by the presence of CBFβ? We performed IP-MS to characterize the interactors of CBFβ, and revealed a list of 23 proteins which we binned as high confidence interactors of CBFβ in OS. Importantly,

the vast majority of these proteins have not been profiled in the literature at the time of writing this. Additionally, by performing IP-MS on our mutant form of CBFβ, we revealed seven (7) proteins which are dependent upon CBFβ residues G61, N63, and/or N104 for their binding to CBFβ. Next, we performed direct detection of biotinylated peptides (DiDBiT) as well as Ribo-Seq, with the goal of elucidating which proteins may have their translation influenced by CBFβ. These studies revealed hundreds of proteins which experience altered production in the presence of CBFβ, with gene ontology (GE) of this list revealing strong enrichment of biological process terms cell division, cell adhesion, and cell migration. These processes are strongly implicated in cancer, and it's possible CBFβ may influence these processes by altering production of proteins involved in them. Additionally, Reactome analysis of these proteins saw enrichment of Rho GTPase signaling and VEGF signaling terms, suggesting CBFβ may play a role in regulating these processes. GO terms cell adhesion, migration, and division, were also enriched among proteins decreased in production in the presence of CBFβ _FLAG_3xMut as compared to CBFβ_WT_FLAG, suggesting these mutated residues may be important in the production of these proteins.

Future Directions

While the data from this project has significantly enhanced our understanding of CBFβ in OS, there are numerous additional studies which could build on this work and dive deeper into whether this protein presents a viable therapeutic target. In **Chapter 2** we demonstrate that RUNX2 protein levels are affected by the presence of CBFβ, and a decrease in RUNX2 stability upon loss of CBFβ does not fully explain this occurrence. A limitation exists in the second portion of that statement, as the stability assays we employed run into confounding variables when used to study proteins with particularly long half-lives, such as RUNX2. As mentioned in the **Chapter 2 Discussion**, treatment with MG132 or Cycloheximide for these extended periods is likely to perturb normal cellular function, hampering accurate measure of the shift in RUNX2 stability upon loss of CBFβ. As mentioned previously, these longer treatments may stimulate lysosomal degradation of RUNX2, which could be addressed by use of lysosomal protease inhibitors, although this would introduce additional variables to an already precarious experiment. For this reason, it may be better to switch approaches entirely.

To get a better picture of RUNX2 half-life, a useful assay involves growing cells in methionine-free media supplemented with L-azidohomoalanine (AHA), a methionine analog compatible with click chemistry conjugation. In short, cells would be incubated with AHA for ~4h, then switched to incubation in normal media for various durations. Lysate is then extracted, AHA is click conjugated to biotin, then RUNX2 is immunoprecipitated (IP) and quantified by western blot. Western blotting for biotin within the RUNX2 IP, and normalizing that to total RUNX2 signal, would yield a measure of quantity of labeled RUNX2 remaining over time. Usage of various post-AHA incubation durations in normal media would allow measure of the degradation of tagged RUNX2, without introducing toxicity into cells as, since AHA does not

interfere with protein translation or degradation. As mentioned in chapter 2, it's possible that lysosomal trafficking of RUNX2, potentially by SOX9, is confounding the stability data we generated, and an AHA pulse-chase experiment would avoid this issue.

AHA pulse chase would require significant optimization of RUNX2 IP, which we found intractable within our timeframe for this work, but is likely not impossible given adequate resources. Optimization of RUNX2 IP would also allow for treatment of cells with MG132, a proteasome inhibitor, followed by immunoblotting for ubiquitination of RUNX2, which would present clear data on altered degradation of RUNX2 based on CBFβ status, and dovetail with stability data from AHA pulse-chase. While these would be useful, their overall benefit balanced against their cost would need to be evaluated first.

In chapter 2 we also re-introduced WT CBFβ back into CBFβ KO cells and observed a recovery of low RUNX2 expression. While we had verified the decrease in RUNX2 protein expression upon loss of CBFβ occurs in a post-transcriptional manner, it would be useful to validate that the increase in RUNX2 protein expression upon re-introduction of CBFβ also occurred via a post-transcriptional mechanism. This could be validated by way of qPCR of RUNX2 in each cell line normalized to HPRT, in the same manner as was originally tested in U2OS WT vs. U2OS CBFβ KO cells in the beginning of chapter 2.

In chapter 3 we introduced key mutations into CBFβ at residues G61, N63, and N104 (CBFβ _FLAG_3xMut), with the goal of inhibiting binding to RUNX proteins, thereby preventing RUNX-mediated nuclear shuttling of CBFβ from complicating study of its translational role. We demonstrated that our mutant exhibited decreased CBFβ-RUNX2 binding and subsequent nuclear shuttling, as was the goal, however our mutant was unable to recover low RUNX2 expression seen in Empty Vector (EV) cells. Usage of the aforementioned AHA pulse chase assay on these 3xMut

cells would provide useful information as well, to test if RUNX2 stability differed between CBFβ CBFβ WT and 3xMut cells. RUNX2 expression may be unchanged relative to EV due to low stability, or perhaps these residues we mutated on CBFβ also play a role in the translation of RUNX2 specifically. Usage of AHA pulse chase would assist in revealing which of these is the dominant factor at play. Additionally, usage of qPCR for RUNX2 expression in CBFβ_3xMut_FLAG-expressing cells would also be informative.

In chapter 4 we conducted three large assays with the goal of answering two key questions: 1) what are all the proteins which CBFβ interacts with in OS cells? And 2) what are all the proteins which CBFβ may translationally regulate. To answer question 1, we performed IP-immunoprecipitation mass spectrometry, (IP-MS), and identified numerous new proteins which interacted with CBFβ_WT_FLAG, the lion's share of which have not been reported anywhere in the literature. A necessary next step to further validate these proteins as specific interactors is to conduct IP followed by western blotting. Of course, it would not be feasible to purchase an antibody for every identified protein, as costs for that would be prohibitive, but blotting for certain proteins of interest for confirmation would be wise. Particularly interesting targets, such as NCK2, USP39, BTF3, and NACA2 could then be further validated via reciprocal co-IP, such as was performed towards the end of chapter 2 studying CBFβ-hnRNPK interaction. Additionally, interaction between these proteins and CBFβ could also be revealed by conducting cellular electrothermal shift assay (CETSA) on these proteins, in the event their stoichiometry in binding to CBFβ is not high enough to be detected in a pulldown, or antibodies suitable to IP them are not available. These same experiments would be useful to validate the proteins we suggested to rely on CBFβ residues G61, N63, and N104 for their interaction, as listed in **Figure 4.6**.

To answer question 2, we performed two orthogonal assays; direct detection of biotinylated peptides (DiDBiT) and Ribo-Seq. These are both complex assays that generated a myriad of data, and therefore a myriad of potential research directions. Building on DiDBiT data, further studies into the characteristics of CBFβ _FLAG_3xMut cells compared to CBFβ_WT_FLAG would prove very useful in unraveling the significance of these residues of CBFβ on overall cancer cell behavior. For example, cell adhesion, migration, division, and osteoblast differentiation showed up as highly ranked biological processes among CBFβ_WT_FLAG cells as compared to CBFβ _FLAG_3xMut cells, suggesting our mutated residues of CBFβ play a role in these processes. This could be further studied by use of migration/invasion or proliferation assays. These phenotypic experiments would bridge the gap between the specific molecular consequences revealed in this study and global effects which would influence cancer cell malignancy. This would also add more data which may further support CBFβ as a therapeutic target in OS.

While our goal in generating CBFβ_3xMut_FLAG was to decouple the transcriptional and translational roles of CBFβ, the appearance of so many proteins which experienced diminished production in the presence of CBFβ_3xMut_FLAG suggests we may have also affected the translational component of CBFβ. In order to fully utilize CBFβ_3xMut_FLAG as a tool in solely investigating the translational role of CBFβ without the transcriptional role confounding data, Ribo-Seq could be performed on CBFβ_3xMut_FLAG cells vs CBFβ_WT_FLAG to measure how drastically these mutations did influence the role of CBFβ in protein translation.

In terms of data from Ribo-Seq, while there was a small cohort of proteins which were upregulated in translational efficiency in the presence of CBFβ, there were many more proteins which experienced a positive change in translational buffering upon loss of CBFβ. That is to say, these proteins experienced a decrease in transcription, but this was coupled with a compensatory

increase in translational efficiency. Although this may not necessarily lead to a bulk increase in the quantity of these proteins, they did experience alterations in translational efficiency in the presence of CBFβ, which is still important to analyze. Future studies which delve deeper into the effect of translational buffering in OS would be useful in giving these results greater context. Translational buffering has been implicated in cancer, although with it being a newly identified phenomenon, our knowledge on it and the overall impacts are more limited than that of more classical gene expression regulatory mechanisms.

The importance of CBFβ in OS could also be measured via assays which compare CBFβ KO cells to WT cells in terms of susceptibility to chemotherapies. While our lab has U2OS CBFβ KO cells, the reliance of other parental cell lines on CBFβ could be assessed by use of siRNA against CBFβ combined with a chemotherapeutic. Functional assays such as migration/invasion would also be interesting to get a picture of the importance of CBFβ in OS cell lines other than U2OS.